Information Theoretic Aspects of some Non-Gaussian Classical and Quantum Optical Fields

Thesis Submitted for the Degree of

Doctor of Philosophy (Sc.)
in Physics (Theoretical)

by

Soumyakanti Bose

Department of Physics

University of Calcutta

2018

I dedicate the thesis to my thesis adviser Dr. M. Sanjay Kumar.

Acknowledgement

I express my heartfelt gratitude to my thesis adviser Dr. M. Sanjay Kumar for his invaluable guidance that shaped my concepts and ideas. I am also thankful to all my thesis committee members and other faculty personnel for their insightful suggestion/remark (s) during the entire tenure of my doctoral research. I am indebted to my fellow scholars for their continuous support, inspiration and maintaining a healthy academic environment.

Nonetheless, I am grateful to the academic and administration office personnel for their relentless support and cooperation that have had helped me in completing my doctoral research in due time.

Abstract

In recent years, non-Gaussian entangled states of light have gained much importance in various information processing tasks. In this thesis, we have investigated various information theoretic aspects of a class of two-mode non-Gaussian entangled resources that are generated by a beam splitter (BS) from input single mode non-Gaussian states, termed MNIO states, arising from two distinct nonclassicality (NC) inducing operations, namely, photon addition/subtraction and squeezing. An interesting aspect of the MNIO states is the presence and/or absence of the squeezing sub-Poissonian character in different parameter regimes. We have shown how various quantitative features of BS generated entanglement, with MNIO states, can be understood in terms of the competition between the different NC-inducing operations, as manifest in the contours of the associated Q distributions. We explain this quantitative features in terms of a Wehrl entropy based measure of NC, as we find the existing measures to be inadequate in this respect. We have investigated aspects of quantum teleportation (QT) with the BS generated non-Gaussian entangled resource states. Our focus has been to assess whether attributes of entangled resource states such as squeezed vacuum affinity and EPR correlation are necessary/sufficient for QT. Our results suggest that these are neither necessary nor sufficient. We have looked into yet another attribute not considered earlier, namely, $U(2)$-invariant two-mode squeezing in this context. Our numerical studies on both the de-Gaussified squeezed vacuum states studied earlier as well as the BS generated states point us to the conclusion that $U(2)$-invariant two-mode squeezing could be a necessary condition for QT. We have examined which particular aspect of NC, viz., the squeezing or the sub-Poissonian character, contributes more towards conversion of input NC into BS output entanglement. Finally, we have addressed the question of how to regenerate the entanglement destroyed by the first BS when two other BSs are placed at the two output ports. We have given a scheme using BSs and other linear optical elements that accomplishes this task. Our scheme also accomplishes the task of regenerating entanglement at various sites on a 1-dimensional lattice.

Key Results of the Thesis

Chapter 2

- While in the case of input MNIO states, the BS generated entanglement shows monotonic dependence on input NC as quantified by the photon addition number m and squeeze parameter r generally, in the particular case of PAS, it turns out a non-monotonic dependence.
- We explain this non-monotonicity in terms of the relative competition between the NC-inducing operations of photon addition and squeezing as manifest in the contours of the associated Husimi-Kano Q distribution.
- Attempts to quantify the NC of the MNIO class of states in terms of the existing measures of NC fail, as these measures are not well defined for these states.

Chapter 3

- We propose a new measure of NC for the pure states in terms of the Wehrl entropy.
- Our measure gives a correct quantification of the effective NC of the MNIO class of states. Further the dependence of the Wehrl entropy based NC measure on the input state parameters is consistent with that of the BS entanglement curves.

Chapter 4

- Squeezed vacuum affinity regarded as an essential attribute of two-mode entangled resource states in the literature turn out to be zero for a large subclass of BS-MNIO states, and hence is not a genuine attribute in general.
- EPR correlation, another such attribute considered in the literature, is found not be sufficient for QT. Our results together with other specific results known in the literature, indicate that EPR correlation is neither necessary nor sufficient for QT.

- We further examine the question of whether $U(2)$-invariant squeezing of two-mode entangled states could be a necessary condition for QT and our extensive numerical results point us to the conclusion that this could well be true.

Chapter 5

- We have found that the sub-Poissonian character of the input states contributes to the larger extent towards conversion of input NC into BS output entanglement in comparison with the squeezing character.

- A scheme, using multiple BSs and other linear optical elements, has been proposed for regenerating and redistributing BS output entanglement originally generated and destroyed at the site of the first BS.

Contents

List of Figures

Introduction

Quantum entanglement is at the heart of a new discipline that has emerged in the last decades, called Quantum Information Science. The first conceptualization of quantum entanglement was given by Einstein, Podolsky and Rosen [1] where they talked about the *spooky action* at a distance between two spatially separated particles with correlated positions and momenta. This *spooky action* at a distance was first termed as *entanglement* by Schrodinger [2]. Quantum Information Science encompasses several sub-disciplines including quantum information theory, quantum information processing, quantum computation *etc.* Entanglement plays a central role in several information processing tasks such as quantum teleportation, dense coding, quantum cryptography *etc.* [3]. In last decades, the theory of entanglement as well as the characterization of different entanglement based information theoretic protocols have been explored to a great extent, both on theoretical and experimental grounds [4]. Various theoretical issues such as characterization and quantification of entanglement, and the use of entanglement in information processing tasks, and experimental issues relating to realization of qubits, quantum gates, various protocols have been explored.

While classical information is stored in bits, quantum information is stored in qubits which are essentially any quantum two state system. Qubits can be realized in several physical systems such as atomic or nuclear spin, two-lowest energy levels of a semiconductor quantum dots, polarization degrees of a single photon *etc.* More generally, quantum information can be stored in qudits which are states in a d-dimensional Hilbert space. In case of qubits, $d = 2$. Alternatively, one may store quantum information in continuous variables such as position and momentum of a particle or the quadrature variables of a single mode quantized electromagnetic field or the vibrational modes of molecules or solids *etc.* The information storage unit here are states that live in an infinite dimensional Hilbert space [5].

Continuous variable QIT with optical resources is centered largely around Gaussian states [6, 7]. This is due the fact that Gaussian states could be well-characterized in terms

of a real symmetric matrix of all second order moments [8, 9], known as the *variance matrix*. The Gaussian entangled states generated typically in various non-linear optical experiments [10] have been extensively studied in several information processing tasks, both theoretically and experimentally [11]. However, in recent years, non-Gaussian entangled resources, generated by several de-Gaussification processes applied on two-mode entangled Gaussian states, have been found to be useful due to their superiority over Gaussian states in different information processing tasks [12].

An alternative way of generating such non-Gaussian entangled states of light is by using linear devices like a passive beam splitter (BS). A necessary and sufficient condition [13–16] for the BS output state to be entangled is that light fed at one of the input ports of a BS with other port left with vacuum, is *nonclassical* [18–20]. The quantitative aspect of BS output entanglement with input nonclassical states has attracted some attention in the literature. Earlier studies on BS generated entanglement have used as input states, the squeezed vacuum, squeezed thermal or the photon number state. They have found a monotonic relation between BS output entanglement and input NC as measured by the squeezed parameter r or the photo number m as the case may be.

My thesis is dedicated to an extensive analysis of the various *information theoretic aspects* of a class of two-mode non-Gaussian entangled states light, generated by a BS from input single mode nonclassical non-Gaussian states. These states have been studied in the literature in respect of their nonclassical properties, photon number distributions *etc.* [21–25]. However, we find it useful to look upon these states as a class of states generated under two distinct nonclassicality (NC) inducing operations, namely photon addition/subtraction and quadrature squeezing, applied on the vacuum state in different orders. The particular single mode states that we have considered are photon added squeezed vacuum state (PAS), photon subtracted squeezed vacuum state (PSS) and squeezed number state (SNS). More generally, one could conceive of states generated under *multiple nonclassicality inducing operations* (MNIO). From this perspective it is convenient to refer to the states PAS, PSS and SNS as belonging to the "MNIO class". The two-mode entangled states generated by the BS with input MNIO states we have conveniently termed as the BS-MNIO states. The outline of the thesis is as given below.

In Chapter 1 we have briefly discussed some basic concepts related to the single mode and two-mode quantum optical states. In particular, we have first reviewed various aspects of these states such as NC and non-Gaussianity (NG). Both NC as well as NG are defined in terms of appropriate phase space distributions associated with these states. Hence we

have given a brief description of phase space distributions and some of their important properties. We have also discussed the basic notion of quantum entanglement, ways to characterize it and measure it. Finally, we have briefly discussed the Braunstein-Kimble (BK) protocol for quantum teleportation (QT) using entangled optical resources.

In Chapter 2 we have carried out an extensive analysis regarding the different nonclassical aspects of the MNIO class of states and the BS output entanglement with such states at input. to begin with, we have brought out some interesting nonclassical features of these states in terms of the presence and/or absence of sub-Poissonian and squeezing character, in different parameter regimes. The main thrust of this chapter is the study of quantitative and qualitative aspects of BS generated entanglement, with MNIO states at input, in relation to the amount of NC in the input states. The BS output entanglement in the case of SNS as input is found to be a monotonic function of the input NC as measured by the input state parameters, viz., number of photon addition (m) and the squeeze parameter (r), in line with the earlier results obtained with either of number state or squeezed vacuum state. However, in the case of PAS as input, the BS output entanglement shows a *non-monotonic* dependence. We have sought to understand this counterintuitive result in terms of an effective NC measure of the states SNS and PAS, relying on existing measures. However, we have found that the existing measures are not even well defined for the MNIO class of states. However, we have *qualitatively explained this non-monotonic behavior in terms of the mutual competition between the NC-inducing operations*, i.e., photon addition and quadrature squeezing, as manifest in the contours of the associated Husimi-Kano Q distributions.

In Chapter 3, we have returned to the question of how to explain quantitatively the non-monotonicity in the BS generated entanglement, with input MNIO class of states, as is observed in Chap. 2, in terms of an effective measure of input NC. To this end, we have proposed propose a new measure of single mode NC for pure states in terms of the Wehrl entropy. We have demonstrated that our newly proposed measure reproduces the NC curves for the MNIO class of states, consistent with that of the respective BS generated entanglement curves. We have also shown that our Wehrl entropy based measure is a monotonically increasing function of a well-known measure of NC known as *nonclassical depth*, in the special case of Gaussian states. This measure, however, can't be extended to the mixed states.

In Chapter 4 we have studied quantitative and qualitative aspects of QT, using the BK protocol with the BS-MNIO states as entangled resources. The primary objective of our study has been to identify what are, besides entanglement, the necessary and/or sufficient conditions on the two-mode entangled states to achieve QT. To this end, we have first in-

vestigated the existing well-known attributes of the two-mode entangled resources such as *squeezed vacuum affinity* (SVA) and *EPR correlation*. Our results indicate that while SVA is not a genuine attribute of the two-mode entangled resource states, as it is not non-zero for a large subclass of the BS-MNIO states, EPR correlation is not sufficient for QT. In conjunction with the earlier work by Lee *et. al.* [Phys. Rev. A **84**, 012302 (2011)] and Wang *et. al.* [Phys. Rev. A **91**, 063832 (2015)], where the EPR correlation has been found not to be *always necessary for QT*, our work leads us to the conclusion that *EPR correlation is neither necessary nor sufficient for QT*, in general. We then have gone into the question of whether $U(2)$-invariant two-mode squeezing could be relevant for QT. Our numerical results on the BS-MNIO states as well as the de-Gaussified TMSV indicate that QT is achieved only when $U(2)$-invariant squeezing is present. However, the converse is not true. In other words, for the class of states that we have considered, $U(2)$-invariant squeezing appears to be necessary for QT, but not sufficient. We have provided an analytical proof of this *necessary criterion* in the case of a subclass of two-mode entangled Gaussian states, namely the symmetric Gaussian states. Our overall conclusion based on our numerical results as well as some limited analytical results is that $U(2)$-*invariant squeezing could be a necessary condition for QT*, in general.

In Chapter 5 we have revisited the question of the extent to which input NC is converted into BS output entanglement that was studied earlier by Ge *et. al.* [Phys. Rev. A **92**, 052328 (2015)]. Our results corroborate the conservation law relating input NC, output NC and BS output entanglement. We have looked into the question of conversion of input NC into BS output entanglement in the non-Gaussian case by focussing on two particular aspects of NC, viz., sub-Poissonian and quadrature squeezing character. We have shown analytically that, compared to the squeezing character, sub-Poissonian character is used up by the BS to greater extent for generating entanglement. Finally, we address the question of regenerating the entanglement destroyed due to the placement of two other BSs at the output ports of the first BS, at some different location. In this regard we have proposed a scheme, using BSs and other linear optical elements such as phase shifter and perfect mirrors, to accomplish this task. We have further demonstrated that our scheme also accomplishes the task of redistributing the BS generated entanglement at different sites on a 1-dimensional lattice.

In Chapter 6 we have summarized the various results obtained in the thesis. We have also indicated in what ways some of these results could be extended in future works. We have also discussed the possibility of examining some of the questions addressed in the thesis in the context of classical optical beams which, as is well known, are analogous to two-mode

quantum states under paraxial approximation.

Chapter 1

Background

In this chapter we briefly discuss important characteristics of quantum states of light such as nonclassicality (NC) and non-Gaussianity (NG) of quantum states of light and related literature. We also describe the of generation of two-mode entanglement from the nonclassical states of light and quantum teleportation with entangled optical resources.

1.1 Phase Space Distributions in Quantum Optics

The expectation value of an operator $\hat{A}$ for the quantum state ρ is given by $\langle\hat{A}\rangle = \mathrm{Tr}\,[\hat{\mathrm{A}}\rho]$. For the first time E. P. Wigner [26] suggested how one can calculate $\langle\hat{A}\rangle$ as the average value of the classical function $A_{\mathrm{cl}}(x,p)$ associated with the operator $\hat{A}$ with respect to the phase space probability distribution $W_\rho(x,p)$, called the Wigner distribution, associated with the quantum state ρ.

There are several such phase space distributions [27]. Here, we discuss some of the distributions that are commonly used in quantum optics, viz., Wigner (W) distribution [26], Glauber-Sudarshan (P) distribution [28] and Husimi-Kano (Q) distribution [29]. For any quantum state of light ρ, these distributions are defined as,

$$\begin{aligned} W(\alpha,\alpha^*) &= \int \frac{d^2\lambda}{\pi}\, e^{\alpha\lambda^*-\alpha^*\lambda}\, \mathrm{Tr}\,[\rho\, \mathrm{e}^{\lambda \mathrm{a}^\dagger - \lambda^* \mathrm{a}}] \\ P(\alpha,\alpha^*) &= \int \frac{d^2\lambda}{\pi}\, e^{\alpha\lambda^*-\alpha^*\lambda}\, \mathrm{Tr}\,[\rho\, \mathrm{e}^{\lambda \mathrm{a}^\dagger}\, \mathrm{e}^{-\lambda^* \mathrm{a}}] \\ Q(\alpha,\alpha^*) &= \int \frac{d^2\lambda}{\pi}\, e^{\alpha\lambda^*-\alpha^*\lambda}\, \mathrm{Tr}\,[\rho\, \mathrm{e}^{-\lambda^* \mathrm{a}}\, \mathrm{e}^{\lambda \mathrm{a}^\dagger}], \end{aligned} \tag{1.1}$$

where, a and $a^\dagger$ are the single mode annihilation and creation operators respectively. The complex numbers $\{\alpha,\alpha^*\}$ are the phase space C-number analogues of the ladder operators a and $a^\dagger$ related to the real quadrature variables ($\{x,p\}$) as $\alpha = \frac{1}{\sqrt{2}}(x + ip)$ and $\alpha^* = \frac{1}{\sqrt{2}}(x - ip)$. Note that the phase space distributions W, P and Q in Eq. (1.1) are in fact special cases of

the family of s-ordered distributions [27, 30] as,

$$F(\alpha,\alpha^*) = \int \frac{d^2\lambda}{\pi}\, e^{\alpha\lambda^*-\alpha^*\lambda}\, e^{s\frac{|\lambda|^2}{2}}\, \mathrm{Tr}\,[\rho\, \mathrm{D}(\alpha)], \tag{1.2}$$

where, $D(\alpha) = e^{\lambda a^\dagger - \lambda^* a}$. One obtains W, P and Q distributions for $s = 0, 1$ and -1 respectively. A detailed description of these phase-space distributions in quantum optics could be found in [27, 31].

It is worth noting that these phase space distributions are not true classical probability distributions as they fail to satisfy some of the requirements on the latter for example the Wigner distribution is not always non-negative whereas the P distribution can become more singular than a delta function for some states. Hence these phase space distributions are referred to as quasi-probability distribution.

1.2 Nonclassical States of Light

Any quantum state of light ρ could be represented in terms of P distribution as

$$\rho = \int \frac{d^2\alpha}{\pi}\, P(\alpha,\alpha^*)\, |\alpha\rangle\langle\alpha|, \tag{1.3}$$

where $|\alpha\rangle$ is the coherent state basis. The state ρ is said to *nonclassical if* its associated P distribution as defined in Eq. (1.3) becomes negative or more singular than a delta function [32]. For the sake of illustration let's consider the photon number state $|m\rangle$ ($\rho = |m\rangle\langle m|$) for which Glauber-Sudarshan P distribution is given by

$$P_{\,|m\rangle}\,(\alpha,\alpha^*) = \frac{\partial^{2m}}{\partial_\alpha^m\, \partial_{\alpha^*}^m}\, \delta^2(\alpha), \tag{1.4}$$

where $\delta^2(\alpha)$ is the delta function $\delta(\mathrm{Re}\ \alpha)\ \delta(\mathrm{Im}\ \alpha)$. Clearly, the P distribution being given by higher derivatives of the delta function is more singular than the delta function. Another simple example is that of the squeezed vacuum sate $\left|\psi_{\mathrm{sv}}\right\rangle = S(r)\ |0\rangle$, $S(r) = \exp\,[\frac{r}{2}(a^{\dagger 2} - a^2)]$. The uncertainty in the quadrature operator $X = \frac{1}{i\sqrt{2}}(a - a^\dagger)$, $V(X) = \Delta X = \langle X^2\rangle - \langle X\rangle^2$ in the state $\left|\psi_{\mathrm{sv}}\right\rangle$ is given by $\Delta X = \frac{1}{2}\, e^{-2r}$, whereas in the vacuum state $|0\rangle$, $\Delta X = \frac{1}{2}$. More generally, a squeezed state is defined as one of which $\Delta X_\phi < \frac{1}{2}$ where ΔX_ϕ is the quadrature variable $\Delta X_\phi = \frac{1}{\sqrt{2}}\,(ae^{i\phi} + a^\dagger e^{-i\phi})$. The condition that in any state ρ, $\Delta X_\phi < \frac{1}{2}$, when expressed in terms of the P distribution leads to the condition $P < 0$ [10]. Thus, the photon number state and a squeezed state are examples of nonclassical states.

In general, a classical state [36] can becomes nonclassical under operations such as *photon excitation* [37], *quadrature squeezing* [38], *amplitude squeezing* [39] *etc.*

1.2.1 Signatures of Nonclassicality

It is not always possible to evaluate P distribution for a given state to check it it is a true probability distribution or not to determine if ρ is nonclassical or not. Hence one would like to detect the nonclassical character of the single mode quantum states of light by checking if some inequalities involving lower order moments of the mode operators are violated or not. To this end one defines NC of states in terms of attributes such as sub-Poissonian photon statistics, quadrature squeezing *etc.* It is well-known that a coherent state $|\alpha\rangle$ has a Poissonian photon number distribution, $P_{|\alpha\rangle}(n) = e^{-|\alpha|^2} \sum_n \frac{(|\alpha|^2)^n}{n!}$ with variance in photon number $\langle(\Delta N)^2\rangle$ being equal to the mean photon number $\langle N\rangle$, where $N = a^\dagger a$ is the photon number operator. If for any state ρ, $\langle(\Delta N)^2\rangle$ becomes less than $\langle N\rangle$, the corresponding photon number distribution $P(n)$ becomes sub-Poisson and the state is said to possess sub-Poissonian character. This is characterized in terms of the Mandel Q parameter given by

$$Q = \frac{\langle(\Delta N)^2\rangle}{\langle N\rangle} - 1 = \frac{\langle N^2\rangle - \langle N\rangle^2}{\langle N\rangle} - 1. \tag{1.5}$$

Note that Q being negative indicates that the photon number distribution is sub-Poissonian. More negative Q is more sub-Poissonian the state is. In the case of the photon number state $|m\rangle$, Q is identically equal to -1, since $\langle(\Delta N)^2\rangle$ is zero. Hence the NC of the photon number state $|m\rangle$ is detected by its sub-Poissonian character. As we have already noted in the previous subsection, if a state ρ is squeezed the P distribution is not a true probability distribution and hence is nonclassical. Thus, squeezing is another signature of NC.

However, in general, NC of quantum optical states may show several signatures, such as *sub-Poissonian statistics* [40], *oscillatory number distribution* [41], *nonclassical relation between moments of the photon number operator* [42] *etc.* A comprehensive review on the nonclassical states of light is given in [43–45].

1.2.2 Measures of Nonclassicality

Let's first consider the cases of $|m\rangle$ and $|\psi_{\rm sv}\rangle$. In the case of $|m\rangle$, with increase in m, P distribution becomes more singular than the delta function (Eq. 1.4). As a consequence, one might consider the value of m as a measure of the nonclassical character of $|m\rangle$. On the other hand, in the case of $|\psi_{\rm sv}\rangle$, as we have noted before $V(X) = \frac{1}{2}e^{-2r} \leq \frac{1}{2}$ (i.e., $r \geq 0$) implies $P(\alpha) < 0$ and hence the state $|\psi_{\rm sv}\rangle$ is nonclassical. In fact as r increases $P(\alpha)$ becomes more negative and hence more nonclassical the state becomes. Hence r can be taken to be a measure of NC of the state $|\psi_{\rm sv}\rangle$.

However, in case of quantum optical states, in general, one requires a measure of NC

that doesn't refer explicitly to state parameters. There have been several proposals for the quantification of NC of single mode quantum states of light [46–52]. While some of them are defined in terms of the distance from the nearest classical states [46,47] in Hilbert space, others are described in terms of certain properties of the associated phase-space distributions [48–50]. Measure of NC have been proposed also in terms of negativity in normal ordered operators [51] as well as quantum superpositions [52]. We shall describe a few commonly used measures in the following.

A. Trace Norm Distance from Nearest Classical State

Trace norm of an operator A is defined as $\|A\|_1 = \mathrm{Tr}\,[|A|] = \mathrm{Tr}\,[\sqrt{A^\dagger A}]$, i.e., the sum of the singular values of A. In terms of the trace norm, NC of any quantum state of light ρ is defined as [46],

$$\delta(\rho) = \inf_{\sigma} \|\rho - \sigma\|_1, \tag{1.6}$$

where the infimum is taken over the set of all classical states σ. It is worth noting that for all pure states of light, $\rho = |\psi\rangle\langle\psi|$, the minimal trace norm distance from the classical state is independent of the choice of classical reference state and is given by

$$\delta(|\psi\rangle) \geq [1 - \sup_{\beta} Q_{|\psi\rangle}(\beta, \beta^*)]. \tag{1.7}$$

where $Q_{|\psi\rangle}(\beta, \beta^*)$ is the Husimi-Kano Q distribution of $|\psi\rangle$. However, in the case of mixed states, it depends on the choice of reference state and thus one has to minimize over the set of all classical states. Note that in the case of $|m\rangle$ as well as $|\psi_{\mathrm{sv}}\rangle$, nonclassical distance increases with both number of photon addition (m) as well as squeezing strength (r) [46].

B. Hilbert-Schmidt Distance from Nearest Classical State

Similar to the trace norm distance NC (Eq. 1.6), this measure is defined as the Hilbert-Schmidt distance of a given density operator ρ from the nearest classical state [47] as,

$$d_{\mathrm{NC}}(\rho) = \inf_{\sigma} \sqrt{\mathrm{Tr}\,[(\rho - \sigma)^2]}, \tag{1.8}$$

where the infimum is taken over set of all classical states σ. Again as in the case of trace norm distance, it can be shown that the minimal Hilbert-Schmidt distance based NC of a nonclassical pure state, $\rho = |\psi\rangle\langle\psi|$, is independent of the choice of classical reference and is given by

$$d_{\mathrm{NC}}(|\psi\rangle) = \inf_{\beta} \sqrt{2}\,[1 - |\langle\beta|\psi\rangle|^2]^{1/2} = \sqrt{2}\,[1 - \sup_{\beta} Q_{|\psi\rangle}(\beta, \beta^*)]^{1/2}, \tag{1.9}$$

where, $Q_{|\psi\rangle}(\beta,\beta^*)$ is the Husimi-Kano Q distribution of $|\psi\rangle$. It may be noted that, in general, the trace norm and Hilbert-Schmidt norm are the special cases of Schatten p norm defined as,

$$\|A\|_p = (\mathrm{Tr}\ [|\mathrm{A}|^{\mathrm{p}}])^{1/\mathrm{p}}, \tag{1.10}$$

where, $p = 1$ and 2 corresponds to trace norm and Hilbert-Schmidt norm respectively.

C. Nonclassical Depth

As we have mentioned earlier nonclassical states of light are defined as those for which The associated P distribution is not a true probability distribution. On the other hand, the Husimi-Kano Q distribution associated with any state is a well-defined positive semi-definite regular distribution. The Q distribution is related to the P distribution by a Gaussian convolution,

$$Q(z,z^*) \ = \ \int \frac{d^2\omega}{\pi}\ e^{\ -\ |z-\omega|^2}\ P(\omega,\omega^*). \tag{1.11}$$

The Kernel of the convolution, $e^{\ -\ |z-\omega|^2}$, is the Wigner distribution corresponding to the vacuum state. In the spirit of the transformation in Eq. (1.11), one can, in general, define an η convoluted P distribution as

$$R(z,\eta) \ = \ \frac{1}{\eta}\ \int \frac{d^2\omega}{\pi}\ e^{-\frac{|z-\omega|^2}{\eta}}\ P(\omega,\omega^*), \tag{1.12}$$

where η is bounded above by unity as $0 \leq \eta < 1$. Accordingly, one can define as measure of NC of any optical state ρ, as the minimum value of η needed to make $R(z,\eta)$ a positive semidefinite regular function [48]. This minimum value η_{min}, is said to be the nonclassical depth of ρ. This depth can be interpreted as the minimal smoothing needed to wash out the negativity (and singularity) of Glauber-Sudarshan P distribution.

However, in the case of pure states with non-Gaussian Wigner distribution, for any $0 \leq \eta < 1$, the positive semi-definiteness of $R(z,\eta)$ can't be ensured. In such cases, the nonclassical depth is taken to be unity [48] as in that case, i.e. with $\eta = 1$ one retrieves Q distribution which a well-behaved distribution. Thus, the concept of nonclassical depth can't be applied to the non-Gaussian pure states as it declares all non-Gaussian pure states as being equally nonclassical [53].

D. Wigner Negativity

It is well known that the Wigner distribution $W_\rho(z,z^*)$ of any state of light ρ, being negative in phase space indicates that the state ρ is nonclassical. Hence it has been proposed that the phase space integral of the negative part of the Wigner function, called the Wigner

negativity, defined by

$$\delta_{\rm w} \;=\; \frac{\int \frac{d^2z}{\pi}\,|W_\rho(z,z^*)| \;-\; 1}{2}, \tag{1.13}$$

may be regarded as a measure of NC [49]. A larger $\delta_{\rm w}$ implies that the Wigner distribution spans a larger volume in phase space and hence state is more nonclassical. For example, in the case of photon number state $|m\rangle$, $\delta_{\rm w}$ increases monotonically with increase in the photon number m [49]. Clearly, this measure is not applicable to states whose Wigner distribution is Gaussian and hence always positive.

1.3 Gaussian and Non-Gaussian States of Light

Several non-linear optical processes such as second harmonic generation, four wave mixing *etc.* [10] are described by effective Hamiltonian that are quadratic in the mode operators. The states generated under evolution generated by quadratic Hamiltonian are characterized by Gaussian Wigner distribution. Any quantum optical state for which the Wigner distribution is Gaussian is said to be a Gaussian state, otherwise a non-Gaussian state. A well known result is that any single mode Gaussian state ($\rho^{\rm G}$) can be expressed as a displaced squeezed thermal state [54], i.e.,

$$\rho^{\rm G} \;=\; D(\alpha)\,S(\zeta)\,\rho_{\rm th}(\bar{n})\,S^\dagger(\zeta)\,D^\dagger(\alpha), \tag{1.14}$$

where, $\rho_{\rm th}(\bar{n})$ is the thermal states and $\bar{n}$ is the average number of thermal photons. In the special case of $\bar{n}=0$, $\rho^{\rm G}$ in Eq. (1.14) represents a pure Gaussian state that can be expressed as a *displaced squeezed vacuum state*, namely $\big|\psi\rangle \;=\; D(\alpha)\;S(\zeta)\;|0\rangle$. Note that in the case ofHowever, for multimode states, the decomposition in Eq. (1.14) can be very involved.

A Gaussian state is determined entirely by its first and second order moments are non-zero. In other words, all cumulants of a Gaussian state of order $n>2$ are zero. In general, an n-mode Gaussian state is described in terms of the $2n\times 2n$ real symmetric matrix, known as the variance matrix. A comprehensive review of different forms of the variance matrix and the allowed Gaussian (symplectic) operations is given in [56, 57]. The question of how to detect if a given single mode state ρ is non-Gaussian has been addressed in the literature. There have been several proposals for detecting the single mode non-Gaussian states of light [58–63]. The question of how to quantify how non-Gaussian a state is, is also an important one. This we shall discuss in the next subsection.

1.3.1 Measures of Non-Gaussianity

To quantify the non-Gaussian character of single mode quantum optical states, several measures are proposed, defined in terms of distance from the corresponding Gaussian counter-

part, both in Hilbert space and in phase space. The Gaussian counterpart ρ^{g} of any non-Gaussian quantum optical state ρ is defined as the state that has first and second order moments equal to those of ρ itself. These distance measures essentially tell how far the state is from the Gaussian state that resembles most to it. Next, we describe some well-known *distance* measures.

A. Measure Based on Hilbert-Schmidt Distance

This measure of NG is defined as the Hilbert-Schmidt distance of the given non-Gaussian quantum optical state ρ from its Gaussian counterpart ρ^{g} [64]

$$d_{\mathrm{NG}}(\rho) = \frac{\mathrm{Tr}\left[(\rho - \rho^{g})^{2}\right]}{\mathrm{Tr}\left[\rho^{2}\right]}. \tag{1.15}$$

It is worth noting that $d_{\mathrm{NG}}(\rho)$ is neither additive nor multiplicative for product states. As a consequence, in the case of multimode quantum optical states, it can't be considered a good measure of NG.

B. Measure Based on Quantum Relative Entropy

Non-Gaussianity of quantum states of light has also been described in terms of the quantum relative entropy between the given state and its Gaussian counterpart as [65]

$$\delta_{\mathrm{NG}} = S(\rho \parallel \rho^{g}) = -\,\mathrm{Tr}\left[\rho \ln \rho^{g}\right] - \mathrm{S}(\rho), \tag{1.16}$$

where, $S(\rho) = \mathrm{Tr}\left[\rho \ln \rho\right]$ is the von-Neumann entropy of ρ. It is worth pointing out that δ_{NG} is defined only in the case of mixed states of light. In the case of pure states, δ_{NG} depends only on the Gaussian counterpart, not the state since $S(\rho) = 0$. According to this measure all pure states with same Gaussian counterpart, have same amount of NG.

C. Measure Based on Wehrl Entropy

Unlike the Glauber-Sudarshan P distribution and the Wigner distribution W Husimi-Kano distribution associated with the state ρ defined by $Q_{\rho}(z, z^{*}) = \langle z|\rho|z\rangle$, enjoys all the properties of a classical probability distribution, in particular, *point-wise positivity and no more singular than a delta function*. An entropy analogous to the von-Neumann entropy of a quantum state of light is the Wehrl entropy [66] that is defined in terms of the Q distribution of ρ as $H_{\mathrm{w}}(\rho) = -\int \frac{d^{2}z}{\pi}\, Q_{\rho}(z) \ln Q_{\rho}(z)$. Ivan *et. al.* [67] have defined a measure of NG of a state ρ in terms of its Wehrl entropy as

$$\mathcal{N}_{\mathrm{G}}(\rho) = H_{\mathrm{w}}\left(\rho \parallel \rho^{g}\right) = H_{\mathrm{w}}(\rho^{g}) - H_{\mathrm{w}}(\rho). \tag{1.17}$$

The quantity $\mathcal{N}_{\rm G}(\rho)$ could be considered as the Kullback-Leibler distance between the classical like Q distributions corresponding to ρ and its Gaussian counterpart $\rho^{\rm g}$. Unlike the quantifications based on Hilbert-Schmidt distance [64] and quantum relative entropy [65], the measure of NG based on Wehrl entropy [67] enjoys several important properties such as *additivity*, *covariance under uniform phase-space scaling etc.*

1.4 Entangled States of Light

1.4.1 Entangled States

A pure state of a bipartite quantum system $\left|\psi_{AB}\right\rangle$ termed separable if it cant be written as a product of states $\left|\psi_A\right\rangle$ and $\left|\psi_B\right\rangle$ corresponding to the individual subsystems, i.e.,

$$\left|\psi_{AB}\right\rangle \;=\; \left|\psi_A\right\rangle \otimes \left|\psi_B\right\rangle. \tag{1.18}$$

The state $\left|\psi_{AB}\right\rangle$ is said to be entangled if it can't be written as in Eq. (1.18). Note that if $\left|\psi_A\right\rangle$ and $\left|\psi_B\right\rangle$ are states in Hilbert spaces of dimension m and n, the bipartite state $\left|\psi_{AB}\right\rangle$ lives in an $m \times n$ dimensional Hilbert space. In the case of mixed states, where states are represented by density operators, the condition for separability generalizes to [68]

$$\rho_{\rm AB} \;=\; \sum_k p_k \; \rho_{\rm A}^k \otimes \rho_{\rm B}^k, \tag{1.19}$$

where, $\rho_i^k \;=\; \left|\psi_i^k\right\rangle\!\left\langle\psi_i^k\right|$ $(i \;=\; A, B)$ is a pure state projection, with $p_k \;\geq\; 0$ and $\sum\; p_k \;=\; 1$. A mixed bipartite state that is not separable in the sense of Eq. (1.19) is said to be entangled. Entangled states could be realized in terms of several physical systems such as pair of atomic spins, nuclear spins, optical modes [3] *etc.* Here, we focus on the entanglement generated between the modes of a quantized electromagnetic field. As a simple example of entangled pure state of light one can think of the *two-mode squeezed vacuum state* (TMSV) given by,

$$\left|\psi_{\rm tmsv}\right\rangle \;=\; S_{ab}(r)\;|0,0\rangle \;=\; \frac{1}{\cosh r}\;\sum_{k=0}^{\infty}(\tanh r)^k\;|k,k\rangle, \tag{1.20}$$

where $S_{ab}(r) \;=\; \exp\left[r(a^\dagger b^\dagger \;-\; ab)\right]$. The TMSV can't be written as a product of the states of the individual modes and hence it is entangled. Bipartite quantum optical states of which TMSV is an example, are called continuous variable states.

1.4.2 Detection of Entanglement

A criterion for separability of a bipartite state was first proposed by A. Peres [69] in terms of the positivity of the bipartite state under the partial transposition operation. However, soon after his proposal, Horodecki *et. al.* proved that the positiveness of the partially transposed

density matrix is a *necessary and sufficient* condition for separability in the case of bipartitte states in 2×2 or 2×3 dimensions [70]. In the case of bipartite states in higher dimensional Hilbert space negativity under partial transposition is a sufficient criterion only.

Separability conditions for bipartite continuous variable states were formulated independently by Duan *et. al.* [71] and R. Simon [72]. While Duan criterion is based on canonical uncertainty relation between non-commuting observables, Simon's condition is an extension of Peres-Horodecki condition to continuous variable systems. In the case of non-Gaussian states, stronger separability criteria were proposed by Schchukin and Vogel [73] and Miranowicz and Plenio [74] that includes the condition of positive partial transposition as a special case.

1.4.3 Quantification/Measure (s) of Entanglement

In the case of pure bipartite states $|\psi_{\rm AB}\rangle$, entanglement is easily computed in terms of the *entropy of entanglement* [75]. It is defined as the von-Neumann entropy of the reduced state given as

$$E(|\psi_{\rm AB}\rangle) \;=\; S(\rho^{\rm r}) \;=\; -\,{\rm Tr}\,[\rho^{\rm r}\,\ln\,\rho^{\rm r}], \tag{1.21}$$

where the reduced state $\rho^{\rm r}$ is obtained by tracing over any of the subsystems ($\rho^{\rm r} \;=\; {\rm Tr}_{\rm A}[|\psi_{\rm AB}\rangle\langle\psi_{\rm AB}|] \;=\; {\rm Tr}_{\rm B}[|\psi_{\rm AB}\rangle\langle\psi_{\rm AB}|]]$). This measure of entanglement is valid for finite dimensional as well as continuous variable systems.

On the other hand, in the case of bipartite mixed entangled states, the notion of entropy of entanglement is generalized to the *entanglement of formation* (EOF) [76] which is defined as the *minimal amount of pure state entanglement required* to reproduce the concerned state. For a mixed entangled state $\rho_{\rm AB}$ is defined as

$$EOF(\rho_{\rm AB}) \;=\; \inf_{\{p_k,|\psi_k\rangle\langle\psi_k|\}} \sum_k p_k\, E(\psi_k), \tag{1.22}$$

where the infimum is taken over all possible pure state ensemble $\{p_k, \left|\psi_k\right\rangle\left\langle\psi_k\right|\}$ and $E(\psi_k)$ is the entropy of entanglement for $\left|\psi_k\right\rangle$. As is evident from the definition of EOF (Eq. 1.22), for a pure state $\rho_{\rm AB} \;=\; \left|\psi_{\rm AB}\right\rangle\left\langle\psi_{\rm AB}\right|$, EOF converges to the entropy of entanglement (Eq. 1.21). Unlike in the case of pure states, in the case of mixed entangled states of light an explicit formula for EOF could be given only in the case of symmetric Gaussian states [77]. We shall have occasion to put to use such a formula for EOF of two-mode symmetric Gaussian state in Chap. 5.

In the case of two-mode non-Gaussian entangled states of light there have been several proposals for quantification of entnaglement such as *logarithmic negativity* [78], *Einstein-*

Podolsky-Rosen correlation [71], *Hillery-Zubairy correlation* [79] *etc.* However, finding a computable measure of entanglement for the non-Gaussian entangled states of light has yet not been settled. In this cnnection it is worth mentioning that the axiomatic theory of entanglement measures was first formulated by Vedral and co-workers [80]. Later, a more mathematical description was provided by G. Vidal [81] in terms of *entanglement monotones*. Logarithmic negativity is an example of an entanglement monotone. A comprehensive review on measures of entanglement is given in [4, 82].

1.5 Quantum Teleportation with Optical Resources: Braunstein-Kimble Protocol

This protocol for quantum teleportation (QT), where two parties [say Alice and Bob] can send an unknown quantum state to each other by sharing an entangled pair of state and using classical communication, was first given by Bennett *et. al.* [83] in the case of qubits. Later, an experimentally realizable extension of this protocol to quantum optical systems was given by Braunstein and Kimble [84]. Quantum teleportation with entangled optical resources, implementing the Braunstein- Kimble (BK) protocol, has also been experimentally realized [85–89]. A detailed review on the recent advances in teleportation with optical resources has been given in [90].

1.5.1 Schematic of Braunstein-Kimble Protocol for Continuous Variable Teleportation

The BK protocol for QT using entangled states of light is schematically described in the Fig. 1.1. First an entangled EPR pair is sent to two parties, say Alice and Bob. Alice then sends her state and an unknown quantum state of light through a homodyne mixer. Subsequently, Alice makes joint *bell-type measurements* on the quadrature variables corresponding to her state and the unknown state via balanced beam splitters. After the measurement, Alice communicates her results to Bob over a classical channel (say telephone). Depending upon the particular outcome that Alice has obtained, Bob performs appropriate (as specified in the protocol) operations (for example displacement) on his state and eventually retrieves the unknown input state.

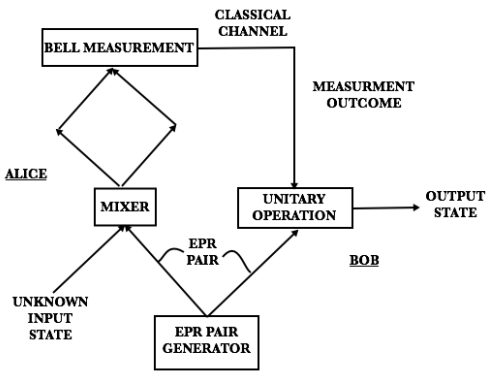

Figure 1.1: Schematic of BK Protocol.

Chapter 2

Beam Splitter Generated Entanglement from Quantum States with Multiple Nonclassicality Inducing Operations

It is well-known that two mode entangled states can be generated at the output of a linear device like beam splitter (BS) provided atleast one of the two input ports is fed with nonclassical state of light [13–17]. The simplest examples of nonclassical states of light are the photon number state $|m\rangle$ and the quadrature squeezed state $\left|\psi_{\rm sv}\right\rangle = S(r)\,|0\rangle$. Slightly more general examples of nonclassical states are $\rho_m = {\rm N_m\ a^{\dagger m}\ \rho_{cl}\ a^m}$ and $\rho_{\rm sq} = S(r)\,\rho_{\rm cl}\,S^\dagger(r)$, where $\rm N_m$ is the normalization constant and $\rho_{\rm cl}$ is any *classical state*. Evidently, the photon excitation ($a^{\dagger m}$) and squeezing operations ($S(r)$) are *nonclassicality (NC) inducing operations*, as the states ρ_m and $\rho_{\rm sq}$ considered above are nonclassical. Quantitative studies on BS generated entanglement with nonclassical input states are known to exhibit a monotonic dependence of BS output entanglement on input NC, in the case of the states $|m\rangle$ and $\left|\psi_{\rm sv}\right\rangle$ [13, 14, 17].

The purpose of the chapter is to carry out similar quantitative studies on more general input nonclassical states and investigate the dependence of BS output entanglement on input NC. In particular, we have focussed on the class of nonclassical states that are generated under *multiple NC-inducing operations* (MNIO), as discussed in the introduction. The particular states that we have considered in this context are the squeezed number state (SNS) [21] and photon added squeezed vacuum state (PAS) [22], which as mentioned earlier are generated under two NC-inducing operations, viz., squeezing and photon addition, in two different orders. After briefly reviewing the BS generated entanglement with input number state

and squeezed vacuum states, i.e., states generated under *single* NC-inducing operations, we analyze the dependence of BS output entanglement on relevant state parameters in the case of MNIO class of states.

Contrary to the cases with input states having single NC-inducing operations, in the case of MNIO states, in particular in the case of PAS, we observe that the BS generated entanglement is a *non-monotonic* function of the input state parameters, viz. the number of photon addition (m) and the squeeze parameter (r). To understand this non-monotonic behavior we further analyze certain well known measures of input NC such as nonclassical depth [48], Wigner negativity [49] and Hilbert-Schmidt distance from nearest classical state [47]. Our numerical results indicate that these measures of NC exhibit behavior that is not consistent with BS output entanglement curves in the case of PAS and hence fail to account for the non-monotonicity.

Finally, *we explain this monotonic dependence* of the BS generated entanglement for input PAS in terms of the *mutual competition between the NC-inducing operations*, namely photon addition and quadrature squeezing, as manifest in the contours of the Husimi-Kano Q distribution associated with these states. We find that while the relative competition is insignificant in the case of SNS and hence leads to the monotonic dependence of BS output entanglement upon m and r, this competition in the case of PAS is quite significant. This is our view is what renders the BS output entanglement curves non-monotonic.

2.1 Generation of Entanglement by a BS from Nonclassical Input States

A passive BS can be realized in terms of a silvered mirror for which the total photon count (intensity for classical E.M. field) at the input remains conserved at the output. In this thesis, we consider only passive 50 : 50 BS which reflects half of the incident beam and transmits the rest. A passive 50 : 50 BS is mathematically described by the transmission matrix, i.e., the matrix relating the input and the output mode operators,

$$\begin{pmatrix} a_{\text{out}} \\ b_{\text{out}} \end{pmatrix} = \begin{pmatrix} 1/\sqrt{2} & 1/\sqrt{2} \\ -1/\sqrt{2} & 1/\sqrt{2} \end{pmatrix} \begin{pmatrix} a_{\text{in}} \\ b_{\text{in}} \end{pmatrix} \tag{2.1}$$

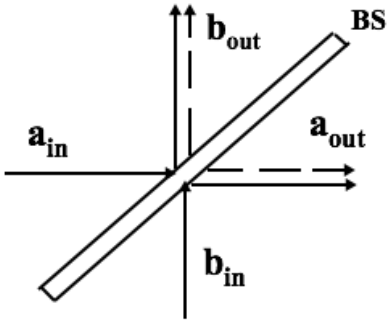

Figure 2.1: Schematic of a Beam Splitter.

In the Fig. 2.1, we show the basic schematic of a BS. It is well known that, if one of the input ports of a passive BS is fed with a nonclassical state of light while the other input port is left with vacuum, output state will necessarily be entangled [13–15]. In the above mentioned

setting, input single mode NC is *not only necessary but also sufficient* to yield entanglement at the output [16]. On the other hand, if the input state is classical, output state is separable [17].

2.2 BS Generated Entanglement from Input Number State and Squeezed Vacuum State

To set the stage for the analysis in the case of the MNIO class of nonclassical states, we briefly review, in this section, the BS generated entanglement for input single mode nonclassical states of light, generated under single NC-inducing operations, fed at one of the input ports while the other port is left with vacuum. We consider, in particular, photon number state, $|m\rangle$, and quadrature squeezed vacuum state, $S(r)|0\rangle$. The entanglement of the BS output states (which are in our case are pure states) is measured in terms of von-Neumann entropy of the reduced state since it is a pure state. We denote the BS output entanglement with the input state $|\psi\rangle$ by $E_{\rm BS}(|\psi\rangle)$.

For input single mode photon number state $|m\rangle$, the BS output state becomes,

$$|m\rangle \xrightarrow{\rm BS} \frac{1}{2^{m/2}} \sum_{k=0}^{m} \binom{m}{k}^{1/2} |m-k,k\rangle \tag{2.2}$$

with entanglement given by

$$E_{\rm BS}(|m\rangle) = -\sum_{k=0}^{m} \frac{1}{2^m} \binom{m}{k} \ln\Big[\frac{1}{2^m}\binom{m}{k}\Big]. \tag{2.3}$$

Since a passive BS doesn't change the Gaussian character of the input states at the output, we can analytically evaluate, by first computing the variance matrix of the reduced output state, the BS generated entanglement in the case of input squeezed vacuum state as,

$$E_{\rm BS}(|\psi_{\rm sv}\rangle) = \frac{e^{\frac{r}{2}}+1}{2} \ln\Big[\frac{e^{\frac{r}{2}}+1}{2}\Big] - \frac{e^{\frac{r}{2}}-1}{2} \ln\Big[\frac{e^{\frac{r}{2}}-1}{2}\Big]. \tag{2.4}$$

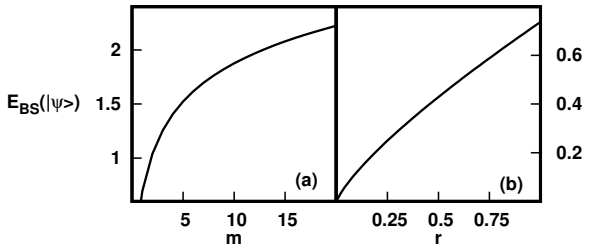

Figure 2.2: Dependence of $E_{\rm BS}$ for input **(a)** $|m\rangle$ and **(b)** $|\psi_{\rm sv}\rangle$.

In Fig. 2.2, we plot the BS generated entanglement in the case of input number state and squeezed vacuum state. In the case of number state [Fig. 2.2(a)], $E_{\rm BS}(|m\rangle)$ monotonically increases with increase in m. On the other hand, it can be analytically shown that $E_{\rm BS}(|\psi_{\rm sv}\rangle)$

given by Eq. (2.4) is a monotonically increasing function of r since the slope

$$\frac{\partial}{\partial r} E_{\rm BS}(|\psi_{\rm sv}\rangle) = -\frac{e^{\frac{r}{2}}}{4} \ln\left[\frac{1 - e^{\frac{-r}{2}}}{1 + e^{\frac{-r}{2}}}\right] \tag{2.5}$$

is always strictly positive for all $r > 0$.

2.3 States Generated Under MNIO

In this section we give a description of states generated under MNIO, in particular under photon addition/subtraction and quadrature squeezing operations acting on the vacuum in different orders. We then bring out some interesting properties of these states that will be relevant for later discussions. The *MNIO class* of states that we would like to focus on in this thesis are mathematically represented as

$$\left|\psi_{\rm pas}\right\rangle = \frac{1}{\sqrt{\mathrm{N}^{\rm m}_{\rm pas}}}\, a^{\dagger m}\, S(r)\, |0\rangle, \tag{2.6a}$$

$$\left|\psi_{\rm pss}\right\rangle = \frac{1}{\sqrt{\mathrm{N}^{\rm m}_{\rm pss}}}\, a^{m}\, S(r)\, |0\rangle, \tag{2.6b}$$

$$\left|\psi_{\rm sns}\right\rangle = S(r)\, |m\rangle = S(r)\, \frac{a^{\dagger m}}{\sqrt{m!}}\, |0\rangle, \tag{2.6c}$$

where the normalization constants $\mathrm{N}^{\rm m}_{\rm pas}$ and $\mathrm{N}^{\rm m}_{\rm pss}$ are defined given by $\mathrm{N}^{\rm m}_{\rm pas} = \mathrm{m}!\mu^{\rm m}\mathrm{P}_{\rm m}(\mu)$, $\mathrm{N}^{\rm m}_{\rm pss} = \mathrm{m}!\nu^{2\rm m}\sum_{\rm k=0}^{\rm m}\frac{\mathrm{m}!}{(\mathrm{m}-\mathrm{k})!\mathrm{k}!}\,(\frac{-\mu}{2\nu})^k\frac{H_k^2(0)}{k!}$, $\mu = \cosh r$ and $\nu = \sinh r$. Here $P_n(x)$ and $H_n(x)$ are respectively $n^{\rm th}$ order Legendre and Hermite polynomials.

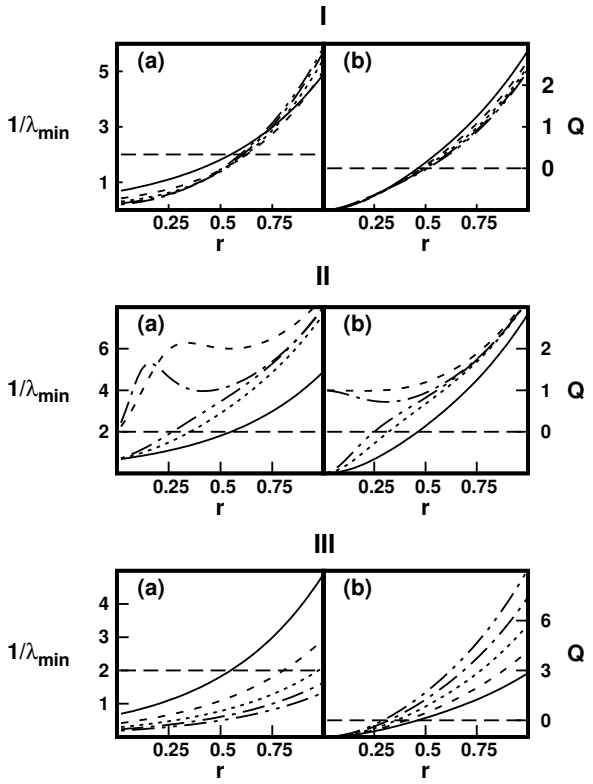

Figure 2.3: Dependence of **(a)** $1/\lambda_{\rm min}$ and **(b)** Q on r for PAS (**I**), PSS (**II**) and SNS (**III**). Different curves correspond to $m = 1$ (solid line), 2 (dashed line), 3 (dotted line), 4 (dash-dotted line) and 5 (dash-double-dotted line). Horizontal long dashed lines correspond to the values 2 in **(a)** and 0 in **(b)**.

As the MNIO class of states listed in Eq. 2.6 are generated under the squeezing and photon addition/subtraction operations, it will be interesting to analyze the nonclassical properties of these states as characterized by **(a)** the amount of squeezing, defined in terms of the minimum eigenvalue of the variance matrix associated with the concerned states and **(b)** the sub-Poissonian character quantified by the Mandel Q parameter. In Fig. 2.3 we plotted $1/\lambda_{\rm min}$ and Mandel Q parameter as a function of r for various values of m in the case of PAS, PSS and SNS. Note that the state is

squeezed when $\lambda_{\min} < \frac{1}{2}$ and exhibits sub-Poissonian statistics when $Q < 0$ (by definition Q is bounded from below by -1). Note that in the case of PSSs with even m ($m = 2, 4$ in Fig. 2.3), the states don't exhibit sub-Poissonian character for any values r.

It is instructive, in the present context, to characterize nonclassical states as follows:

(i) squeezed ($\lambda_{\min} < \frac{1}{2}$) but not exhibiting sub-Poissonian character ($Q < 0$),

(ii) exhibiting sub-Poissonian character ($Q < 0$) but not squeezed ($\lambda_{\min} < \frac{1}{2}$),

(iii) neither exhibiting sub-Poissonian character ($Q < 0$) nor squeezed ($\lambda_{\min} < \frac{1}{2}$) and

(iv) both exhibiting sub-Poissonian character ($Q < 0$) and squeezed ($\lambda_{\min} < \frac{1}{2}$).

Note that nontrivial examples of already known nonclassical states with property (i) are the Kerr states [38, 39] while those with property (ii) are the photon added coherent state studied in [37]. The nonclassical states with the property (iii) were first studied by Agarwal and Tara [91] and their NC was characterized in terms of violation of inequalities involving higher-order moments of the number operator. We would like to study the nonclassical properties of the MNIO class of states in the light of the above characterization.

A careful reading of Fig. 2.3 suggests that there are region of the parameter r where the states PAS, PSS and SNS are either squeezed only (property (i)) or exhibit sub-Poissonian character only (property (ii)). However, to make these results more manifest, we find it convenient to define *witnesses* $d_{\rm sq}$ and $d_{\rm sp}$ associated with the squeezing character ($\lambda_{\min} < \frac{1}{2}$) and the sub-Poissonian character ($Q < 0$) as follows

$$d_{\rm sq} \;=\; \min\{0,\; 2\lambda_{\min} \;-\; 1\}, \quad d_{\rm sp} \;=\; \min\{0,\; Q\}. \tag{2.7}$$

Note that both $d_{\rm sq}$ and $d_{\rm sp}$ are defined in the range $[-1, 0]$. In fact $d_{\rm sq} \;=\; 0$ implies that the state is squeezed and $d_{\rm sp} \;=\; 0$ implies that the state doesn't exhibit sub-Poissonian character. We have replotted in Fig. 2.4 the results that we have already shown in Fig. 2.3, in terms of the witnesses $d_{\rm sq}$ and $d_{\rm sp}$ for $m = 1$ and 3 including $m = 5$.

Let's focus on the $m = 1$ plots first. The $d_{\rm sp}$ (dashed line) and $d_{\rm sq}$ (solid line) curves fall in non-overlapping regions of the squeezing parameter r. For small values of r, the photon addition/subtraction operations completely contributes to the NC of these states, whereas for large r (beyond a certain critical value of r that is dependent on the state) the squeezing operation is what completely contributes and hence does not exhibit any sub-Poissonian character at all. Hence these states have properties (i) and (ii) in two different

non-overlapping parameter regions. However, as is evident from Fig. 2.4, there is an intermediate region where both $d_{\rm sq}$ and $d_{\rm sp}$ are zero, hence the NC of these states, in this region, is characterized by the property (iii), i.e., they exhibit neither squeezing nor sub-Poissonian character.

Let's next focus on the $m = 3$ and $m = 5$ plots. Qualitatively the behavior is as in the case of $m = 1$. However, there are some quantitative differences. In the case of PAS, the regions of r where $d_{\rm sq} = 0$ and $d_{\rm sp} = 0$ has becomes *wider* in comparison to the $m = 1$ case. In the case of SNS, this widening is even more prominent. It turns out that this trend persists as m increases. Hence, we can conclude that, in general, PAS and SNS are characterized by the NC obeying properties (i), (ii) and (iii) in different regions of r. On the other hand, in the case of PSS, the region where $d_{\rm sq} = 0$ and $d_{\rm sp} = 0$ is much *narrower* compared to that in $m = 1$ case. Hence, we expect that for larger values of m (> 5), the curves for $d_{\rm sq}$ and $d_{\rm sp}$ will cross each other and a region of r will appear where both $d_{\rm sq}$ and $d_{\rm sp}$ will be non-zero. In this region, the NC of PSS will be characterized by the property (iv).

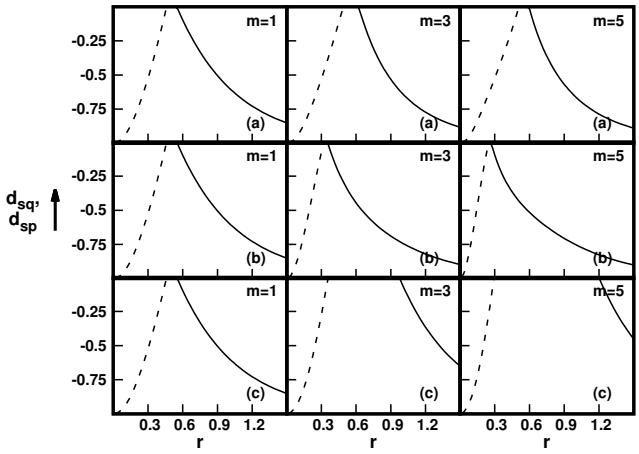

Figure 2.4: Plot of $d_{\rm sq}$ (solid line) and $d_{\rm sp}$ (dashed line) vs r for $m = 1$, $m = 3$ and $m = 5$ in the cases of **(a)** PAS, **(b)** PSS and **(c)** SNS.

Thus, we have found that the MNIO class of states provide examples of nonclassical states whose NC is characterized by the sets of properties **(a)** (i), (ii) and (iii) or **(b)** (i), (ii) and (iv), in different parameter regions of r, for given values of m. In fact the figures in Fig. 2.4 could be looked upon as an *NC phase diagram* since they depict the parameter regions in which only one of the nonclassical characters, viz., squeezing, sub-Poissonian character or higher-order NC is present. These regions are like the *NC phases*. The region where $d_{\rm sq} < 0$ and $d_{\rm sp} < 0$ in the case of PSS for $m > 5$ is like the *coexistence* region.

2.4 BS Generated Entanglement from PAS and SNS

In this Sec. we discuss generation of entanglement by a passive 50 : 50 BS with MNIO class of states (as discussed in Sec. 2.3) at one of the input ports while the other port is left in the vacuum state. For simplicity we deal with only PAS and SNS in this section. We investigate the question of the dependence of BS output entanglement on input NC when either SNS or

PAS is input at one of the ports of the BS.

Using Eq. 2.2 we get the BS output states for input SNS and PAS as,

$$|\psi_{\rm pas}\rangle \xrightarrow{\rm BS} \frac{1}{\sqrt{{\rm N}^{\rm m}_{\rm pas}}} \sum_{k=0}^{\infty} \frac{\sqrt{(2k+m)!}}{k!} \left(\frac{\tau}{2}\right)^k \frac{1}{2^{k+\frac{m}{2}}} \sum_{p=0}^{2k+m} \binom{2k+m}{p}^{1/2} |2k+m-p, p\rangle \text{ and} \tag{2.8a}$$

$$|\psi_{\rm sns}\rangle \xrightarrow{\rm BS} \sum_{n=0}^{m} C_m^n \frac{1}{2^{n/2}} \sum_{p=0}^{n} \binom{n}{p}^{1/2} |n-p, p\rangle, \tag{2.8b}$$

where, $\binom{A}{B}$ denotes the binomial coefficient and the coefficients C_m^n are as given in [21, 92]

We measure the entanglement of the BS output state by its local von-Neumann entropy (Eq. 1.21). In Fig. 2.5 we have plotted the BS generated entanglement for the input PAS and SNS, i.e., $E_{\rm BS}(\left|\psi_{\rm pas}\right\rangle)$ and $E_{\rm BS}(\left|\psi_{\rm sns}\right\rangle)$ respectively. It is clear from Fig. 2.5(a) that $E_{\rm BS}(\left|\psi_{\rm pas}\right\rangle)$ (except in the case of $m = 1$) shows a *non-monotonic* dependence on both r and m. For all values of m (≥ 2), $E_{\rm BS}(\left|\psi_{\rm sns}\right\rangle)$ first decreases and then increases with increase in r. For sufficiently large r ($\gtrsim 0.60$) in fact $E_{\rm BS}(\left|\psi_{\rm pas}\right\rangle)$ depends predominantly on r. Further, it can be seen from Fig. 2.5(a) that $E_{\rm BS}(\left|\psi_{\rm pas}\right\rangle)$ curve depends nonmonotonically on r for various values of m; $E_{\rm BS}(\left|\psi_{\rm pas}\right\rangle)$ for larger values of m, in fact, is less than that for smaller values of m, beyond $r \sim 0.60$.

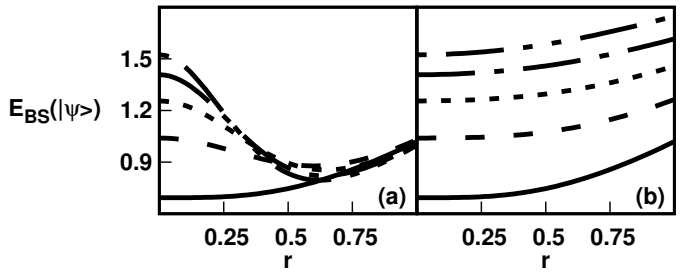

Figure 2.5: Plot of $E_{\rm BS}(\left|\psi\right\rangle)$ for **(a)** PAS and **(b)** SNS vs r for $m = 1$ (solid line), 2 (dashed line), 3 (dotted line), 4 (dash-dotted line) and 5 (dash-double-dotted line).

In contrast, for SNS, $E_{\rm BS}(\left|\psi_{\rm sns}\right\rangle)$ [Fig. 2.5(b)] increases monotonically with both r and m. This monotonic dependence is quite similar to what one has either $S(r)|0\rangle$ or $|m\rangle$ as input at the BS, as discussed in Sec. 2.2.

From a comparison of the results in the cases of SNS and PASVS, it is evident that the dependence of BS output entanglement, $E_{\rm BS}^{|\psi\rangle}$, on r and m depends critically on the order in which the squeezing, $S(r)$, and photon addition, $a^{\dagger m}$, operations act on the initial vacuum state. This nonmonotonic dependence in the case of PAS is, indeed, counterintuitive, given that the BS input states, generated under single NC-inducing operation, lead to monotonically increasing BS output entanglement, as observed in the previous section.

It is noteworthy that in the case of $m = 1$, entanglement curves for $\left|\psi_{\rm pas}\right\rangle$ and $\left|\psi_{\rm sns}\right\rangle$ are identical. This feature can be understood from the following argument. For $m = 1$, using

the properties of the squeezing operator one can show that

$$\begin{aligned}\left|\psi_{\text{pas}}\right\rangle &= \frac{a^\dagger\, S(r)\,|0\rangle}{\mu} = \frac{S(r)\,(\mu a^\dagger + \nu a)\,|0\rangle}{\mu} \\ &= S(r)\,a^\dagger|0\rangle = S(r)\,|1\rangle,\end{aligned} \tag{2.9}$$

where $\mu = \cosh(r)$ and $\nu = \sinh(r)$. Thus we see that for $m = 1$, $|\psi_{\text{pas}}\rangle$ and $|\psi_{\text{sns}}\rangle$ are identical. On the other hand, for $m = 2$, a similar calculation yields

$$\begin{aligned}\left|\psi_{\text{pas}}\right\rangle &= \frac{a^{\dagger 2}\, S(r)\,|0\rangle}{\mu\sqrt{2(3\mu^2-1)}} = \frac{S(r)\,(\mu a^\dagger + \nu a)^2\,|0\rangle}{\mu\sqrt{2(3\mu^2-1)}} \\ &= \frac{S(r)\,(\mu^2 a^{\dagger 2} + \mu\nu(2a^\dagger a + 1))\,|0\rangle}{\mu\sqrt{2(3\mu^2-1)}} \\ &= \frac{1}{\mu\sqrt{2(3\mu^2-1)}}\Big(\mu\sqrt{2}\,S(r)\,|2\rangle + \nu S(r)\,|0\rangle\Big) \\ &\neq S(r)\,|2\rangle\end{aligned} \tag{2.10}$$

Note that here $\left|\psi_{\text{pas}}\right\rangle$ is a superposition of two different squeezed number states, namely, $S(r)\,|2\rangle$ and $S(r)\,|0\rangle$. For higher photon excitation ($m \geq 2$), $\left|\psi_{\text{pas}}\right\rangle$ contains superposition of more SNSs and differs from the particular $S(r)\,|m\rangle$ even more. As a consequence, with an increase in m, $E_{\text{BS}}(\left|\psi_{\text{pas}}\right\rangle)$ differs more from $E_{\text{BS}}(\left|\psi_{\text{sns}}\right\rangle)$ as observed in Fig. 2.5.

2.5 Effective NC of Input PAS and SNS

In a first attempt to resolve the non-monotonic dependence mentioned above, we argue that for states generated under multiple NC-inducing operations, SNS and PASVS in particular, r and m individually may not measure the nonclassicality of these states, but one should perhaps work with an effective measure. Several nonclassicality measures have been proposed in the literature such as the nonclassical depth [48], Wigner negativity [49] and the Hilbert-Schmidt distance [47] from the nearest classical state. In this Sec. we shall investigate if any of these measures faithfully captures the NC of these states, and if they do, working with such effective measure (s) will allow us to understand this nonmonotonic dependence.

2.5.1 Nonclassical Depth

The nonclassical depth is defined as the minimum value of smoothing, η_{min}, needed to make an η convoluted Glauber-Sudarshan P distribution, $R(z,\eta) = \frac{1}{\eta}\int \frac{d^2\omega}{\pi}\, e^{-\frac{|z-\omega|^2}{\eta}}\, P(\omega)$, a positive semidefinite regular function [48]. The function $R(z,\eta)$, for PAS and SNS are given by (Ap-

pendix A)

$$R(z,\eta)_{\text{pas}} = \frac{A_1^m e^{\frac{|z|^2}{1-\eta}} W_0(z,z^*,\eta)}{\mu N_m \sqrt{\eta^2-\tau^2(1-\eta)^2}} \sum_{k=0}^{m} \frac{(-1)^m m!}{k!(m-k)!} \left(\frac{D_1}{A_1}\right)^k L_{m-k}\left(\frac{|B_1|^2}{4A_1}\right), \tag{2.11a}$$

$$R(z,\eta)_{\text{sns}} = \frac{A_2^m e^{\frac{|z|^2}{1-\eta}} W_0(z,z^*,\eta)}{\mu \sqrt{\eta^2-\tau^2(1-\eta)^2}} \sum_{k=0}^{m} \frac{(-1)^{m-k} m!}{k!(m-k)!} \left(\frac{D_2}{A_2}\right)^k L_{m-k}\left(\frac{|B_2|^2}{4A_2}\right), \tag{2.11b}$$

where

$$W_0(z,z^*,\eta) = \exp\left(-\frac{\frac{\eta}{1-\eta}|z|^2 - \frac{\tau}{2}[z^2+z^{*2}]}{\eta^2-\tau^2(1-\eta)^2}\right),\ A_1 = \frac{\tau(1-\eta)^2}{2[\eta^2-\tau^2(1-\eta)^2]},\ A_2 = \frac{A_1}{\mu^2} - \frac{\tau}{2},$$
$$B_1 = \frac{\eta z - \tau(1-\eta)z^*}{\eta^2-\tau^2(1-\eta)^2},\ B_2 = \frac{B_1}{\mu},\ D_1 = \frac{\eta(1-\eta)}{\eta^2-\tau^2(1-\eta)^2},\ D_2 = \frac{D_1}{\mu^2},\ \mu = \cosh r,\ \tau = \tanh r. \tag{2.12}$$

$L_n(x)$ is the n^{th} order Laguerre polynomial. Because of the presence of the Laguerre polynomial in Eq. (2.11a) and Eq. (2.11b), the positiveness of the function $R(z,\eta)$ is not guaranteed for all choices of $\eta < 1$. In such cases, as prescribed in [48], the nonclassical depth has to be taken to be unity. Thus we have a situation where the nonclassical depth for $|\psi_{\text{sns}}\rangle$ is the same as that of $|\psi_{\text{pas}}\rangle$ or a photon number state and hence it is independent of the squeeze parameter r. Clearly, the nonclassical depth fails to be a faithful measure of NC as far as these states are concerned. Further, our conclusion, specifically in the context of these states, is in agreement with the general conclusion that nonclassical depth is always unity for all non-Gaussian pure states [53].

2.5.2 Wigner Negativity

Wigner negativity, δ_{w}, for any quantum state ρ is defined as the phase-space integral of the negative part of the Wigner distribution $W_\rho(z,z^*)$ [49]. It is mathematically defined as (Eq. 1.13)

$$\delta_{\text{w}} = \frac{\int \frac{d^z}{\pi} |W_\rho(z,z^*)| - 1}{2} \tag{2.13}$$

The Wigner distributions for PAS and SNS (Appendix B) are given by,

$$W_{\text{pas}}(\alpha,\alpha^*) = \frac{2(-1)^m m! e^{-2|\beta|^2} \mu^m \nu^m}{2^m N_m} \sum_{k=0}^{m} \frac{m!(\frac{\tau}{2})^{-k}}{k!(m-k)!} L_{m-k}\left(\frac{2|\beta|^2}{\tau}\right), \tag{2.14a}$$

$$W_{\text{sns}}(\alpha,\alpha^*) = (-1)^m e^{-2|\beta|^2} L_m(4|\beta|^2), \tag{2.14b}$$

where $\mu = \cosh r$, $\nu = \sinh r$, $\tau = \tanh r$ and $\beta = \mu\alpha - \nu\alpha^*$.

In Fig. 2.6, the Wigner negativity of PAS is plotted as a function of the squeeze parameter r for various values of the photon addition number m. For all values of m, the

Wigner negativity falls off with increasing r. This can be understood as being due to the photon addition operation for large r. In the case of SNS, however, Wigner negativity is independent of r and hence it is the same as that of the number state $|m\rangle$. The independence of Wigner negativity on r, in the case of SNS, can be easily understood from the following fact. If $W_\rho(x,p)$ is the Wigner function of a given state ρ, then the Wigner function of the state $\rho' = S(\zeta)\rho S^\dagger(\zeta)$ is $W_\rho(x',p')$, where x',p' and x,p are related to each other by a linear canonical transformation. Since the Jacobian of any linear canonical transformation is unity, the Wigner negativity of $\rho \to \rho'$ remains the same.

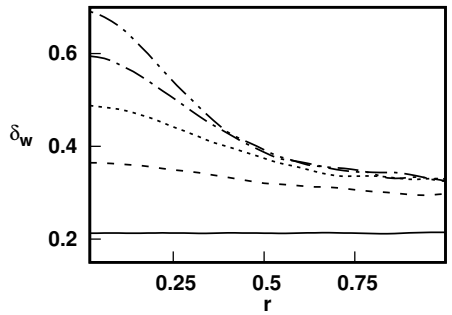

Figure 2.6: Dependence of δ_w on r for m=1 (solid line), 2 (dashed line), 3 (dotted line), 4 (dash-dotted line) and 5 (dash-double-dotted line) for PAS.

As in the case of the nonclassical depth, again, we have a situation where the Wigner function negativity fails to be a faithful measure of NC as far as SNS is concerned. As our aim is to do a comparative study of PAS and SNS in the context of entanglement of the BS output state with these states as the input, it is desirable that we have a measure of NC that works equally well for both the NC-inducing operations, i.e., photon excitation and quadrature squeezing.

2.5.3 Hilbert-Schmidt Distance from Nearest Classical State

The Hilbert-Schmidt distance based measure of single mode quantum state ρ, $d_{\rm NC}(\rho)$, is defined as its distance from the nearest classical state, where, hilbert-Schmidt metric has been used as the distance function [47]. Since coherent states $|\beta\rangle$ are the only pure classical states $|\beta\rangle$ [36], $d_{\rm NC}$ for a pure state $|\psi\rangle$ is defined as,

$$d_{\rm NC}(|\psi\rangle) = \inf_{\beta} \sqrt{2}[1 - |\langle\beta|\psi\rangle|^2]^{1/2}. \tag{2.15}$$

where infimum is taken over the set of all coherent states $|\beta\rangle$, with β being a complex number.

We have calculated $d_{\rm NC}$ for the two states PASVS and SNS. While $d_{\rm NC}$ for PAS has a closed-form analytic expression given by

$$d_{\rm NC}\Big)_{\rm PAS} = \sqrt{2}\Big[1 - \frac{m^m e^{-m}}{(1-\tau)^m N_m}\Big]^{\frac{1}{2}}, \tag{2.16}$$

$d_{\rm NC}$ for SNS can at best be reduced to the simple form

$$d_{\rm NC}\Big)_{\rm SNS} = \inf_{\beta} \sqrt{2}\Big[1 - \frac{\tau^m e^{-|\beta|^2+\frac{\tau}{2}(\beta^2+\beta^{*2})}}{\mu 2^m} L_m\Big(\frac{|\beta|^2}{2\mu\nu}\Big)\Big]^{\frac{1}{2}}, \tag{2.17}$$

from which the computation proceeds via a numerical minimization.

In Fig. 2.7, we have plotted $d_{\rm NC}$ for PASVS and SNS. For PAS, $d_{\rm NC}$ first decreases and then increases with an increase in r for all m; however, for $r \lesssim 0.20$, we observe a monotonic dependence of $d_{\rm NC}$ upon m while for larger $r(\gtrsim 0.20)$ such monotonicity breaks down. For $m \geq 2$, $d_{\rm NC}$ shows a non-monotonic behavior [Fig. 4(a)] consistent with that of $E_{\rm BS}$ [Fig. 2(a)]. In contrast, in the case of $m = 1$, $d_{\rm NC}$ reveals non-monotonic behavior that is inconsistent with $E_{\rm BS}$. Here, we have a situation, in particular, for $m = 1$, in the case of PASVS, where **NC** (as measured by $d_{\rm NC}$) decreases while the corresponding $E_{\rm BS}$ [Fig. 2.5(a)] increases, which is unphysical. On the other hand, for SNS, we observe a non-monotonic dependence of $d_{\rm NC}$ [Fig. 2.5(b)] on r but a monotonic dependence on m. For all m, as r increases, it first decreases and then increases. Similar to the case for PAS, for SNS, we also have an unphysical situation where the NC (as measured by $d_{\rm NC}$) decreases while $E_{\rm BS}$ [Fig. 2.5(b)] increases with r for all m. This leads us to the conclusion that $d_{\rm NC}$ is not an acceptable measure of NC of states generated under multiple NC-inducing operations, in particular SNS and PAS.

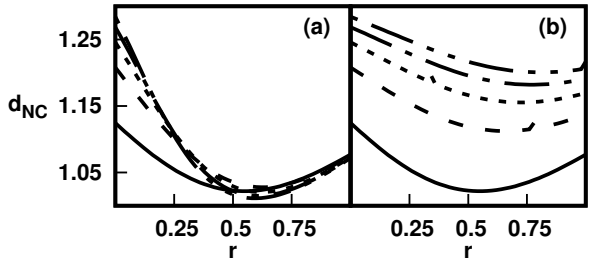

Figure 2.7: Dependence of $d_{\rm NC}$ for (**a**) PASVS and (**b**) SNS on r for m=1 (solid line), 2 (dashed line), 3 (dotted line), 4 (dash-dotted line) and 5 (dash-double-dotted line)

It appears from the above discussion that none of the three measures considered above is an acceptable measure of NC of the states we have considered here. Whether a suitable measure of **NC** can be given that shows a dependence on r and m for such states that is consistent with the dependence of $E_{\rm BS}$ on these parameters remains to be investigated. We shall return to this question in Chap. 3. For the present, we shall deal with the question of how to understand the monotonicity of the entanglement curves in the case of SNS and the non-monotonicity in the case of PAS, in terms of the contours of the Q distributions associated with these states. This shall be the subject of the next section.

2.6 Monotonicity Versus non-Monotonicity question; Role of Competing Nonclassicalities

In this Sec. we shall outline our point of view that the nonmonotonicity in the $E_{\rm BS}$ curves (in the case of PAS) is a consequence of a *competition* between the two different kinds of NC-inducing operations underlying these states. Various counterintuitive features seen in Fig. 2.5(a) can be attributed to the effects of such a competition. In particular the feature that we discussed after Fig. 2.5, that $E_{\rm BS}$ for larger values of m is in fact less than that for smaller values of m beyond $r \sim 0.60$.

2.6.1 Contours of Q Distribution and NC-inducing Operations

We illustrate this competition in terms of contours of the Q function associated with these states. To begin with, it is helpful to visualize the effect of the two NC-inducing operations acting individually on an initial vacuum state in terms of the deformation induced in the circular Q function contour of the vacuum state. As is well known, light (initially in a coherent state) propagating through a medium with a Kerr nonlinearity undergoes radial squeezing [39] and the photon number state can be thought of as an extreme case of a radially squeezed state. Here, figuratively speaking, the photon excitation (addition) operation $(a^\dagger)^m$ can be thought of as deforming the circular Q function contour of the vacuum state into an extreme crescent shape. On the other hand, the squeezing operation $S(r)$ can be thought of as deforming the initial circular Q function contour of the vacuum state into an ellipse [38].

2.6.2 Competing Nonclassicalities and Non-monotonicity of Entanglement

The above picture can now be applied to states with two NC-inducing operations applied in succession. As is evident from Fig. 2.8, in the case of PAS, for small r, with an increase in m, the contours become more crescent shaped indicating the dominant number state character. However, as r increases, except for the case of $m = 1$, the crescent-shaped contours smooth out and become more elliptic. This points to a crossover in the dominant character of the state, from a photonic to a quadrature squeezed one. Such a crossover arises due to an *overwhelming competition* between photon addition and quadrature squeezing operations. For higher r ($\gtrsim 0.60$), the Q function contours tend to become more and more elliptic. It is our view that this competition, as manifest in terms of the crossover from crescent-shaped to elliptic contours of the Q function, is what is behind the change in slope that is evident in the $E_{\rm BS}$ curve for PAS in Fig. 2.2(b).

On the other hand, in the case of SNS (Fig. 2.9), unlike in the case of PAS, there does not appear to be any significant crossover from crescent-shaped to predominantly elliptic Q-function contours. This points to a rather *insignificant competition* between the two NC-inducing operations, namely, photon excitation and quadrature squeezing. Consequently, no change in slope is evidenced in the corresponding $E_{\rm BS}$ curve [Fig. 2.5(b)].

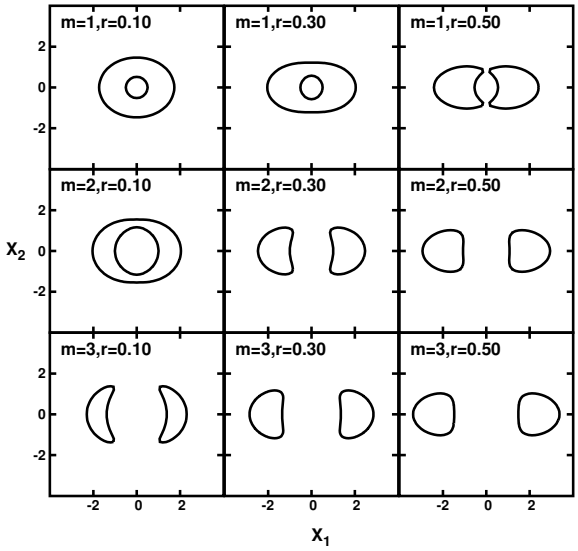

Figure 2.8: Contour plots of the Q function for PAS for different m and r. The axes of the subplots are the quadrature components given by $X_1 = \frac{\beta+\beta^*}{\sqrt{2}}$ and $X_2 = \frac{\beta-\beta^*}{i\sqrt{2}}$.

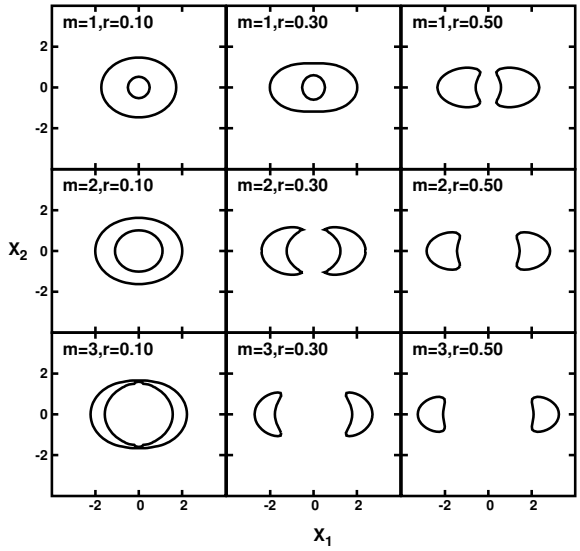

Figure 2.9: Contour plots of the Q function for SNS for different m and r. The axes of the subplots are the quadrature components given by $X_1 = \frac{\beta+\beta^*}{\sqrt{2}}$ and $X_2 = \frac{\beta-\beta^*}{i\sqrt{2}}$.

To sum up, the key to understanding the monotonicity vs nonmonotonicity question is, therefore, the degree of competition between the two NC inducing operations. An overwhelming competition leads to a slope change in the $E_{\rm BS}$ curve and hence a non-monotonic dependence. Whether, this competition is overwhelming or insignificant, can be inferred from the contours of the Q functions associated with the states depending on whether or not they undergo a crossover from crescent shaped to elliptic, as r or m is increased.

2.7 Discussion and Conclusion

In this chapter, we have introduced a useful notation of NC inducing operations. We have then introduced a class of nonclassical states that are generated under multiple (in fact two) NC-inducing operations, viz., the states PAS, PSS and SNS. We have analyzed the nonclassical properties of these states in relation to the presence or absence of squeezing/sub-Poissonian character and displayed these results with the help of what we have called NC-

phase diagram.

We have quantitatively studied the BS output entanglement for input single mode states generated from successive application of two different NC-inducing operations that lead to, in particular, SNS and PAS. We have observed that while BS output entanglement shows a monotonic dependence on the squeeze parameter and the number of photon addition in the case of SNS, this dependence is nonmonotonic in the case of PASVS. We show that any attempt to understand this issue of monotonicity vs nonmonotonicity fails since none of the well-known measures such as the nonclassical depth, the Wigner negativity and the Hilbert-Schmidt distance proves to be an acceptable measure of NC of these states. We have offered an intuitive picture in terms of contours of the associated Q function of these states and pointed out that the competition between these two different NC-inducing operations is the key to understand the monotonicity vs nonmonotonicity issue.

Chapter 3

Analysis of non-monotonicity of entanglement in terms of an effective nonclassicality measure

Let's recall that in Sec. 2.5 of Chapter 2 we have examined in detail the question of whether any known measure of single mode NC may be used to understand the non-monotonic dependence of entanglement for the photon added squeezed vacuum state on number of photon addition (m) and squeeze parameter (r). In this context we have examined several well-known measures, viz. (i) *nonclassical depth*, (ii) *Hilbert-Schmidt distance* from nearest classical state and (iii) *Wigner negativity*. However, we have found that none of these measures succeed in accounting for the non-monotonicity of the entanglement curves.

A question naturally arises as to whether one can construct a *measure of NC* that, when used to quantify the effective NC of states with MNIO, reproduces the non-monotonic dependence when present, as in the example mentioned above. In this chapter, we address this question. We shall restrict our attention to pure states. First we shall give the construction of such a measure and list its various properties. Then we shall use this measure to revisit the problem of the dependence of the BS output entanglement on the effective NC of various input states.

3.1 NC measure in terms of a suitably chosen function of the state

A way to quantify the NC of a state ρ is by the distance *in the Hilbert space* between ρ and the nearest classical state. It is well-known that the only pure states that are classical are the coherent states [36]. Thus, one may define a generic distance-based measure of NC of a

pure state ρ ($= \big|\psi\rangle\langle\psi\big|$) as,

$$\mathcal{N}(\rho) = \inf_{\alpha} D\,(\rho\ ,\ |\alpha\rangle\langle\alpha|), \tag{3.1}$$

where, $D(\rho_1, \rho_2)$ defines a distance between the two states ρ_1 and ρ_2. Indeed, the Hilbert-Schmidt measure, discussed in Sec. III, Chapter 2, is an example where D defines the Hilbert-Schmidt distance between ρ and $|\alpha\rangle\langle\alpha|$.

An alternative approach that we propose here is to construct a NC measure in terms of the difference between $E(\rho)$ and $E(|\alpha\rangle\langle\alpha|)$, where, $E(\rho)$ is a suitably chosen function of ρ such that $E(|\alpha\rangle\langle\alpha|)$ *is independent of* α. Of course one must ensure that this difference is always positive. This alternative approach has the advantage that one can obviate the need of taking an infimum over all values of α. One simple choice of such a function is,

$$E(\rho) \ = \ \lambda_{\min}\Big(V(\rho)\Big), \tag{3.2}$$

where, $\lambda_{\min}\Big(V(\rho)\Big)$ is the minimum eigenvalue of the variance matrix $V(\rho)$ corresponding to ρ as defined in [56]. For this choice of $E(\rho)$, one has $E(|\alpha\rangle\langle\alpha|) = \frac{1}{2}$ as a consequence of the fact that both the eigenvalues of $V(|\alpha\rangle\langle\alpha|)$ are equal to $\frac{1}{2}$. Clearly, $E(|\alpha\rangle\langle\alpha|)$ is independent of α. Note that this choice makes sense only in the case of Gaussian states as $E(\rho)$ depends only on the first and second moments of ρ. Accordingly, one could then define a NC measure $\mathcal{N}_{\rm V}(\rho)$ as

$$\begin{aligned}\mathcal{N}_{\rm V}(\rho) &= E(|\alpha\rangle\langle\alpha|) \ - \ E(\rho) \\ &= \frac{1}{2} \ - \ \lambda_{\min}\Big(V(\rho)\Big)\end{aligned} \tag{3.3}$$

We would like to ensure that $\mathcal{N}_{\rm V}(\rho)$ is always positive, i.e., $\mathcal{N}_{\rm V}(\rho) \geq 0$ for all ρ. Hence it is convenient to redefine $\mathcal{N}_{\rm V}(\rho)$ as

$$\mathcal{N}_{\rm v}(\rho) = \max\ \Big\{\ 0,\ \frac{1}{2} \ - \ \lambda_{\min}\Big(V(\rho)\Big)\ \Big\}. \tag{3.4}$$

Evidently, $\mathcal{N}_{\rm v}(\rho) > 0$ whenever $\lambda_{\min}\Big(V(\rho)\Big) < \frac{1}{2}$, i.e.,$\rho$ is squeezed. This immediately implies that the NC of a single mode Gaussian state is entirely due to its squeezing character. Interestingly, the result (Eq. 3.4) holds true for Gaussian mixed states as well. Here, it is worth mentioning that the $\mathcal{N}_{\rm v}(\rho)$ matches well with the nonclassical depth [48] of a Gaussian state, i.e., $\tau \ = \ \frac{1}{2} \ - \ \lambda_{\min}\Big(V(\rho)\Big)$. We shall have occasion to make use of this result in Chap. 5.

3.2 NC measure in terms of the Wehrl entropy

The choice in Eq. (3.2) is by no means unique. Another choice of $E(\rho)$ that one could make, as we have discovered, is

$$E(\rho) = H_{\rm w}(\rho), \tag{3.5}$$

where, $H_{\rm w}(\rho) = -\int \frac{d^2z}{\pi}\, Q(z,z^*)\, \ln\, Q(z,z^*)$ is the Wehrl entropy of ρ [66]. The Husimi-Kano Q distribution is defined as $Q(z,z^*) = \langle z|\rho|z\rangle$, where $|z\rangle$ forms the coherent state basis. It can be easily checked that $H_{\rm w}(|\alpha\rangle\langle\alpha|) = 1$ for all values of α. This choice will work for *all pure states* ($\rho = \left|\psi\right\rangle\left\langle\psi\right|$) as $H_{\rm w}(\rho)$ depends on *all moments of* ρ. Thus we propose a measure of NC for pure states as

$$\begin{aligned}\mathcal{N}_{\rm w}(|\psi\rangle) &= E(\left|\psi\right\rangle\left\langle\psi\right|) \;-\; E(|\alpha\rangle\langle\alpha|) \\ &= H_{\rm w}(\left|\psi\right\rangle) - 1.\end{aligned} \tag{3.6}$$

The positiveness of $\mathcal{N}_{\rm w}(|\psi\rangle)$ is ensured by the fact that minimum Wehrl entropy for any single mode quantum optical state is unity and the minimum value is attained for the coherent states [93]. It is pertinent to note that the Wehrl entropy has been used earlier to define a measure of non-Gaussianity [67], as in Eq. 1.17 in Chapter 1. In fact, our definition of $\mathcal{N}_{\rm w}$ is inspired by the definition of NG measure mentioned above.

3.3 Invariance Properties of $\mathcal{N}_{\rm w}$

In this section we shall discuss the transformations on the state ρ under which $\mathcal{N}_{\rm w}(\rho)$ remains invariant, i.e., $\mathcal{N}_{\rm w}(\rho) \;=\; \mathcal{N}_{\rm w}(U\rho U^\dagger)$, where, U is the unitary operator corresponding to the transformation. These invariance properties of $\mathcal{N}_{\rm w}$ follow from the transformation properties of the Q distribution under relevant phase space transformations.

3.3.1 Invariance under Phase Space Displacements

Under the action of a phase-space displacement, $D(z) : \rho \to \tilde{\rho} = D(z)\, \rho\, D^\dagger(z)$, the Husimi Q distribution associated with ρ changes to

$$D(z) : Q_\rho(\beta) \to Q_{\tilde{\rho}}(\beta) = Q_\rho(\beta - z). \tag{3.7}$$

This indicates that the phase-space displacement works as the *rigid translation* [66, 93] that leaves Wehrl entropy unchanged, i.e. $D(z) : H_{\rm w}(\rho) \to H_{\rm w}(\rho)$. Hence, it is evident from the Eq. 3.6, that under the transformation $D(z) : |\psi\rangle \to D(z)|\psi\rangle$, its NC does not change, i.e.,

$$D(z) : \mathcal{N}_{\rm w}(|\psi\rangle) \to \mathcal{N}_{\rm w}(|\psi\rangle). \tag{3.8}$$

3.3.2 Invariance under Passage through a Passive Linear System

A passive linear system is represented by the map

$$U_\theta : \rho \rightarrow \tilde{\rho} = U_\theta \rho U_\theta^\dagger \; ; \; U_\theta = e^{-i\theta a^\dagger a}. \tag{3.9}$$

U_θ maps a coherent state $|\alpha\rangle$ to another coherent state $\left|\beta\right\rangle = \left|e^{-i\theta}\alpha\right\rangle$. This is equivalent to a proper rotation in phase space. Under the transformation U_θ, the Husimi Q distribution changes as [67]

$$U_\theta : \; Q_\rho(\beta) \rightarrow Q_{\tilde{\rho}}(\beta) = Q_\rho\,(e^{-i\theta}\beta), \tag{3.10}$$

i.e., the Wehrl entropy does not change. Consequently, under a proper phase space rotation $U_\theta : \left|\psi\right\rangle \rightarrow |\tilde{\psi}\rangle$, $\mathcal{N}_{\rm w}(|\psi\rangle)$, as defined in Eq. 3.6 remains invariant.

Note that the transformations represented by **(a)** $U = D(z)$ and **(b)** $U = e^{-i\theta a^\dagger a}$ can be looked upon as NC preserving operations in the contrast to the NC-increasing transformations that we have discussed in Chap. 2.

3.4 $\mathcal{N}_{\rm w}$ for some pure quantum states of light

In this section we shall evaluate the measure of NC proposed above (Eq. 3.6) for some well-known single mode states studied in the literature earlier, as well as the states that we have considered in the previous chapter.

3.4.1 Photon Number State:

A photon number state $|m\rangle$ is obtained by applying photon excitation operator $\left(\frac{a^{\dagger m}}{\sqrt{m!}}\right)$ on the vacuum state $|0\rangle$. The Wehrl entropy of the photon number state $|m\rangle$ is given by [67]

$$H_{\rm w}(|m\rangle) = 1 \; + \; m \; + \; \ln \; m! \; - \; m \; \Psi(m+1), \tag{3.11}$$

where, $\Psi(m+1) = \sum_{k=1}^{m} \; \frac{1}{k} \; - \; \gamma$ is the di-gamma function and $\gamma \approx 0.5772..$ is the Euler constant. Thus in the case of $|m\rangle$, we obtain an analytic expression for NC as,

$$\mathcal{N}_{\rm w}(|m\rangle) = m \; + \; \ln \; m! \; - \; m \; \Psi(m+1). \tag{3.12}$$

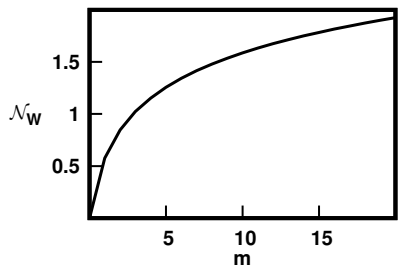

Figure 3.1: Plot of $\mathcal{N}_{\rm w}(|m\rangle)$ with m.

We plot $\mathcal{N}_{\rm w}(|m\rangle)$ for various values of m in Fig. 3.1. For small $m(\leq 4)$ we observe a rapid increase in $\mathcal{N}_{\rm w}(|m\rangle)$. As m increases, $\mathcal{N}_{\rm w}(|m\rangle)$ increases monotonically. This behaviour of $\mathcal{N}_{\rm w}(|m\rangle)$ is consistent with that of Wigner negativity as noted in [49].

Let's look at the large m limit of $\mathcal{N}_{\rm w}(|m\rangle)$ given in Eq. (3.12). In the limit $m \to \infty$, $\ln\, m! \sim m\ln m - m + \frac{1}{2}\ln\, 2\pi m$. On the other hand, $\lim_{m\to\infty} m\Psi(m+1) \sim \frac{m}{2}\Big(\ln(m+1)+\ln m\Big)$. Putting these expressions in Eq. (3.12) we get

$$\lim_{m\to\infty} \mathcal{N}_{\rm w}(|m\rangle) \sim \frac{1}{2}\ln\, 2\pi m \,-\, \frac{m}{2}\ln\Big(\frac{m+1}{m}\Big) \tag{3.13}$$

The logarithmic growth in $\mathcal{N}_{\rm w}(|m\rangle)$ with m for large m is evident from the Fig. 3.1.

3.4.2 Squeezed Coherent State:

A squeezed coherent state, $|\psi_{\rm sc}\rangle = S(\zeta)|\alpha\rangle$, is generated under quadrature squeezing operation, $S(\zeta) = \exp\Big(\frac{\zeta a^{\dagger 2} - \zeta^* a^2}{2}\Big)$, applied on a coherent state $|\alpha\rangle$, where $\zeta = re^{i\theta}$; r and θ being the squeezing strength and the squeezing direction respectively. We obtain an analytic expression of $\mathcal{N}_{\rm w}$ for $|\psi_{\rm sc}\rangle$ given by

$$\mathcal{N}_{\rm w}(|\psi_{\rm sc}\rangle) = \ln\, \cosh r. \tag{3.14}$$

As one would expect $\mathcal{N}_{\rm w}(\big|\psi_{\rm sc}\rangle)$ depends only on the degree of squeezing and not the direction of squeezing indicated by θ. Moreover, the state $|\psi_{\rm sc}\rangle$ could be written as $|\psi_{\rm sc}\rangle = S(\zeta)|\alpha\rangle = D(\beta)S(\zeta)|0\rangle$, where, $\beta = \mu\alpha - \nu e^{i\theta}\alpha^*$, $\nu = \sinh r$. Further, $S(\zeta)|0\rangle = e^{-i\theta a^\dagger a}S(r)|0\rangle$, implying that the squeezing angle θ plays the role of rotation of quadratures in phase space. We have already discussed in Sec. 3.3 that $\mathcal{N}_{\rm w}$ is independent of displacements as well as rotations in phase space. This explains the fact that $\mathcal{N}_{\rm w}(\big|\psi_{\rm sq}\big\rangle)$ in Eq. 3.14 depends only on the squeezing strength r. As evident from Fig. 3.2, $\mathcal{N}_{\rm w}(\big|\psi_{\rm sc}\rangle)$ increases logarithmically with r for small r whereas it increases linearly for large r. This is so because in the large r limit ($r \to \infty$), $\cosh r \sim \frac{e^r}{2}$ and hence $\ln\, \cosh r \;=\; r \,-\, \ln\, 2$.

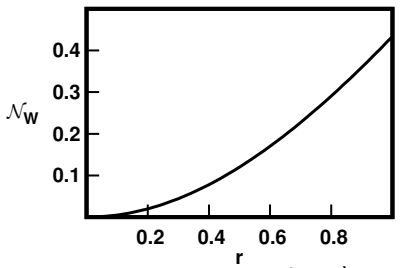

Figure 3.2: Plot of $\mathcal{N}_{\rm w}(\big|\psi_{\rm sq}\big\rangle)$ with r.

It is worth emphasizing here that in case of $|m\rangle$ as well as $\big|\psi_{\rm sq}\big\rangle$, $\mathcal{N}_{\rm w}$ increases monotonically with m and r respectively, mimicking the monotonic dependence of the BS output entanglement on m and r with these states as input. This implies that the BS output entanglement with these states as input increases monotonically with the amount of NC in these states.

$\mathcal{N}_{\rm w}(\big|\psi_{\rm sq}\big\rangle)$ is a monotone of $\mathcal{N}_{\rm v}(\big|\psi_{\rm sq}\big\rangle)$

In this conjunction, we further emphasize that the newly proposed measure of NC, $\mathcal{N}_{\rm w}(|\psi\rangle)$ (Eq. 3.6) is, in fact, a monotone of the NC measure $\mathcal{N}_{\rm v}(\rho)$ (Eq. 3.3), in the case of Gaussian pure state, namely $\big|\psi_{\rm sq}\big\rangle$. This can be appreciated in the following way.

The minimum eigenvalue of the variance matrix of the Squeezed coherent state is given by, $\lambda_{\min}\Big(V(\big|\psi_{sq}\big\rangle)\Big) = \frac{e^{-2r}}{2}$. Putting the expression of $\lambda_{\min}\Big(V(\big|\psi_{sq}\big\rangle)\Big)$ in Eq. (3.14) it can be easily shown that

$$\mathcal{N}_w(|\psi_{sc}\rangle) = \ln\Big[\frac{1 - \mathcal{N}_v\Big(\big|\psi_{sq}\big\rangle\Big)}{\sqrt{1 - 2\mathcal{N}_v\Big(\big|\psi_{sq}\big\rangle\Big)}}\Big]$$

$$\Rightarrow \frac{\partial\, \mathcal{N}_w(|\psi_{sc}\rangle)}{\partial\, \mathcal{N}_v\Big(\big|\psi_{sq}\big\rangle\Big)} = \frac{\mathcal{N}_v\Big(\big|\psi_{sq}\big\rangle\Big)}{\Big[1 - \mathcal{N}_v\Big(\big|\psi_{sq}\big\rangle\Big)\Big]\Big[1 - 2\mathcal{N}_v\Big(\big|\psi_{sq}\big\rangle\Big)\Big]} > 0. \tag{3.15}$$

Evidently, $\mathcal{N}_w(\big|\psi_{sq}\big\rangle)$ increases monotonically with $\mathcal{N}_v(\big|\psi_{sq}\big\rangle)$. From the example of $\big|\psi_{sq}\big\rangle$ it is quite natural to consider that $\mathcal{N}_w$ *is a monotone of* $\mathcal{N}_v$ *for any Gaussian pure nonclassical state*. It would be nice to prove that result, in general; however, currently the proof is unknown and we shall address it elsewhere.

3.4.3 Photon Added Coherent State:

An m-photon added coherent state (PAC) is given by

$$\big|\psi_{pac}\big\rangle = \frac{1}{\sqrt{N_m}} a^{\dagger m}|\alpha\rangle, \tag{3.16}$$

where, $N_m = m!\, L_m\,(-|\alpha|^2)$ is the normalization constant. For the sake of simplicity we consider real displacement. In Fig. 3.3, we plot the dependence of $\mathcal{N}_w(|\psi_{pac}\rangle)$ on α for different values of m. The NC of this state, $\mathcal{N}_w(|\psi_{pac}\rangle)$, increases monotonically with m whereas it decreases with $|\alpha|$. For sufficiently high α (>> 1), $\mathcal{N}_w(|\psi_{pac}\rangle)$ becomes almost independent of m. As is evident form the Fig. 3.3, for fixed α, a larger photon excitation makes the state more nonclassical. On the other hand, for a given m, a sufficiently large value of α renders the state almost classical.

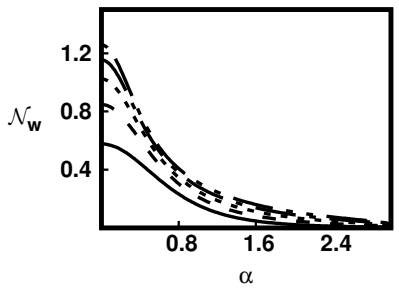

Figure 3.3: Plot of $\mathcal{N}_w(\big|\psi_{pac}\big\rangle)$ vs α for $m = 1$ (solid line), 2 (dashed line), 3 (dotted line), 4 (dash dotted line) and 5 (dash double dotted line).

3.4.4 Even and Odd Coherent States:

Next we study the even ($|\psi_+\rangle$) an the odd ($|\psi_-\rangle$) superposition of coherent states given by

$$|\psi_\pm\rangle = \frac{1}{\sqrt{2(1 \pm e^{-2|\alpha|^2})}}(|\alpha\rangle \pm |-\alpha\rangle). \tag{3.17}$$

For the sake of simplicity we again consider real displacement. We show the dependence of NC on α for $|\psi_\pm\rangle$ in Fig. 3.4. It is worth noting that for small α ($\lesssim 1.0$), $|\psi_-\rangle$ is more nonclassical than $|\psi_+\rangle$; however, for large α (~ 1.5) both $|\psi_\pm\rangle$ contain almost equal amounts of NC. This can be explained in the following way. The Husimi-Kano Q distributions for the even and odd superposition states are given as

$$Q_{|\psi_\pm\rangle}(z) = \frac{e^{-\alpha^2}e^{-|z|^2}}{1+2e^{-2\alpha^2}}\Big(\cosh[2\alpha x] \pm \cos[2\alpha p]\Big), \tag{3.18}$$

where, we have rewritten the phase space coordinate z as $z = x + ip$. In the expression of the Q distribution for the $\left|\psi_\pm\right\rangle$, the second term in the bracket is a circular function that is bounded by ± 1 while the first term is unbounded. As a consequence, in the large α limit only the first term dominates while the contribution from the second term becomes negligible. That is to say that in the limit $\alpha \to \infty$, the Q distributions for both $\left|\psi_\pm\right\rangle$ in Eq. (3.18) reduce to

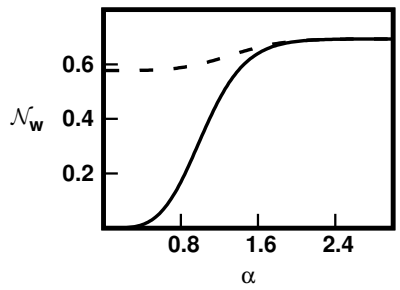

Figure 3.4: Plot of $\mathcal{N}_w$ vs α for $|\psi_+\rangle$ (solid line) and $|\psi_-\rangle$ (dashed line).

$$\lim_{\alpha\to\infty} Q_{|\psi_\pm\rangle}(z) \to \frac{e^{-\alpha^2}}{1+2e^{-2\alpha^2}}\, e^{-|z|^2}\, \cosh[2\alpha x]. \tag{3.19}$$

As a consequence, with increase in α, the amount of NC in the states $\left|\psi_\pm\right\rangle$ tend to become equal.

3.4.5 Photon Added Squeezed Vacuum State and Squeezed Number State:

Here, we shall evaluate $\mathcal{N}_w$ for the photon added squeezed vacuum state (PAS) and the squeezed number state (SNS). These are given as,

$$\begin{aligned} |\psi_{\rm pas}\rangle &= \frac{1}{\sqrt{N_m}} a^{\dagger m} S(r)|0\rangle \\ |\psi_{\rm sns}\rangle &= S(r)|m\rangle, \end{aligned} \tag{3.20}$$

where, $N_m = m!\mu^m P_n(\mu)$, $\mu = \cosh r$ and $P_n(x)$ is the $n^{\rm th}$ order Legendre polynomial. Note that although these states $\left|\psi_{\rm pas}\right\rangle$ and $\left|\psi_{\rm pas}\right\rangle$ are quite different, we have considered these together because they are obtained by the application of squeezing ($S(r)$) and photon addition ($a^{\dagger m}$) operations on the vacuum state in different orders.

In Fig. 3.5 we have plotted the dependence of N_w on r for PAS and SNS. In the case

of PAS [Fig. 3.5(a)], we observe that $\mathcal{N}_w$ is non-monotonic both on r and m. For $m = 1$ it increases monotonically with r. However, for all $m \geq 2$, as r increases it first decreases and then increases. In addition to that, we also notice that for a moderate r ($0.30 \leq r \leq 0.60$), $\mathcal{N}_w$ for higher m becomes smaller than the lower m. It becomes prominent with increase in m. For very high value of r ($\gtrsim 0.80$), $\mathcal{N}_w$ becomes predominantly dependent on r.

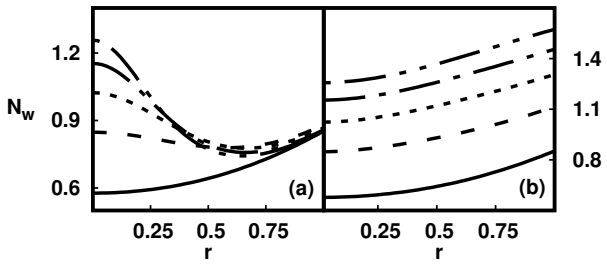

Figure 3.5: Plot of $\mathcal{N}_w$ vs r for $m = 1$ (solid line), 2 (dashed line), 3 (dotted line), 4 (dash dotted line) and 5 (dash double dotted line) for **(a)** PAS and **(b)** SNS.

In the case of SNS [Fig. 3.5(b)] we observe a monotonic dependence of $\mathcal{N}_w$ on both r and m. For $m = 1$, both SNS and PAS yield similar NC; however for $m \geq 2$ they are different. This is due to the fact that $a^\dagger S(r)|0\rangle = S(r)|1\rangle$ and for $m \geq 2$, states are very much different as discussed in the previous chapter.

Here, we would like to emphasize that the non-monotonic dependence of the BS generated entanglement on m with PAS at the input [Fig. 2.5(a)], as is discussed in Sec. 2.4, is similar to the non-monotonic dependence of the NC of PAS on m [Fig. 3.5(a)]. Moreover, the monotonicity of entanglement that we observed in the case of SNS [Fig. 2.5(b)] is also similar to the monotonic dependence of $\mathcal{N}_w$ on m in Fig. 3.5(b). Hence, we infer that the BS generated entanglement depends monotonically on the amount of NC of the input non-classical states, as measured by $\mathcal{N}_w$, as one would expect. This, therefore establishes $\mathcal{N}_w$ as a *good measure of NC of single mode pure states*. Recall our discussion in Chapter 2 where we argued that *none of the other known measures of NC served as good measure* in this respect.

3.5 Conclusion

In summary, we have proposed a new measure of NC of single mode states based on the Wehrl entropy. We have verified that in the case of squeezed vacuum state, $S(r)|0\rangle$, and photon number state, $|m\rangle$, $\mathcal{N}_w$ shows a monotonic dependence on m and r respectively as one would expect. In the case of states with MNIO as well, viz. $S(r)|m\rangle$ and $\frac{1}{\sqrt{N_m}} a^{\dagger m} S(r)|0\rangle$, we have demonstrated that $\mathcal{N}_w$ plays the role of effective NC measure of the states and the BS output entanglement in these cases exhibits a monotonic dependence on $\mathcal{N}_w$. Thus our studies establish that $\mathcal{N}_w$, the measure of NC that we have proposed, is *indeed a good measure of NC for all Gaussian as well as non-Gaussian pure states*.

We would like to remark that our definition of NC measure doesn't extend to mixed states. This is because one doesn't know (*unlike in the case of pure states*) how to characterize all classical mixed states. Although, nonclassical depth serves as a good measure in the case of Gaussian mixed states, *the problem of finding a measure of NC that works for all mixed states is an open one*.

Chapter 4

Quantum Teleportation with Beam Splitter Generated Entangled Non-Gaussian Resource States

The most commonly used Gaussian entangled quantum optical resource in teleportation is the two-mode squeezed vacuum state (TMSV) which could be generated in several nonlinear optical processes [33–35]. However, certain de-Gaussification processes such as photon addition and subtraction along with their coherent superpositions, quantum catalysis *etc.* have been found to improve the amount of entanglement as well as the success of teleportation compared to TMSV. [94–101]. Dell'Anno *et. al.* [95] showed that optimized teleportation could be achieved by tuning entanglement, non-Gaussianity (NG) and squeezed vacuum affinity (SVA) of the entangled resource state. There has been some discussion in the literature on what could possibly be the essential ingredients, besides entanglement, to achieve QT. While Dell'Anno *et. al.* [95] clearly recognized SVA as such an essential ingredient, later developments [96,97,99,100] have pointed to the possibility that Einstein-Podolosky-Rosen (EPR) correlation of the resource states could be a sufficient condition for quantum teleportation (QT). However, Lee *et. al.* [97] and Wang *et. al.* [99] have argued that EPR correlation is not always necessary for QT - for example, the symmetrically photon added TMSV yields QT even without EPR correlation. Further, Hu *et. al.* [101] have addressed the question of whether there could be other attributes of the resource states, besides EPR correlation, that may be crucial for QT. In this respect they considered the Hillery-Zubairy (HZ) correlation. However, they concluded that EPR correlation is a better witness of QT than HZ correlation, i.e., there exist resource states that yield QT that are not HZ correlated but are EPR

correlated.

It may be noted that all the non-Gaussian entangled states considered in earlier works [94–101] were generated by de-Gaussifying the TMSV. Another way to generate non-Gaussian entangled states is by using a passive BS with single mode nonclassical non-Gaussian states at one of the input ports. In chapter 2, we have undertaken a detailed study of the MNIO class of single mode non-Gaussian states in respect of their nonclassical properties and BS output entanglement characteristics when these states are used as input.

In this chapter, we would like to investigate the question of what could be the essential attributes of entangled resource states that contribute to QT, within the context of the BS generated entangled states with the MNO class of states at one of the input ports. Let's call these resource states as BS-MNIO resource states. To this end, we have analyzed several aspects of the BS-MNIO resource states such as NG, squeezed vacuum affinity (SVA) and EPR correlation. We observe that while SVA is not non-zero (hence not a genuine attribute) in a large subset of the BS-MNIO resource states, EPR correlation is found to be not sufficient for QT. This result, together with that of Lee *et. al.* [97] and Wang *et. al.* [99], indicates that *EPR correlation is in general neither necessary nor sufficient for QT*.

We propose that $U(2)$-invariant two-mode quadrature squeezing as defined by Simon and his co-workers [56] could be an important ingredient for QT. In this connection, we have carried out numerical studies using two classes of entangled resource states **(a)** those generated by de-Gaussifying two-mode squeezed vacuum and **(b)** the BS-MNIO class of states. Our results on both these classes of states indicate that $U(2)$-invariant two-mode quadrature squeezing could well be *necessary to achieve QT*. We must point out that except for the overwhelming numerical evidence we do not have a proof of this assertion in general. However, by way of a plausibility argument, we provide an analytical proof of this assertion in the case of a subclass of two-mode Gaussian resource states., viz. the symmetric two-mode Gaussian states.

4.1 Success of Teleportation: Teleportation Fidelity

In the case of the BK protocol for continuous variable teleportation [84], with TMSV as the entangled resource, an unknown coherent state from Alice is completely recovered at Bob's end at asymptotically large value of squeezing. Note that in this limit, the resource state attains maximal correlation between quadratures of the individual modes. Consequently, in the case of entangled quantum optical resource states with non-maximal correlation, the performance/success of the teleportation is measured in terms of a *figure of merit known* as

the fidelity of teleportation (F). It is defined as the overlap between the unknown input state and the output state (the retrieved state), $F = \mathrm{Tr}\,[\rho_{\rm in}\rho_{\rm out}]$. Clearly $F = 1$ in the case of TMSV in the infinite squeezing limit.

The evaluation of F becomes particularly simple in the characteristic function (CF) description [102]. The CF of an n mode quantum optical state ρ is defined as $\chi_\rho(\{\lambda_i\}) = Tr[\rho D(\{\lambda_i\})]$ where $D(\{\lambda_i\}) = \Pi_{i=1}^{n} \exp[\lambda_i a_i^\dagger - \lambda_i^* a_i]$ is the displacement operator associated with the $i^{\rm th}$ mode, a_i being the corresponding mode operator. For any two-mode state $\rho_{\rm AB}$ as a resource, the fidelity of teleportation of an unknown input state $\rho_{\rm in}$ can be expressed in terms of the CFs as [102],

$$F = \int \frac{d^2\lambda}{\pi}\, \chi_{\rm in}(-\lambda)\, \chi_{\rm in}(\lambda)\, \chi_{\rm AB}(\lambda, \lambda^*), \tag{4.1}$$

where, $\chi_{\rm in}(\lambda)$ and $\chi_{\rm AB}(\lambda, \lambda^*)$ are the CFs of $\rho_{\rm in}$ and $\rho_{\rm AB}$ respectively. In the case of a coherent state $|\alpha\rangle$ as the unknown input state, Eq. (4.1) simplifies to,

$$F = \int \frac{d^2\lambda}{\pi}\, e^{-\lambda^2}\, \chi_{\rm AB}(\lambda, \lambda^*), \tag{4.2}$$

Note that the above expression of F is independent of the input coherent state $|\alpha\rangle$. The maximum fidelity of teleportation of any coherent state attainable by a separable state in the BK protocol turns out to be 1/2 [84]. Hence, $F > \frac{1}{2}$ indicates QT. In this chapter, as we shall consider teleportation of an input coherent state only, the fidelity of teleportation with entangled resource $\rho_{\rm AB}$ shall always be given by Eq. (4.2). In Fig 4.1 we plot the dependence of F on the squeeze parameter r and the number of photon addition/subtraction m in the case of non-Gaussian BS output entangled states generated from PAS, PSS and SNS. As is evident from Fig. (4.1), in the case of

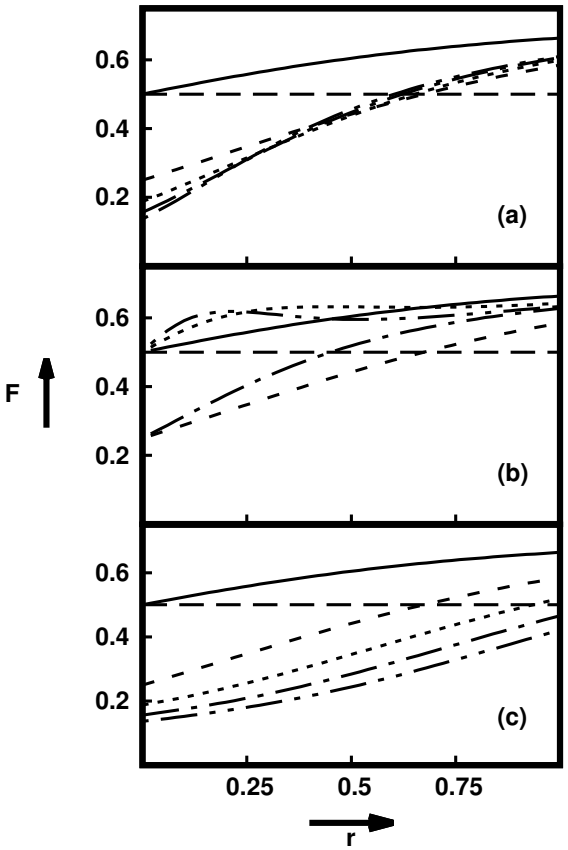

Figure 4.1: Plot of F vs r for $m = 0$ (solid line), 1 (dashed line), 2 (dotted line), 3 (dash dotted line) and 4 (dash double dotted line) with BS output states generated from input **(a)** PAS, **(b)** PSS and **(c)** SNS. Long dashed line corresponds to the value $F = 1/2$.

all three resource states, the teleportation fidelity F exhibits a rather complex, in particular non-monotonic, dependence on the state parameters r and m.

The rest of the chapter is devoted to understanding the various ramifications of the principal numerical results reported in Fig. 4.1. In the next few sections we shall assess the role of various attributes of the resource states, viz. entanglement, NG, squeezed vacuum affinity (SVA) and EPR correlation on teleportation fidelity in respect of the results in Fig. 4.1. We shall now study quantitative and qualitative aspects of teleportation in the case of the BS-MNIO class of resource states.

4.2 Attributes of the Resource States I: Entanglement, Non-Gaussianity and Squeezed Vacuum Affinity

In this section we essentially extend the analysis of Dell'Anno *et. al.* [95] to BS generated resource states. It is pertinent to recall here the observation of Dell'Anno *et. al.* [95], in the context of resource states generated by certain de-Gaussifications of the TMSV, that in order to achieve optimal teleportation, one has to tune values of entanglement, NG and SVA of the resource states. The purpose of this section is to verify if this observation of Dell'Anno *et. al.* is borne out in the case of BS generated resource states with $|\psi_{\rm pas}\rangle$, $|\psi_{\rm pss}\rangle$ and $|\psi_{\rm sns}\rangle$ at the input.

4.2.1 Entanglement and Teleportation Fidelity

In Fig 4.2, we plot the dependence of BS entanglement for different input states. The specific dependence of $E_{\rm BS}(|\psi_{\rm pas}\rangle)$ [Fig. 4.2(a)] and $E_{\rm BS}(|\psi_{\rm sns}\rangle)$ [Fig. 4.2(c)] on r and m have already been discussed in detail in chapter 2. Here, we reproduce the figures for $E_{\rm BS}(|\psi_{\rm pas}\rangle)$ and $E_{\rm BS}(|\psi_{\rm sns}\rangle)$ from chapter 2 for the sake of future discussion. However, the results for $E_{\rm BS}(|\psi_{\rm pss}\rangle)$ are new and we discuss them in some detail.

In the case of $E_{\rm BS}(|\psi_{\rm pss}\rangle)$ [Fig. 4.2(b)], we find that for small r (≤ 0.40), odd photon subtracted states [$m = 1, 3$] are more entangled than the even photon subtracted states [$m = 2, 4$]. However, with increase in r, $E_{\rm BS}(|\psi_{\rm pss}\rangle)$ for even photon subtracted states becomes higher than that for odd photon subtracted states. In general, $E_{\rm BS}(|\psi_{\rm pss}\rangle)$, for all values of m, increases monotonically with increase in r.

As it is quite explicit from Fig. 4.1 and Fig. 4.2, the dependence of the fidelity of teleportation on input parameters r and m for different input states is very different from that of the respective BS output entanglement. In the cases of both PAS, PSS and SNS as input, BS output entanglement, for all non-zero values of m and r, is always greater than that for the

input Gaussian single mode squeezed vacuum state ($m = 0$). However, in the case of teleporation, we observe that F for all input states, except for the case of even PSS in the small r ($\lesssim 0.60$) limit, is always smaller compared to the case of input squeezed vacuum state for all non-zero values of m and r.

In the case of even PSS input, in the small r ($\lesssim 0.30$) region, all input odd PSSs yields more entanglement at the output of BS than the input even PSSs. However, F for all even PSSs at BS input is greater than all input odd PSSs. These results indicate the well-known fact that, although entanglement is necessary for QT, *increase in entanglement does not always ensure increase in fidelity of teleportation.*

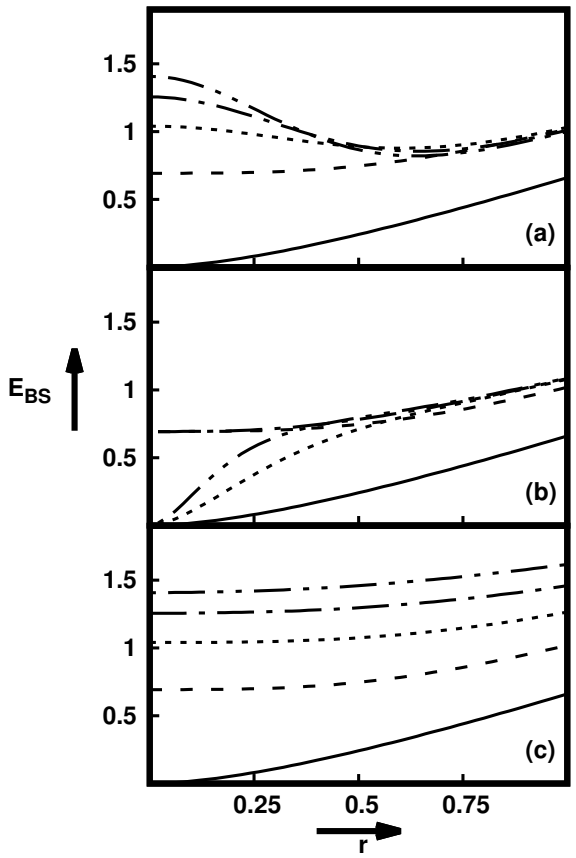

Figure 4.2: Dependence of $E_{\rm BS}$ on r for $m = 0$ (solid line), 1 (dashed line), 2 (dotted line), 3 (dashed dotted line) and 4 (dashed double dotted line) for the input states **(a)** PAS, **(b)** PSS and **(c)** SNS.

4.2.2 Non-Gaussianity and Teleportation Fidelity

In this subsection we study how teleportation fidelity depends on the NG of the BS generated resource states. Here we consider the Wehrl entropy based measure defined by Ivan *et. al.* [67] of NG. For a quantum state of light, described by the density operator ρ, its

non-Gaussianity is defined in Eq. (1.17) as

$$\mathcal{N}_{\rm G}(\rho) \;=\; H_{\rm w}(\rho^{\rm G}) \;-\; H_{\rm w}(\rho), \tag{4.3}$$

where $H_{\rm w}(\rho)$ $[= -\int \frac{d^2z}{\pi} Q_\rho(z) \log Q_\rho(z)]$ is the Wehrl entropy of ρ defined in terms of the Husimi-Kano $Q_\rho(z)$ $[= \langle z|\rho|z\rangle]$ distribution. Here $\rho^{\rm G}$ is the Gaussian counterpart of ρ, i.e., the state formed with the first and the second moments equal to those of ρ itself.

It is further shown by Ivan *et. al.* [67] that, in the case of product state input at any passive linear system like BS, NG of the output state becomes equal to the sum of NG of the input states, i.e.,

$$\mathcal{N}_{\rm G}(\rho_{\rm out}) \;=\; \mathcal{N}_{\rm G}\left(\mathscr{U}_{\rm BS}\,(\rho_a \otimes \rho_b)\,\mathscr{U}_{\rm BS}^{\dagger}\right) \;=\; \mathcal{N}_{\rm G}(\rho_a) + \mathcal{N}_{\rm G}(\rho_b), \tag{4.4}$$

where, $\mathscr{U}_{\rm BS}$ is the unitary operation corresponding to the evolution of the input state $(\rho_a \otimes \rho_b)$ through BS. In the current work we have considered the cases where one of the input ports of the BS is fed with single mode non-Gaussian states $\rho_{\rm in}$ while the other port is left with vacuum. Since, vacuum ($|0\rangle$) is a Gaussian state with $\mathcal{N}_{\rm G}(|0\rangle) = 0$, Eq. (4.4) immediately implies that the NG of the BS generated resource states ($\rho_{\rm out}$) is same as the NG of the corresponding input state $\rho_{\rm in}$.

In Fig. 4.3 we plot $\mathcal{N}_{\rm G}$ as a function of r for different values of m, for the BS output states generated from different input states. From a comparison of Fig. 4.1 and Fig. 4.3 that the fidelity of teleportation (F) does not depend monotonically on the NG ($\mathcal{N}_{\rm G}$) of the resource states. In the case of input PAS, $\mathcal{N}_{\rm G}$ increases monotonically with increase in both m and r, while corresponding F shows a non-monotonic dependence. In the case of input PSS, while the odd m states are more non-Gaussian than the even m states at low r ($\lesssim 0.30$) limit, F for input even PSSs is always higher than that for input odd PSSs. Besides, in the case of input SNS, $\mathcal{N}_{\rm G}$ shows

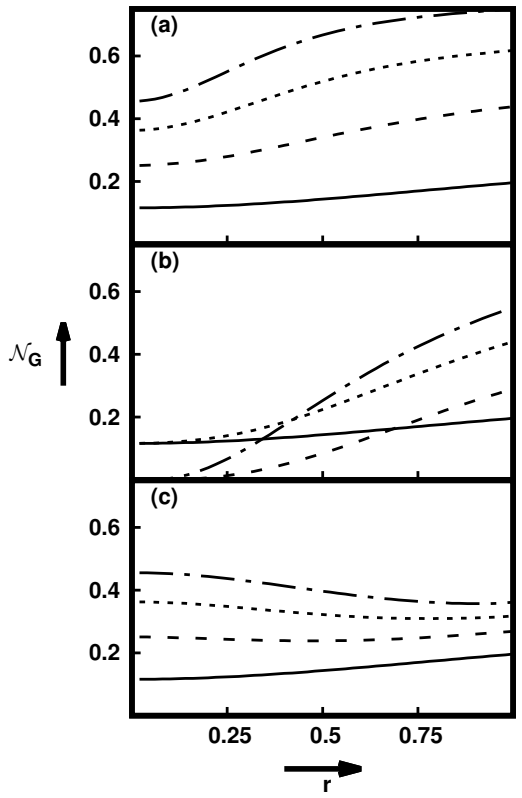

Figure 4.3: Plot of $\mathcal{N}_{\rm G}$ of the BS output states vs r for $m = 1$ (solid line), 2 (dashed line), 3 (dotted line) and 4 (dash dotted line) for input **(a)** PAS, **(b)** PSS and **(c)** SNS.

a non-monotonic dependence on r for higher values of m while corresponding F is a monotonically increasing function of r for all values of m.

4.2.3 Squeezed Vacuum Affinity and Teleportation Fidelity

Dell'Anno *et. al.* [95] identified yet another attribute called squeezed vacuum affinity (η) that entangled quantum optical resources must possess to achieve QT. For any bipartite entangled state $\rho_{\rm AB}$, η is defined as its maximal overlap with the TMSV ($|\xi(s)\rangle$),

$$\eta = \max_{s} |\langle \xi(s)|\rho|\xi(s)\rangle|^2. \tag{4.5}$$

First, We have analyzed the case of even photon added/subtracted states ($m = 0, 2, 4$) at input of the BS for which the output states have nonzero η. In Fig. 4.4, we have shown the dependence of η of the BS generated resource states for different input states. As evident, in the case of all input states, η for the BS output resource states decrease with increase in r for different values of m. The maximum SVA is obtained for $r = 0$ and $m = 0$ that corresponds to the vacuum state ($|0\rangle$).

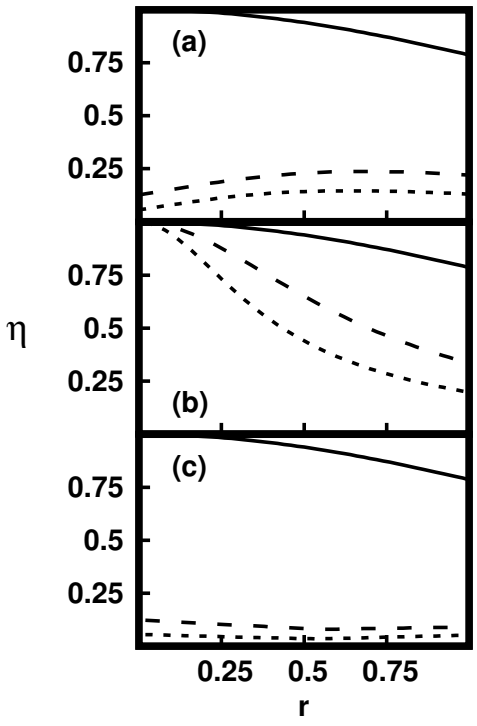

Figure 4.4: η for BS output states with input **(a)** PAS, **(b)** PSS and **(c)** SNS for $m = 0$ (solid line), 2 (dashed line) and 4 (dotted line).

However, we have noticed that η becomes trivially zero in the case of all input states with odd photon addition/subtraction. This could be explained in the following way. The state TMSV has a symmetric expansion in number state basis $|\xi(s)\rangle = \frac{1}{\mu_s}\sum_k \tau_s^k |k,k\rangle$, where $\mu_s = \cosh s$ and $\tau_s = \tanh s$. Let's now consider a bipartite state $\rho = \sum_{\substack{m,n\\k,l}} C_{m,n}^{k,l}\, |m,n\rangle\langle k,l|$. The overlap between $|\xi(s)\rangle$ and ρ is given by,

$$\mathrm{Tr}\left[\rho\ |\xi(\mathrm{s})\rangle\langle\xi(\mathrm{s})|\right] = \frac{1}{\mu_s}\sum_{\substack{m,n\\k,l}} C_{m,n}^{k,l}\, \tau_s^{m+k}\, \delta_{m,n}\, \delta_{k,l} \tag{4.6}$$

.

Evidently, in the case of a bipartite state ρ for which the diagonal elements for all m and k vanish (e.g., $C_{m,m}^{k,k} = 0$), SVA is identically zero. Note that a passive BS simply redistributes the photons in the input modes among the output modes. As a consequence, for all odd

number ($m = 2p+1$, p is any positive integer) of photon added/subtracted states at input, BS output state have diagonal elements identically equal to zero, i.e, $C^{k,k}_{m,m} = 0$ leading to $\eta = 0$.

It is quite clear from Fig. 4.2, 4.3 and 4.4 for entanglement, NG and SVA respectively, that these attributes do not behave quite the same way as the teleprotation fidelity [Fig. 4.1], as far as their dependence on r and m is concerned. In other words, F depends non-monotonically on each of these attributes. One can't achieve a larger value of F merely by increasing any one of these attributes. Thus, our results in the case of those BS generated resource states for which SVA is non-zero are consistent with those of Dell'Anno *et. al.* [95] in the case of de-Gaussified two-mode squeezed vacuum states.

4.3 Attributes of the Resource States II: Einstein-Podolsky-Rosen Correlation

In recent years, besides entanglement, Einstein-Podolsky-Rosen (EPR) correlation [71] of the two-mode resource states have been found to be an important ingredient in achieving QT [96, 100, 101]. However, Lee *et. al.* [97] and Wang *et. al.* [99] have have pointed to examples of states that yield QT even without EPR correlation. In this section, we study this attribute in the case of BS generated non-Gaussian entangled resource states.

In the seminal paper on completeness of quantum mechanics [1], Einstein, Podolsky and Rosen proposed an ideal bipartite state which is a common eigenstate of the relative position and total momentum of the subsystems. In the case of any two-mode quantum optical state one can define an EPR correlation parameter known as EPR uncertainty $\Delta_{\rm EPR}$ [71] as

$$\begin{aligned}\Delta_{\rm EPR} &= \langle(\Delta(X_{\rm A} - X_{\rm B}))^2\rangle + \langle(\Delta(P_{\rm A} + P_{\rm B}))^2\rangle \\ &= 2\Big([1 + \langle A^\dagger A\rangle + \langle B^\dagger B\rangle - \langle A^\dagger B^\dagger\rangle - \langle AB\rangle]\,[\langle A^\dagger\rangle - \langle B\rangle][\langle A\rangle - \langle B^\dagger\rangle]\Big),\end{aligned} \tag{4.7}$$

where, the quadrature operators $\{X_{\rm A}, P_{\rm A}, X_{\rm B}, P_{\rm B}\}$ are defined as $X_{\rm A} = \frac{1}{\sqrt{2}}(A + A^\dagger)$, $P_{\rm A} = \frac{1}{i\sqrt{2}}(A - A^\dagger)$, $X_{\rm B} = \frac{1}{\sqrt{2}}(B + B^\dagger)$ and $P_{\rm B} = \frac{1}{i\sqrt{2}}(B - B^\dagger)$. EPR uncertainty ($\Delta_{\rm EPR}$) being zero indicates perfect correlation between the modes. The correlated state considered by Einstein *et. al.* which is known as the EPR state [103], could be realized in terms of TMSV in the limit of infinite squeezing strength ($r \to \infty$). In the case of two-mode states with $\Delta_{\rm EPR} > 0$, smaller the value of $\Delta_{\rm EPR}$ more correlated the modes are. Further, as shown by Duan *et. al.* [71] $\Delta_{\rm EPR} < 2$ indicates that the two-mode state is entangled.

In this section, we evaluate EPR correlation for the BS generated entangled resources for the different input non-Gaussian states we have considered in this paper. Using the transformation matrix for a 50:50 BS [Eq. (2.1)], $\Delta_{\rm EPR}$ [Eq. (4.7)] for the BS generated resource

states can be expressed in terms of the input mode operators as,

$$\Delta_{\rm EPR} = 2\Big(1 + \langle a^\dagger a\rangle + \langle b^\dagger b\rangle - \langle a^\dagger\rangle\langle a\rangle - \langle b^\dagger\rangle\langle b\rangle\Big) - \Big(\langle a^{\dagger 2}\rangle + \langle a^2\rangle - \langle a^\dagger\rangle^2 - \langle a\rangle^2\Big) - \Big(\langle b^{\dagger 2}\rangle + \langle b^2\rangle - \langle b^\dagger\rangle^2 - \langle b\rangle^2\Big). \tag{4.8}$$

We have considered single mode nonclassical states at one of the input ports (say mode a) while other port (mode b) is left in the vacuum state. This leads to $\langle b\rangle = \langle b^\dagger\rangle = \langle b^2\rangle = \langle b^{\dagger 2}\rangle = \langle b^\dagger b\rangle = 0$. Besides, for the input nonclassical states we have considered, $\langle a\rangle = \langle a^\dagger\rangle = 0$ and $\langle a^2\rangle = \langle a^{\dagger 2}\rangle$. With these results, EPR uncertainty for the BS output states [Eq. (4.8)] reduces to,

$$\Delta_{\rm EPR} = 2\Big(1 + \langle a^\dagger a\rangle - \langle a^2\rangle\Big). \tag{4.9}$$

We denote the $\Delta_{\rm EPR}$ in the case of input state $|\psi\rangle$ as $\Delta_{\rm EPR}(|\psi\rangle)$. Using the expression of Eq. 4.9, we find the analytic forms of the $\Delta_{\rm EPR}$, for input PAS, PSS and SNS as,

$$\Delta_{\rm EPR}(|\psi_{\rm pas}\rangle) = 2\Big[\frac{N_{\rm pas}^{m+1}}{N_{\rm pas}^m} + \frac{\mu^{2m}(m+2)!}{N_{\rm pas}^m}\Big(\frac{\mu\nu}{2}\Big)\sum_{k=0}^{m}\binom{m}{k}\Big(\frac{-\nu}{2\mu}\Big)^k \frac{H_k(0)H_{k+2}(0)}{(k+2)!}\Big], \tag{4.10a}$$

$$\Delta_{\rm EPR}(|\psi_{\rm pss}\rangle) = 2\Big[1 + \frac{N_{\rm pss}^{m+1}}{N_{\rm pss}^m} + \frac{\nu^{2m}(m+2)!}{N_{\rm pss}^m}\Big(\frac{\mu\nu}{2}\Big)\sum_{k=0}^{m}\binom{m}{k}\Big(\frac{-\mu}{2\nu}\Big)^k \frac{H_k(0)H_{k+2}(0)}{(k+2)!}\Big], \tag{4.10b}$$

$$\Delta_{\rm EPR}(|\psi_{\rm sns}\rangle) = 2\Big[1 + m(\mu-\nu)^2 - \nu(\mu-\nu)\Big], \tag{4.10c}$$

where, $\mu = \cosh r$, $\nu = \sinh r$ and $H_n(x)$ is the $n^{\rm th}$ order Hermite polynomial. The expression $\binom{m}{k}$ is the binomial coefficient and the normalization constants $N_{\rm pas}^m$ and $N_{\rm pss}^m$ are defined in Eq. (2.6).

In Fig. 4.5 we have plotted $\Delta_{\rm EPR}$ as a function of r for various values of m for the BS output states, generated from the input single mode states. It is evident from a comparison of Fig. 4.1 for the teleportation fidelity and Fig. 4.5 for the EPR correlation in the case of BS generated resource states with either of the $|\psi_{\rm pas}\rangle$, $|\psi_{\rm pss}\rangle$ and $|\psi_{\rm sns}\rangle$, that there exist regions of r where resource states are EPR correlated ($\Delta_{\rm EPR} < 2$) yet they *don't yield QT* ($F > 1/2$). This leads to the conclusion that *EPR correlation is not sufficient for QT*. Further, as shown by Lee *et. al.* [97] and Wang *et. al.* [99] in the case of non-Gaussian entangled states, in particular the asymmetrically photon added TMSV, QT can be achieved even when the resource state is not EPR correlated, i.e. $\Delta_{\rm EPR} > 2$. Thus, in view of our results together with the results of [97, 99], we conclude that EPR correlation is, in general, *neither necessary nor sufficient* for QT.

Let us summarize our analysis of the various attributes of the resource states so far. The results of Sec. 4.2 lead us to conclude that SVA, as it is not non-zero in general and in

particular in the case of BS generated resource states, it cannot be regarded as an essential attribute of resource states for QT. Moreover, when it is non-zero it is not even sufficient. Further, the results obtained in this section make it clear that EPR correlation as an attribute of resource states is neither necessary nor sufficient. In the backdrop of these results, the question of *what other attributes of the resource states, besides entanglement, play an essential role in QT* remains open.

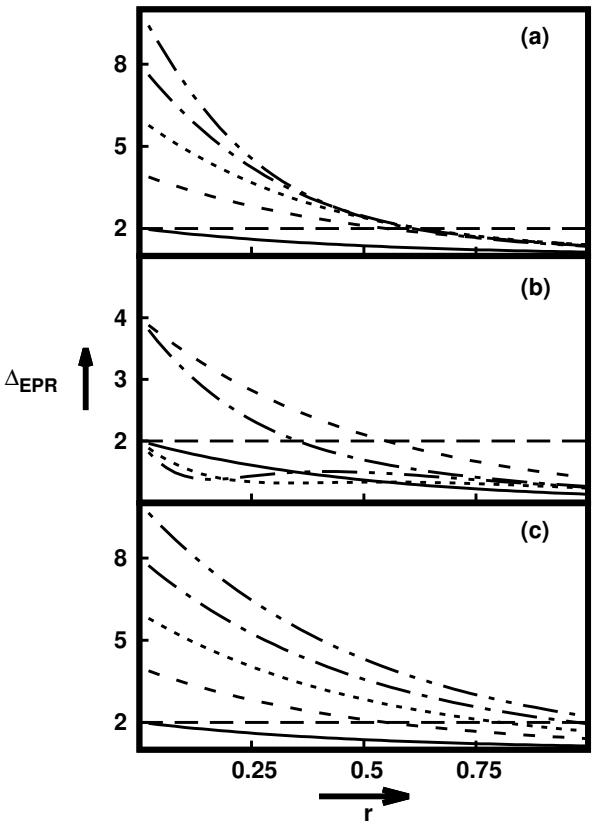

Figure 4.5: Dependence of Δ_{EPR} on r for different $m = 0$ (solid line), 1 (dashed line), 2 (dotted line), 3 (dash dotted line) and 4 (dash double dotted line) for input **(a)** PAS, **(b)** PSS and **(c)** SNS. The long dashed line corresponds to $\Delta_{\mathrm{EPR}} = 2.0$.

4.4 Attributes of the Resource States III: Two-mode Quadrature Squeezing

In this section we analyze yet another attribute of resource states that has not been considered in the literature in the context of QT, namely the $U(2)$-invariant two-mode quadrature squeezing as defined by Simon *et. al.* [56, 57]. Here we focus on examining the role of this attribute in the context of QT.

4.4.1 U(n)-invariant Squeezing Criterion

As we have mentioned in Chap. 1, the condition for a single mode quantum optical states to be squeezed is that the minimum eigenvalue of the variance matrix be less than 1/2. However, it is not straightforward to extend such a characterization of squeezing to the multi-mode case. $U(n)$-invariant quadrature squeezing criterion for an n-mode system defined in terms of a $2n \times 2n$ real symmetric matrix known as the variance matirx, was given by Simon *et. al.* [56, 57]. We shall briefly describe below this criterion in the case of $n = 2$, as our interest is in squeezing properties of BS output states that are 2-mode states.

Let's consider an 2-mode quantum state of light ρ with mode annihilation operators a_k $[k = 1, 2]$ satisfying the commutation relations,

$$\begin{aligned} [a_k, a_l^\dagger] &= \delta_{k,l} \text{ and} \\ [a_k, a_l] &= [a_k^\dagger, a_l^\dagger] = 0. \end{aligned} \tag{4.11}$$

In terms of the quadrature components, namely $x_k = \frac{1}{\sqrt{2}}(a_k + a_k^\dagger)$ and $p_k = \frac{1}{i\sqrt{2}}(a_k - a_k^\dagger)$ $(k = 1, 2)$, one can define a column vector as $R = (x_1 \; p_1 \; x_2 \; p_2)^{\mathrm{T}}$, where "T" stands for transposition. The variance matrix of a two-mode state ρ can be written in a compact form as $V_{k,l} = \frac{1}{2}\,\mathrm{Tr}[\rho\{\Delta \mathrm{R_k}, \Delta \mathrm{R_l}\}]$, where $\Delta R_k = R_k - \mathrm{Tr}[\rho \mathrm{R_k}]$. Here, $\{A, B\}$ stands for the anti-commutator of the operators A and B. The state ρ is said to be n-mode quadrature squeezed if

$$\lambda_{\min} < \frac{1}{2}, \tag{4.12}$$

where, $\lambda_{\min}$ is the least eigenvalue of the 4×4 variance matrix V [56] associated with state ρ. Accordingly, the degree of quadrature squeezing is defined as,

$$f_{\mathrm{sq}} = \frac{1}{\sqrt{2\lambda_{\min}}}, \tag{4.13}$$

and it follows from Eq. 4.12 that the state is said to be quadrature squeezed if $f_{\mathrm{sq}} > 1$.

4.4.2 U(2)-invariant Squeezing for BS Generated Resource States

Using the relation between variance matrices of the input and output state of a BS, it is easy to show (Appendix C) that $\lambda_{\min}$ for the BS output states is given by, $\lambda_{\min} = \min[1/2, \Delta Q]$, where, ΔQ is the value of the uncertainty of the squeezed quadrature of the input state.

In Fig. 4.6 we show the dependence of f_{sq} on r for the BS output two-mode states generated from input PAS, PSS and SNS. In the case of input PAS [Fig. 4.6(a)], f_{sq}, for all $m \geq 1$, becomes greater than unity beyond a moderate squeezing strength ($r \gtrsim 0.60$). However,

these states yield QT ($F > 1/2$) for higher r. In comparison to the results on F [Fig. 4.1(a)], it explains the absence of QT below $r \sim 0.60$.

In the case of input PSS, all the even photon subtracted states [$m = 2, 4$] as well as no photon subtracted state [$m = 0$] possess two-mode quadrature squeezing ($f_{sq} > 1.0$) [Fig. 4.6(b)] for all values of r. However, all the odd photon subtracted states attain $f_{sq} > 1.0$ for higher values of r. In comparison to the corresponding results on F [Fig. 4.1(b)], it is clear that the states, we consider here, yield quantum teleportation provided they possess two-mode quadrature squeezing.

In the case of input SNS, we observe that f_{sq} [Fig. 4.6(c)] for $m \neq 0$ becomes greater than unity for high values of r. The threshold value of r for two-mode squeezing ($f_{sq} > 1.0$) increases with the increase in m. In the case of corresponding results on F [Fig. 4.1(c)] also, we notice that for $m \neq 0$ states quantum teleportation ($F > 1/2$) is attained for higher values of r.

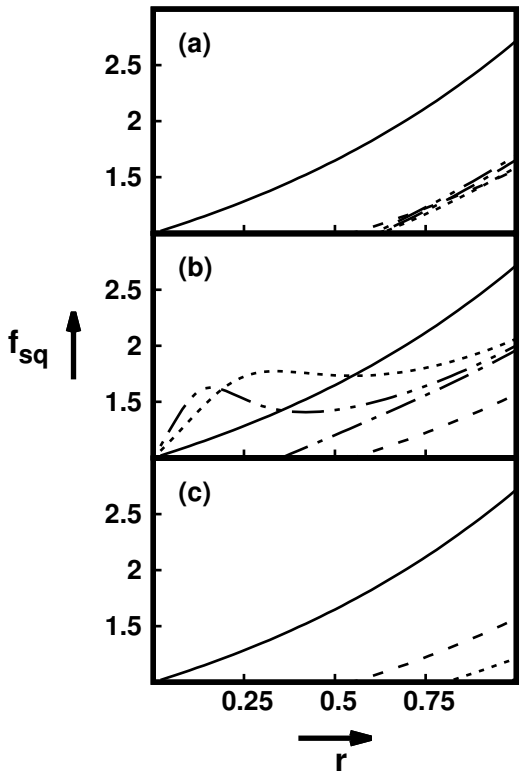

Figure 4.6: Plot of f_{sq} vs r for different $m = 0$ (solid line), 1 (dashed line), 2 (dotted line), 3 (dashed dotted line) and 4 (dashed double dotted line) input **(a)** PAS, **(b)** PSS and **(c)** SNS.

It is worth noting that all the BS output resource states that we have considered attain two-mode quadrature squeezing, depending upon the value of m, beyond a certain value of squeeze parameter r. This could be explained in the following manner. Using the relation between the variance of matrix of the state at input of the BS and that of the output state, it can be easily shown (Appendix C) that the output state is quadrature squeezed if and only if the input single mode is quadrature squeezed. Since, the input single mode states become quadrature squeezed ($f_{sq} > 1$) beyond a moderate value of squeeze parameter r, depending upon the value of m, the same is reflected in the quadrature squeezing of the output states.

The numerical results obtained on the two-mode $U(2)$-invariant quadrature squeezing, in the case of BS output states with different input nonclassical states, indicate that the two-mode $U(2)$-invariant quadrature squeezing might be a necessary condition to obtain

quantum teleportation. In this context, we next analyze our observation in the case of the two-mode non-Gaussian entangled states of light considered by Dell'Anno *et. al.* [95].

4.4.3 $U(2)$-invariant squeezing for states considered by Dell'Anno *et. al.*

Let's denote the states considered in [95] by,

$$|\psi_{\text{TMSV}}\rangle = S_{a,b}(r)|0,0\rangle, \tag{4.14a}$$

$$|\psi_{\text{tmpa}}\rangle = \frac{1}{N_+} a^\dagger b^\dagger S_{a,b}(r)|0,0\rangle, \tag{4.14b}$$

$$|\psi_{\text{tmps}}\rangle = \frac{1}{N_-} ab S_{a,b}(r)|0,0\rangle, \tag{4.14c}$$

$$|\psi_{\text{tmsn}}\rangle = S_{a,b}(r)|1,1\rangle, \tag{4.14d}$$

where, $S_{a,b}(r) = e^{r(a^\dagger b^\dagger - ab)}$, N_+ and N_- are the normalization constants. We have obtained analytic expressions for λ_{min} for the states [Eq. (4.14a), (4.14b), (4.14c) and (4.14d)] as,

$$\begin{aligned}
\lambda_{\text{min}}\Big(|\psi_{\text{TMSV}}\rangle\Big) &= \frac{1}{2} - \nu(\mu - \nu), \\
\lambda_{\text{min}}\Big(|\psi_{\text{tmpa}}\rangle\Big) &= \frac{1}{2} + (1-\tau)(1 - 3\tau + \tau^2 - \tau^3), \\
\lambda_{\text{min}}\Big(|\psi_{\text{tmps}}\rangle\Big) &= \frac{1}{2} - 2\tau(1-\tau)(1 - \tau + \tau^2), \\
\lambda_{\text{min}}\Big(|\psi_{\text{tmsn}}\rangle\Big) &= \frac{1}{2} + (\mu - 2\nu)(\mu - \nu),
\end{aligned} \tag{4.15}$$

where, $\mu = \cosh r$, $\nu = \sinh r$ and $\tau = \tanh r$. The degree of squeezing for the states, then, is calculated using Eq. (4.13). In Fig. 4.7, we plot the dependence of the degree of two-mode quadrature squeezing (f_{sq}), for states given in Eq. (4.14b), (4.14c) and (4.14d), on the squeezing strength r. We also plot, in the same figure, f_{sq} for TMSV as reference.

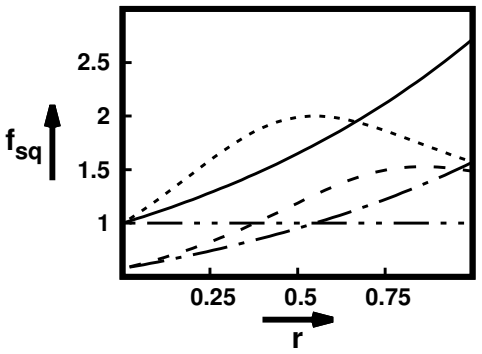

Figure 4.7: Plot of f_{sq} vs r for TMSV (solid line), $|\psi_{\text{tmpa}}\rangle$ (dashed line), $|\psi_{\text{tmps}}\rangle$ (dotted line) and $|\psi_{\text{tmsn}}\rangle$ (dash dotted line). Horizontal dashed double dotted line corresponds to $f_{\text{sq}} = 1$.

The degree of squeezing (f_{sq}) for TMSV is found to be always greater than unity for all non-zero values of r and increases monotonically with r. In the case of $|\psi_{\text{tmpa}}\rangle$, we notice that the state shows two-mode squeezing ($f_{\text{sq}} > 1.0$) beyond $r \sim 0.30$. However, it leads to quantum teleportation for higher r values [95]. In the case of $|\psi_{\text{tmps}}\rangle$, we observe the presence of two-mode squeezing for all values of r which falls in

line with the curve for corresponding teleportation fidelity [95]. It is worth noting that for a small squeeze parameter ($r \lesssim 0.65$), photon subtracted TMSV is more two-mode quadrature squeezed than the TMSV whereas opposite is the case for higher r ($\gtrsim 0.70$). In the case of $|\psi_{\text{tmsn}}\rangle$ we find the dependence of f_{sq} on r very similar to the case of $|\psi_{\text{tmpa}}\rangle$.

From a comparison of the 2-mode squeezing plots (Fig. 4.6) and the teleportation fidelity plots (Fig. 4.1), one can see that there is a parameter region of r where the resource states are 2-mode squeezed ($f_{\text{sq}} > 1$), however they do not lead to QT, i.e., $F > 1/2$. However, in all regions of r where $F > 1/2$ (Fig. 4.1) it turns out that $f_{\text{sq}} > 1$ (Fig. 4.6). Hence, two-mode quadrature squeezing appears to be necessary for QT but not sufficient. Thus a close examination of the numerical results on f_{sq} for the BS-MNIO resource states that we have considered here as well as the states considered by Dell'Anno *et. al.* [95], indicates that *two-mode quadrature squeezing is necessary for QT*. However, as we have noted earlier, two-mode quadrature squeezing is not a sufficient condition.

In summary, our numerical studies on various non-Gaussian resource states lead us to the conclusion that *two-mode $U(2)$-invariant squeezing* could be a necessary condition for QT, in general. In this connection, we next analyze $U(2)$-invariant squeezing in the context of quantum teleportation with symmetric Gaussian entangled resource states. In fact, it turns out (as we show analytically in the next subsection) that in the case of symmetric Gaussian states, two-mode quadrature squeezing is indeed *necessary and sufficient* for QT.

4.4.4 $U(2)$-invariant Squeezing for Quantum Teleportation with Symmetric Gaussian Resource States

Let's consider a symmetric Gaussian state, that without less of generality, is given by the two-mode variance matrix V of the form,

$$V = \begin{bmatrix} \eta & 0 & c & 0 \\ 0 & \eta & 0 & -c \\ c & 0 & \eta & 0 \\ 0 & -c & 0 & \eta \end{bmatrix}. \tag{4.16}$$

The necessary condition on V (set by the uncertainty relation) to be a bona fide quantum variance matrix is that its symplectic eigenvalues [56] (κ_i, $i = 1, 2$) (elements in the Williamson's diagonal form) must be no less than 1/2, i.e. $\kappa_i \geq 1/2$. These, symplectic eigenvalues are obtained as the ordinary eigenvalues of the matrix $iV\Omega$, where,

$$\Omega = \begin{bmatrix} J & 0 \\ 0 & J \end{bmatrix}; \; J = \begin{bmatrix} 0 & 1 \\ -1 & 0 \end{bmatrix}. \tag{4.17}$$

The condition $\kappa_i \geq 1/2$, for the variance matrix V [Eq. 4.16] leads to the condition on the elements of V,

$$\sqrt{(\eta + c)(\eta - c)} \geq 1/2. \tag{4.18}$$

According to the condition of two-mode quadrature squeezing as defined by Simon *et. al.* [56], the variance matrix V is said to be quadrature squeezed if its "*least eigenvalue*" becomes less than 1/2. For the variance matrix V given in Eq. 4.16, its eigenvalues are $l = \eta \pm c$. Evidently, the condition of two-mode quadrature squeezing for V yields

$$\eta - c < 1/2. \tag{4.19}$$

Let's now look at the teleportation of the coherent state with the Gaussian resource states. For any Gaussian entangled resource state with variance matrix $V = \begin{pmatrix} A & C \\ C^T & B \end{pmatrix}$, where, A, C and B are 2×2 matrices, the fidelity of teleportation of a coherent state (Eq. 4.2) is given by Pirandola *et. al.* [90] as,

$$F = \frac{1}{\sqrt{\det[\mathscr{M}]}}, \tag{4.20}$$

where, $\mathscr{M} = A - \{\sigma_z, C\} + \sigma_z B \sigma_z + I$. σ_z is the Pauli spin matrix, $\sigma_z = \begin{pmatrix} 1 & 0 \\ 0 & -1 \end{pmatrix}$.

For the symmetric Gaussian states with variance matrix given in Eq. 4.16, we have $B = A = \mathrm{diag}(\eta, \eta)$ and $C = C^{\mathrm{T}} = \mathrm{diag}(\mathrm{c}, -\mathrm{c})$. This leads to $\mathscr{M} = \mathrm{diag}(1 + 2\overline{\eta - \mathrm{c}}, 1 + 2\overline{\eta - \mathrm{c}})$ with $\det[\mathscr{M}] = (1 + 2\overline{\eta - c})^2$. Now the condition of QT, i.e., $F > 1/2$, leads to,

$$\sqrt{\det[\mathscr{M}]} \leq 2 \Rightarrow \eta - c \leq 1/2. \tag{4.21}$$

Evidently, the condition for quantum teleportation (Eq. 4.21) and the condition for quadrature squeezing (Eq. 4.19), in the case of entangled symmetric Gaussian resource state turns out to be *identical*. This implies that the $U(2)$-invariant quadrature squeezing is a necessary condition for QT with symmetric Gaussian resource states. Further it implies that, in this particular case, it is also sufficient. However, we would like to point out that $U(2)$-invariant quadrature squeezing is not sufficient in the case of Gaussian resource states in general. While numerical evidence suggests (not reported in the thesis) that $U(2)$-invariant two-mode squeezing is necessary for QT in the case of Gaussian states in general it would be nice to have an analytical proof of such a result.

However, in view of the result for the symmetric Gaussian states obtained above, that two-mode quadrature squeezing is *necessary and sufficient* for QT, it is plausible that in the case of non-Gaussian entangled resource states as well *two-mode quadrature squeezing could*

be necessary for QT. We do recognize that we cannot draw too definite conclusions based on our analytical results because of the following two reasons: **(a)** entanglement by itself is known to be necessary and sufficient for QT in the case of symmetric two-mode Gaussian states and **(b)** qualitative results on Gaussian states do not always extend to non-Gaussian states.

4.5 Discussion and Conclusion

In summary, we have studied QT with the non-Gaussian resource states under BS action with the MNIO class of single mode states those are generated under MNIO, viz., the photon added squeezed vacuum state, the photon subtracted squeezed vacuum state and squeezed number state, at one of the input ports. We have extended the analysis of Dell'Anno *et. al.* [95] to these BS generated non-Gaussian resource states and studied in detail the dependence of QT on entanglement, NG and SVA. Consistent with the results of Dell'Anno *et. al.*, we have found that the teleportation fidelity doesn't depend monotonically on either of these properties but one has to tune the values of these to achieve optimal QT fidelity. Moreover, we have found that SVA is, in general, not non-zero for all resource states. In particular, it turns out to be zero in most of the cases for the class of states that we have considered.

We have also examined the EPR correlation of the resource states in order to understand the results of quantum teleportation, obtained in this chapter. While the fact that EPR correlation is not necessary for QT has been known in the literature [97, 99], numerical results on our class of states indicate that *it is not also sufficient*. We, have investigated the question of whether two-mode $U(2)$-invariant squeezing for the BS generated resource states could be necessary/sufficient for QT. Our numerical results on the BS generated non-Gaussian resource states as well as the de-Gaussified TMSV states show that the two-mode $U(2)$-invariant squeezing is in fact *necessary for QT*. this leads us to the conclusion that two-mode squeezing could be a necessary condition for QT in general. To argue that this is a plausible conclusion we have given an analytical proof, in the case of symmetric Gaussian resource states, that $U(2)$-invariant two-mode quadrature squeezing is indeed *necessary and sufficient* for QT.

Chapter 5

Aspects of Conversion of Nonclassicality into Entanglement using Beam Splitters

It is well known that a passive BS converts input single mode NC into output two-mode entanglement [13,16]. In Chapters 2 and 3 we have undertaken a detailed quantitative study of how BS output entanglement depends on input NC. Another important question one may ask, from a quantitative perspective, is to what extent the input NC is used up to generate entanglement at the output of a BS. In a recent work, Ge *et. al.* [104] have shown, in the context of Gaussian states, that a passive BS doesn't convert the entire input NC into output entanglement. Only a part of the input NC is used up to convert to entanglement while the reduced states at the output ports of the BS carry residual NC. They have further obtained a *conservation relation* between the input single mode NC, the BS output entanglement and the residual nonclassicalities at the two output ports. As measures of NC and entanglement, they have considered nonclassical depth and logarithmic negativity respectively.

The purpose of the present chapter is three-fold. First, we revisit the analysis of Ge *et. al.* [104] on the relation between BS output entanglement and the NC of the states at input and output ports, by using a different measure of entanglement, namely, the entanglement of formation [77], in contrast to logarithmic negativity that they have used. Our analysis confirms the conclusion of Ge *et. al.* that the difference between NCs of input and output modes is, indeed, a measure of entanglement generated by the BS. Thereafter, we attempt to examine the conversion of NC into entanglement in the context of non-Gaussian states. A few points worth noting here: **(a)** unlike in the case of Gaussian states, the NC of non-Gaussian states is not determined by squeezing alone, **(b)** even if the input nonclassical state is pure, the reduced states at the output modes of the BS are mixed, in general and

(c) we have argued in Chapter 2, there is no known measure of NC of single mode non-Gaussian states at present. In Chapter 3 we have proposed a Wehrl entropy based measure of NC for pure states that works well for non-Gaussian states also. However, our measure can't be extended to the non-Gaussian mixed states. In view of this handicap, we choose to focus on the limited question of how certain characteristics of NC such as squeezing and antibunching are used by the BS to convert to entanglement.

Lastly, we examine the problem of conversion of NC into entanglement in the most general setting of multiple BSs. Specifically, we investigate the question of how and to what extent one may be able to spatially distribute entanglement using an assembly of BSs and other linear optical elements (if necessary).

5.1 NC-Entanglement Conservation Relation for Gaussian States

We begin by motivating a definition of a measure of NC for Gaussian states. For this purpose the following result is useful.

Statement: A single mode Gaussian state is nonclassical if and only if it is squeezed.

This is easily inferred from the well-known result that a general single mode Gaussian state can always be represented as a displaced squeezed thermal state [54]. In other words, given a Gaussian Wigner distribution, its variance matrix elements can always be parametrized in terms of a complex squeezing parameter ζ and a thermal parameter $\bar{n}$. Any single mode Gaussian state can be written as a squeezed thermal state [54], i.e., $\rho^{\mathrm{G}} = S(\zeta)\, \rho_{\mathrm{th}}(\bar{n})\, S^{\dagger}(\zeta)$, where $\zeta = r\, e^{i\phi}$ with r and ϕ being the squeeze parameter and the direction of squeezing. It is well-known that ρ^{G} is nonclassical if $r > \frac{1}{2} \ln [2\bar{n} + 1]$. Here, the displacement in the expression of a general single mode Gaussian state as pointed out in [54] could be ignored without any loss of generality. Clearly then, the NC of a single mode Gaussian state is contained entirely in its squeezing character, as squeezing is the only NC-inducing operation that is involved.

Consequently, one can quantify the NC of a Gaussian state by the amount of squeezing in it, or equivalently by the minimum eigenvalue of its variance matrix of the state. This is what justifies our use of the measure of NC given by

$$\mathrm{NC}(\rho) = \min \Big\{ 0,\, \frac{1}{2} - \lambda_{\min}\Big(\mathrm{V}(\rho)\Big) \Big\}, \tag{5.1}$$

earlier proposed in Eq. (3.4) of Chapter 3 in the context of Gaussian *pure* states from totally different considerations. Note that nonclassical depth [48] evaluated for a Gaussian state by Ge *et. al.* [104], in fact, reduces to the formula in Eq. (5.1). It is interesting that the NC

measure in Eq. (5.1) we have put forward as an extension of Eq. (1.6) in Chapter 3 to general Gaussian states agrees with nonclassical depth. Evidently, at the root of this agreement is the fact that NC of a single mode Gaussian state is determined by its squeezing character alone.

Let's consider a single mode nonclassical Gaussian state input at one of the input ports of a 50 : 50 BS while the other port is in the vacuum state. Given that the input Gaussian state is nonclassical, i.e., quadrature squeezed, the BS output is a two-mode Gaussian entangled state determined entirely by its two-mode variance matrix. The input variance matrix $V^{\rm in}$ in our case is given by $V^{\rm in} = \begin{pmatrix} \sigma & 0 \\ 0 & \frac{I}{2} \end{pmatrix}$, where σ denotes the 2×2 variance matrix of the input Gaussian state and I is the 2 identity matrix. The matrix $\frac{I}{2}$ is the variance matrix of the vacuum state at the other port. The 4×4 variance matrix of the BS output state ($V^{\rm out}$) is related to the variance matrix $V^{\rm in}$ of the input state by

$$V^{\rm out} \;=\; S\; V^{\rm in}\; S^{\rm T} = \frac{1}{2}\begin{pmatrix} \sigma + \frac{1}{2}I & -\sigma + \frac{1}{2}I \\ -\sigma + \frac{1}{2}I & \sigma + \frac{1}{2}I \end{pmatrix}, \tag{5.2}$$

where, S is the 4×4 symplectic transformation given by (Appendix C)

$$S \;=\; \frac{1}{\sqrt{2}}\begin{pmatrix} I & I \\ -I & I \end{pmatrix}. \tag{5.3}$$

The states at the two output ports of the BS are given by the reduced density operators, $\rho^{\rm out,1} \;=\; {\rm Tr}_2\,[\rho^{\rm out}]$ and $\rho^{\rm out,2} \;=\; {\rm Tr}_1\,[\rho^{\rm out}]$. The output mode states are characterized by the 2×2 variance matrices

$$V^{\rm out,1} \;=\; V^{\rm out,2} \;=\; \frac{1}{2}(\sigma + \frac{I}{2}) \;=\; \frac{1}{2}\begin{pmatrix} \sigma_{11} + \frac{1}{2} & -\sigma_{12} + \frac{1}{2} \\ -\sigma_{12} + \frac{1}{2} & \sigma_{22} + \frac{1}{2} \end{pmatrix}. \tag{5.4}$$

The minimum eigenvalue of the output mode states are found to be

$$\lambda_{\rm min}\Big(V^{\rm out,1}\Big) \;=\; \lambda_{\rm min}\Big(V^{\rm out,2}\Big) \;=\; \frac{1}{2}\Big(\frac{1}{2} + l_{\rm min}\Big), \tag{5.5}$$

where, $l_{\rm min}$ is the minimum eigenvalue of σ. If one measures NC of the Gaussian states by nonclassical depth which is the same as the formula given in Eq. (5.1), then the nonclassical depth of one of the output modes, on using Eq. (5.5), is given by

$$\mathrm{NC}_{\rm out,1} \;=\; \frac{1}{2} \;-\; \lambda_{\rm min}\Big(\mathrm{V}^{\rm out,1}\Big) \;=\; \frac{1}{2}\,\Big(\frac{1}{2} - \mathrm{l}_{\rm min}\Big). \tag{5.6}$$

As $V^{\rm out,1} \;=\; V^{\rm out,2}$, it leads to the result $\mathrm{NC}_{\rm out,1} \;=\; \mathrm{NC}_{\rm out,2}$. On the other hand, NC of the input mode state is $\mathrm{NC}_{\rm in,1} \;=\; \frac{1}{2} \;-\; \mathrm{l}_{\rm min}$, whereas the NC of the vacuum state at the other

port is zero. Thus if one uses nonclassical depth as a measure of NC for input and output modes then, as follows immediately from Eq. (5.1) and Eq. (5.6) that

$$\mathrm{NC}_{\mathrm{in},1} + \mathrm{NC}_{\mathrm{in},2} = \mathrm{NC}_{\mathrm{out},1} + \mathrm{NC}_{\mathrm{out},2}, \tag{5.7}$$

implying that total input NC is equal to total output NC. This result derive d by Ge *et. al.* is counterintuitive as the above relation fails to account for the fact that some input NC may be used up by BS to generate entanglement. However, as suggested by Ge *et. al.* [104], if one uses a modified measure of NC instead, namely,

$$\mathrm{LNC}(\rho) = -\ln\left[2\lambda_{\min}\Big(\mathrm{V}(\rho)\Big)\right], \tag{5.8}$$

then one finds the relation

$$\mathrm{LNC}_{\mathrm{in},1} + \mathrm{LNC}_{\mathrm{in},2} = \mathrm{LNC}_{\mathrm{out},1} + \mathrm{LNC}_{\mathrm{out},2} + \mathrm{S_N}, \tag{5.9}$$

where, S_N, as argued by Ge *et. al.* [104], measures the amount of entanglement generated by the BS and is given by

$$S_N = \ln\left[\frac{\lambda_{\min}(V^{\mathrm{out},1})\,\lambda_{\min}(V^{\mathrm{out},2})}{\lambda_{\min}(V^{\mathrm{in},1})\,\lambda_{\min}(V^{\mathrm{out},2})}\right] = 2\ln\left[\frac{1+2\,l_{\min}}{2\sqrt{2\,l_{\min}}}\right]. \tag{5.10}$$

Clearly, $S_N > 0$ whenever $2\,l_{\min} < 1$, i.e., the input Gaussian state is squeezed (hence nonclassical). The reason why Ge *et. al.* [104] found it compelling to regard S_N as a measure of BS output entanglement is because it not merely resembles the formula for logarithmic negativity, a well-known entanglement monotone [78], but, as they have numerically demonstrated, both S_N as well as the logarithmic negativity of the BS output state increase monotonically with input NC.

5.1.1 NC-Entanglement Conservation Relation with reference to Entanglement of Formation (EOF)

In this section, we would like to reexamine the conservation relation mentioned above using a different measure of entanglement, namely, the *Entanglement of Formation* (EOF) for two-mode symmetric Gaussian states [77]. It is pertinent to note here that in the case of a $50:50$ BS, when a NC state is input at one port and the other port is left with vacuum, the BS output state is always symmetric.

The EOF of a two-mode symmetric Gaussian state is, in fact, the same as as that of a suitably defined two-mode correlated squeezed state $\left|\psi^{\mathrm{sq}}_{\mathrm{AB}}\right\rangle = S_{\mathrm{AB}}(r_\Delta)|0,0\rangle$ and is given by [77]

$$\mathrm{EOF}(\rho^{\mathrm{AB}}) = \mu_\Delta^2 \ln\,\mu_\Delta^2 - \nu_\Delta^2 \ln\,\nu_\Delta^2,, \tag{5.11}$$

where $\mu_\Delta = \cosh r_\Delta$ and $\nu = \sinh r_\Delta$. The effective squeeze parameter r_Δ is given by

$$r_\Delta = -\frac{1}{2} \ln\, \Delta, \tag{5.12}$$

where Δ is defined in terms of $\Delta_{\rm EPR}$ (Eq. 4.7), the EPR uncertainty of $\rho^{\rm G}_{AB}$, as

$$\Delta = \min\, \left\{1, \frac{1}{2}\Delta_{\rm EPR}\right\}. \tag{5.13}$$

It can be easily shown that the EPR uncertainty for the BS output two-mode entangled Gaussian state, generated from the single mode nonclassical Gaussian state $\rho^{\rm G}$ (with $2\, l_{\rm min} < 1$), is given by $\Delta_{\rm EPR} = 1 + 2\, l_{\rm min}$. This leads us to the result

$$r_\Delta = -\frac{1}{2} \ln \left[\min\, \left\{1, \frac{1}{2}(1 + 2\, l_{\rm min})\right\}\right] = -\frac{1}{2} \ln\, [\frac{1 + 2\, l_{\rm min}}{2}]. \tag{5.14}$$

With the choice of r_Δ (Eq. 5.14), it can be shown by a straightforward calculation that the values of μ_Δ and ν_Δ are given by

$$\mu_\Delta = \frac{1}{2}\, \frac{3 + 2\, l_{\rm min}}{\sqrt{2(1 + 2\, l_{\rm min})}}\ ,\ \ \nu_\Delta = \frac{1}{2}\, \frac{1 - 2\, l_{\rm min}}{\sqrt{2(1 + 2\, l_{\rm min})}}. \tag{5.15}$$

On substituting the values of μ_Δ and ν_Δ from Eq. (5.15) in Eq. (5.11) we obtain an analytic expression of the entanglement of formation for the BS output Gaussian state as

$$\begin{aligned} {\rm EOF}(\rho^{\rm out}) = \frac{1}{4(1 + 2\, l_{\rm min})} &\left\{(3 + 2\, l_{\rm min})^2 \ln (3 + 2\, l_{\rm min}) - (1 - 2\, l_{\rm min})^2 \ln (1 - 2\, l_{\rm min})\right\} \\ &- \ln (1 + 2\, l_{\rm min}) - 2 \ln 2\sqrt{2}. \end{aligned} \tag{5.16}$$

For a comparison with the work of Ge *et. al.* [104], we have plotted in Fig. 5.1 the difference of input and output NCs, S_N, the logarithmic negativity $E_{\rm N}$ and the entanglement of formation EOF as a function of $\frac{1}{l_{\rm min}}$. From Eq. (5.1) it is clear that as $\frac{1}{l_{\rm min}}$ increases the nonclassical depth increases and hence $\frac{1}{l_{\rm min}}$ could be taken as a measure of NC for a Gaussian state. It is clear from the Fig. 5.1 that very much like E_N, EOF too is a monotonically increasing function of $\frac{1}{l_{\rm min}}$. Thus our work corroborates the conclusion of Ge *et. al.* that S_N is, indeed, a measure of BS output entanglement, and thus satisfies the conservation relation stated in Eq. (5.9). In fact, one can analytically show that EOF is a monotonically increasing function of $\frac{1}{l_{\rm min}}$. It turns out that

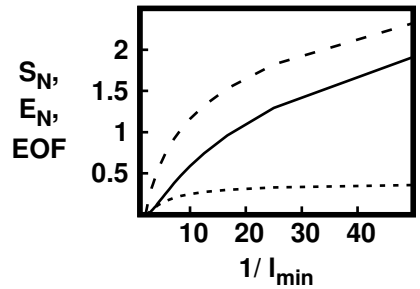

Figure 5.1: Dependence of S_N (solid line), $E_{\rm N}$ (dashed line) and EOF($\rho^{\rm out}$) (dotted line) on $\frac{1}{l_{\rm min}}$.

$$\frac{\partial\, {\rm EOF}(\rho^{\rm out})}{\partial\, (1/l_{\rm min})} = \frac{l_{\rm min}^2 (3 + 2\, l_{\rm min})(1 - 2\, l_{\rm min})}{2(1 + 2\, l_{\rm min})^2} \ln \left(\frac{3 + 2\, l_{\rm min}}{1 - 2\, l_{\rm min}}\right). \tag{5.17}$$

Clearly, the right hand side in Eq. (5.17) is greater than for $2\,l_{\rm min} < 1$ implying that EOF is a monotonically increasing function of $1/l_{\rm min}$. In fact, one can go a step further and show analytically that EOF is a monotonically increasing function of S_N. In view of the expression of S_N (Eq. 5.10), it turns out that

$$\frac{\partial\,\mathrm{EOF}(\rho^{\rm G}_{\rm out})}{\partial\,S_N} = \frac{\partial\,\mathrm{EOF}(\rho^{\rm G}_{\rm AB})}{\partial\,l_{\rm min}} \cdot \frac{\partial\,l_{\rm min}}{\partial\,S_N} = \frac{l_{\rm min}(3\,+\,2\,l_{\rm min})}{2(1\,+\,2\,l_{\rm min})}\,\ln\Big(\frac{3\,+\,2\,l_{\rm min}}{1\,-\,2\,l_{\rm min}}\Big). \tag{5.18}$$

Again the right hand side in Eq. (5.18) is greater than for $2\,l_{\rm min} < 1$ implying that EOF is a monotonically increasing function of S_N. For the sake of illustration, we have looked at the dependence of EOF of the BS output state on S_N in the case of input state being squeezed vacuum state, $\left|\psi_{\rm sv}\right\rangle = S(r)|0\rangle$, where, $S(r) = e^{\frac{r}{2}(a^{\dagger 2}-a^2)}$. The input variance matrix for $\left|\psi_{\rm sv}\right\rangle$ is given by $\sigma_{\rm sv} = \mathrm{diag}\ (\mathrm{e}^{2\mathrm{r}}/2,\ \mathrm{e}^{-2\mathrm{r}}/2)$ for which $l_{\rm min} = \frac{e^{-2r}}{2}$. In Fig. 5.2 we show the dependence of entanglement of formation of the BS output state on $S_{\rm N}$, the difference between total input and total output NCs, in the case of $\left|\psi_{\rm sv}\right\rangle$ as input. As is evident from the Fig. 5.2, output entanglement is a monotonic function of the difference between input and output NCs.

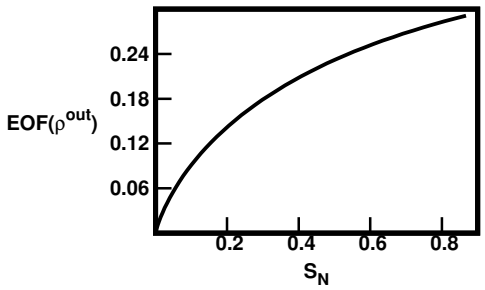

Figure 5.2: Plot of $\mathrm{EOF}(\rho^{\rm out})$ vs S_N for input $\left|\psi_{\rm sv}\right\rangle$.

So far we have analyzed the conservation relation between total input NC, total output NC and the BS generated entanglement, in the case of Gaussian states, in line with the work done by Ge *et. al.* [104]. We have seen that, even with a different measure of entanglement, namely EOF instead of the logarithmic negativity considered in [104], the BS output entanglement is found to be a monotonically increasing function of the difference between total input and output NCs. This, in other words, reaffirms the conclusion that a passive BS uses only a part of the input NC to yield entanglement at the output; the rest of input NC is carried by the reduced states at the BS output ports.

5.2 On Conversion of Input NC into BS Output Entanglement: The non-Gaussian Case

In the previous section, we have considered the quantitative aspects of conversion of input NC into BS output entanglement in the case of Gaussian states. In particular we have revis-

ited the conservation relation between NC of Gaussian states at input and output ports and BS generated entanglement, studied earlier by Ge *et. al.* [104].

Our broad aim in this section is to extend the results of the previous section to non-Gaussian states. However, as we have remarked at the beginning of the present chapter, we are handicapped by the fact that there is no known measure of NC for non-Gaussian mixed states. It is worth recalling here that the NC of a Gaussian state is contained entirely in its squeezing character. Thus, the problem of conversion of input NC into BS output entanglement in the case of Gaussian states is effectively that of the conversion of input squeezing into entanglement. On the other hand, the NC of a non-Gaussian state is contained, in general, not only in its squeezing character but also in other characteristics such as sub-Poissonian character, higher order squeezing *etc.* Thus, as far as the question of conversion of input NC into BS output entanglement is concerned, for non-Gaussian states, all of the above -mentioned quantifications of NC based on the lower-ordered moments of the mode creation and annihilation operators are likely to play a role. Here, we take a pragmatic approach and address the limited question of how only two aspects of NC, namely, squeezing and sub-Poissonian character, contribute towards the conversion of input NC into entanglement at the BS output.

As quadrature squeezing in any state is determined by how small the minimum eigenvalue of the variance matrix is compared to $\frac{1}{2}$, the results on the Gaussian states from the previous subsection will be immediately applicable here. In order to evaluate squeezing for the non-Gaussian states, it is sufficient to compute the $l_{\min}$ for the corresponding Gaussian counterparts, i.e., the states having the same first and second order moments.

On the other hand, sub-Poissonian character of any state is defined in terms of the Mandel Q parameter given by (Eq. 1.5)

$$Q = \frac{\langle N^2\rangle - \langle N\rangle^2}{\langle N\rangle} - 1, \tag{5.19}$$

where, $N = a^\dagger a$ is the number operator. Note that more negative Q is, more sub-Poissonian the state is, and hence more nonclassical. It can be shown by a straightforward calculation (Appendix D) that the Q parameter of the reduced output state is half times the Q parameter of the input state ρ, i.e.,

$$Q^{\text{out,1}} = Q^{\text{out,2}} = \frac{Q}{2}, \tag{5.20}$$

where, $Q^{\text{out,i}}$ $(i = 1, 2)$ is the Q parameter of the reduced state at the i^{th} mode. The Q parameter of the reduced output state is less than that of the input state (in fact exactly half)

implying that the reduced output state is less sub-Poissonian as some of this aspect of NC has been used to generate entanglement.

Let's compare the change in the sub-Poissonian and the quadrature squeezing characters of the input state under BS evolution. It is convenient to define the fractional change in the squeezing as

$$\eta_{\rm sq} \;=\; \frac{l_{\rm min} \;-\; \lambda_{\rm min}(V^{\rm out,1})}{l_{\rm min}}. \tag{5.21}$$

From Eq. (5.5) the value of $\eta_{\rm sq}$ is found to be $\eta_{\rm sq} \;=\; \frac{1}{2}\left(1 \;-\; \frac{1}{2\,l_{\rm min}}\right)$. Clearly, as $l_{\rm min}$ becomes smaller compared to $\frac{1}{2}$, $\eta_{\rm sq}$ becomes more negative implying that squeezing in the output modes is less than that in the input, as some of it has been used up to generate entanglement. One can similarly define a fractional change in sub-Poissonian character as

$$\eta_Q \;=\; \frac{Q \;-\; Q^{\rm out,1}}{Q}, \tag{5.22}$$

which from Eq. (5.20) turn out to have the value $\eta_Q \;=\; \frac{1}{2}$.

As is evident from the Eq. (5.21) and Eq. (5.22), the relative change in the Q parameter is more than that in $l_{\rm min}$, i.e.,

$$\eta_Q \;-\; \eta_{\rm sq} \;=\; \frac{1}{4\,l_{\rm min}} \;>\; 0. \tag{5.23}$$

This indicates that, under BS transformation, sub-Poissonian character decreases faster than the quadrature squeezing character. In other words, *compared to the sub-Poissonian character, quadrature squeezing character of the single mode quantum optical states is less efficient as far as the problem of optimal conversion of input NC into BS output entanglement is concerned*. It is interesting that this conclusion is independent of which non-Gaussian state is input at the BS as long as it has the same $l_{\rm min}$.

5.3 Entanglement Redistribution over a 1-Dimensional Lattice Using a BS Setup

Let's recall that when the output of the first BS is fed to a second BS, the state at the input port of the second BS is given by, for example

$$\rho^{(2)}_{\rm in,1} \;=\; {\rm Tr}_2\,[\rho^{(1)}_{\rm out}], \tag{5.24}$$

where, $\rho^{(1)}_{\rm out}$ is the two-mode state after the first BS and $\rho^{(2)}_{\rm in,1}$ is the reduced density operator corresponding to the state input at one of the ports of the second BS. It is important to realize that *the event of putting a second BS at the output ports of the first BS, which is mathematically equivalent to the operation of state reduction, necessarily destroys the entanglement* of the two-mode output state after the first BS.

In this section, we look into the question of whether two-mode entanglement destroyed at the output of the first BS due to putting two other BSs at the two output ports of the first BS can be regenerated at another location. We give a *basic scheme*, using 50 : 50 BSs, perfect mirrors and phase shifters, that, in fact, accomplishes this task. Thereafter, we embed this basic scheme within an *extended scheme* that accomplishes the task of redistributing the entanglement generated at the output of the first BS over N $(= 1, 2, 3, ..)$ sites on a 1-dimensional lattice.

5.3.1 Schematic of the BS Arrangement for Entanglement Redistribution

Let's consider the setup where passive 50 : 50 BSs are placed at various sites of a 2-dimensional square lattice with $(N+1)^2$ $(N = 1, 2, 3, ..)$ sites (Fig. 5.3). Let's label the lattice points by (m, n), where m and n are positive integers. We place BSs at all diagonal points (m, m) and all boundary points $(0, m)$ and $(m, 0)$ $(m = 0, 1, 2, 3, .., N)$. There is an exception, however. At the extreme points $(N, 0)$ and $(0, N)$ we place perfect mirrors rather than BSs as depicted in Fig. 5.4 and Fig. 5.6 in the cases of $N = 1$ and $N = 2$ respectively. All other lattice sites are empty. Our general notation is as follows. The two-mode state at the output of the BS located at (m, n) is denoted by $\rho_{\text{out}}^{(m,n)}$. Let's index various objects corresponding to the two ports of BS by x and y, the directions of propagation of the fields. In our setup the frequency and the polarization of the fields do not change and hence x and y effectively are the mode indices. The states input at the two ports of the BS located at the site (m, n) are denoted by $\rho_x^{(m,n)}$ and $\rho_y^{(m,n)}$ respectively. In general, $\rho_x^{(m,n)}$ and $\rho_y^{(m,n)}$ are derived from the output state at the the *connected* sites. In the case of boundary sites, we have

$$\begin{aligned} \rho_x^{(m,0)} &= \text{Tr}_y\,[\rho_{\text{out}}^{(\text{m}-1,0)}]\,;\ \rho_y^{(\text{m},0)} = |0\rangle\langle 0| \\ \rho_y^{(0,m)} &= \text{Tr}_x\,[\rho_{\text{out}}^{(0,\text{m}-1)}]\,;\ \rho_x^{(0,\text{m})} = |0\rangle\langle 0| \end{aligned} \tag{5.25}$$

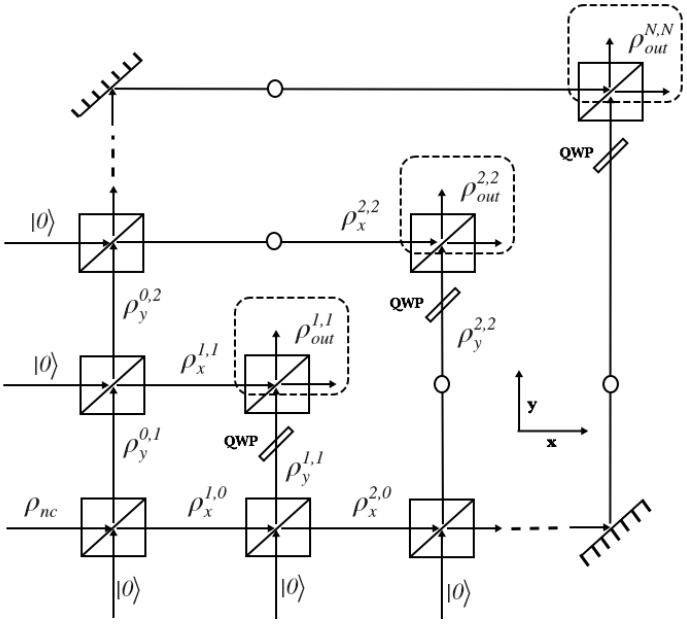

Figure 5.3: Schematic of the BS arrangement for distributing entanglement over 1-dimensional lattice. The dotted boxes represent where entanglement is regenerated. the small circles represent empty sites.

while the in the case of diagonal states we have

$$\begin{aligned} \rho_x^{(m,m)} &= \mathrm{Tr_y}\,[\rho_{\mathrm{out}}^{(0,\mathrm{m})}]\,, \\ \rho_y^{(m,m)} &= \mathrm{Tr_x}\,[\rho_{\mathrm{out}}^{(\mathrm{m},0)}] \;\; ; \;\; \mathrm{m} = 1,2,...,\mathrm{N}-1 \\ \text{and } \rho_{\mathrm{x}}^{(\mathrm{N,N})} &= \rho_y^{(0,N)}\,, \quad \rho_y^{(N,N)} = \rho_x^{(N,0)}. \end{aligned} \tag{5.26}$$

Here, "$\mathrm{Tr_x}$" for example stands for trace over states of the field input along the x direction.

The initial BS at the left bottom corner, i.e. at the point denoted by $(0,0)$, is fed with a nonclassical state ρ_{nc} at one of the input ports while the other port is left with vacuum state. Note that in our notation, $\rho_x^{(0,0)} = \rho_{\mathrm{nc}}$ and $\rho_y^{(0,0)} = |0\rangle\langle 0|$. In general, *one of the ports of any BS placed along the boundary is always in the vacuum state*. Specifically, $\rho_x^{(0,m)} = |0\rangle\langle 0|$ and $\rho_y^{(m,0)} = |0\rangle\langle 0|$ $(m = 1,2,3,..,N)$. From the discussion in the previous sections, it is clear that the states $\rho_x^{(1,0)}$ and $\rho_y^{(0,1)}$ input to the BSs at $(1,0)$ and $(0,1)$ are nonclassical. Hence, these BSs again produce two-mode entangled states at their output. In general, any of the BSs located at the next stage after any given BS will act to destroy the entanglement generated at the output of this BS. However, as we demonstrate below, with a clever arrangement of BSs and other linear optical elements, it is possible to ensure that the entanglement after the BSs at the diagonal points $(1,1)$, $(2,2)$, $(3,3)$ and so on is *not destroyed*.

5.3.2 Regeneration of BS Output Entanglement at a Different Site

Let's illustrate our scheme in the case of $N = 1$ as shown in the Fig. 5.4. The input states at the BSs located at $(1,0)$ and $(0,1)$ sites are denoted by the density operators $\rho_x^{(1,0)}$ and $\rho_y^{(0,1)}$ respectively. The unused ports of the BSs at $(1,0)$ and $(0,1)$ are left in the vacuum state. As we have remarked earlier, the entanglement generated at the output of the BS at $(0,0)$ is destroyed if we place a BS at $(1,0)$ or $(0,1)$ as shown in the Fig. 5.3. This is so, since, the inputs to the BS at $(1,1)$ are, in fact, the reduced density operators $\rho_x^{(1,1)}$ and $\rho_y^{(1,1)}$ and the reduction operation destroys the entanglement.

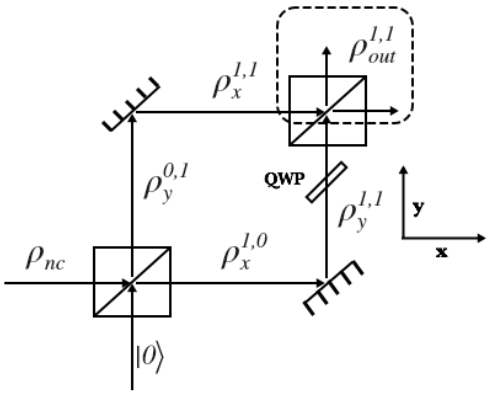

Figure 5.4: Schematic of the BS arrangement for regenerating entanglement at a different lattice site.

Note that $\rho_x^{(1,1)}$ and $\rho_y^{(1,1)}$ are same as the $\rho_y^{(1,0)}$ and $\rho_x^{(0,1)}$ upto the phase factors contributed by free propagation and the perfect mirrors at $(1,0)$ and $(0,1)$. In our geometry, these phase factors are equal and hence are irrelevant. Further, the squeezing phase ϕ_x and ϕ_y corre-

sponding to the Gaussian states $\rho_y^{(1,0)}$ and $\rho_x^{(0,1)}$ are the same as that of the Gaussian state input at the BS at $(0,0)$.

Statement : If a passive 50 : 50 BS is fed with Gaussian state at both the input ports with the squeezing characterized by the complex squeeze parameters $\zeta_x = r\, e^{i\phi_x}$ and $\zeta_y = r\, e^{i\phi_y}$, then (Appendix E)

(a) output state is separable if $\phi_x = \phi_y$,

(b) output state entanglement attains maximal value (dependent on the thermal parameter $\bar{n}$), if $\phi_x = \phi_y + \pi$.

The states input at the two ports of the BS at $(1,1)$, viz. $\rho_x^{(1,1)}$ and $\rho_y^{(1,1)}$, are characterized by equal complex squeeze parameters. From the statement given above, $\rho_{\text{out}}^{(1,1)}$ will be separable, although both $\rho_x^{(1,1)}$ and $\rho_y^{(1,1)}$ are nonclassical. Hence, in order to make $\rho_{\text{out}}^{(1,1)}$ entangled, we insert at one of the ports, an optical element (for example a quarter-wave plate (QWP)) that shifts the squeezing phase by π. As a result of this, $\rho_{\text{out}}^{(1,1)}$ attains maximal possible entanglement. Note that such a phase shifter could have been inserted before any of the input ports of the BS at $(1,1)$ since what is relevant is only the relative phase of squeezing between the states input at the two ports.

Thus, we have demonstrated that the basic scheme in Fig. 5.4 indeed regenerates entanglement at the site $(1,1)$ even though it is destroyed at the site $(0,0)$. However, the entanglement at $(1,1)$ is *less than* what was generated originally at $(0,0)$. This can be understood from the following facts: **(a)** NC of a state is invariant under reflection from a perfect mirror (free propagation and phase shift) as argued in Chap. 3 and **(b)** the total NC at the output of the BS at $(0,0)$, i.e., $\text{NC}(\rho_{\text{x}}^{(1,0)}) + \text{NC}(\rho_{\text{y}}^{(0,1)}) = \text{NC}(\rho_{\text{y}}^{1,1)}) + \text{NC}(\rho_{\text{x}}^{1,1)})$, is less than $\text{NC}(\rho_{\text{nc}})$, the NC of the state input at the BS at $(0,0)$, due to the conservation relation of Ge *et. al.* [104]. Hence, the NC of the states input to BS at $(1,1)$ is less than the NC of states at BS at $(0,0)$ - consequently has less potential to generate entanglement. It is interesting to study quantitatively the dependence of the regenerated entanglement at $(1,1)$ on the NC of the state input to the BS at $(0,0)$ or equivalently $1/l_{\text{min}}$, l_{min} being the minimum eigenvalue of σ, the variance matrix of ρ_{nc}.

We compute the entanglement of formation (EOF) (Eq. 5.11) of the entangled state at $(1,1)$. For comparison, we also evaluate for this state the logarithmic negativity (E_{N}) [105]. A straightforward but tedious calculation involving variance matrices of the relevant reduced

output states after each BS leads us to the analytical results

$$\begin{aligned}\mathrm{EOF}(\rho^{\mathrm{out}}_{\mathrm{site1}}) &= \frac{1}{4(1+2\,l_{\mathrm{min}})}\Big\{(3+2\,l_{\mathrm{min}})\ln(3+2\,l_{\mathrm{min}}) \\ &\quad -(1-2\,l_{\mathrm{min}})\ln(1-2\,l_{\mathrm{min}})\Big\} \\ &\quad -\ln 8(1+2\,l_{\mathrm{min}}), \\ E_{\mathrm{N}}(\rho^{\mathrm{out}}_{\mathrm{site1}}) &= -\ln\frac{1+2\,l_{\mathrm{min}}}{2}. \end{aligned} \tag{5.27}$$

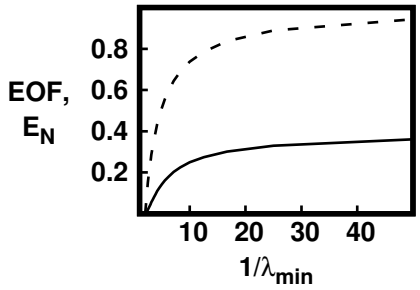

Figure 5.5: Plot of EOF (solid line) and E_{N} (dashed line) vs $\frac{1}{l_{\mathrm{min}}}$.

In Fig. 5.5 we have plotted the dependence of EOF and E_{N} given in Eq. (5.27) on the $\frac{1}{l_{\mathrm{min}}}$. It is evident from Fig. 5.5 that more the input state is nonclassical, more entanglement is regenerated at $(1,1)$.

5.3.3 Spatial Redistribution of the BS Generated Entanglement

We shall now give an outline of how we can embed the basic scheme of Fig. 5.4 within an extended scheme that will allow us to accomplish the task of redistribute entanglement generated at the output of the BS at $(0,0)$ over a 1-dimensional lattice of points (m,m) $(m = 1,2,3,..,N)$.

Let's for simplicity consider the $N = 2$ case as depicted in Fig. 5.6. The present scheme is an extension of the basic scheme in Fig. 5.4 in the sense that while the entire reduced output states after the BS at $(0,0)$ were directed into the BS at $(1,1)$, now, due to presence of BSs (rather than perfect mirrors) at $(1,0)$ and $(0,1)$, a part of this output is available for directing into the BS at $(2,2)$. Two points are worth noting here. *Firstly*, the state at the output of the BS at $(2,2)$ is entangled because the inputs are nonclassical, and we have also made sure that the two input states are characterized by different squeezing phases by putting a phase shifter in the arm between $(2,0)$ and $(2,2)$. *Secondly*, the entanglement generated at the output of the BS at $(1,1)$ *is not destroyed* because there are no BSs placed at the output of the BS at $(1,1)$. Clearly, the entanglement at $(1,1)$ is less than what it was in the basic scheme of Fig. 5.4 because some of it has been regenerated at $(2,2)$. Thus, we have managed to redistribute the entanglement at the output of the BS at $(0,0)$ by regenerating it at two different sites,

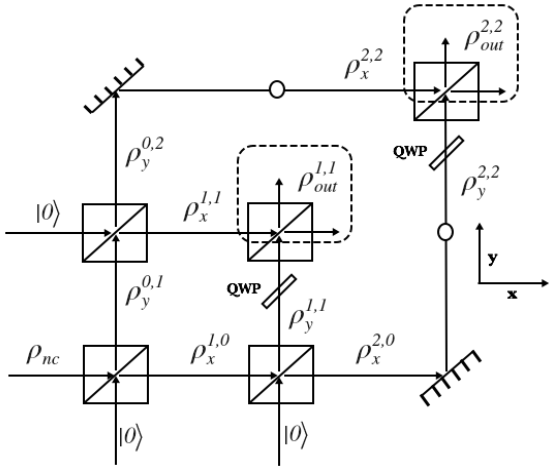

Figure 5.6: Schematic of the BS arrangement for redistributing entanglement at two different lattice sites.

viz, $(1,1)$ and $(2,2)$.

The scheme of Fig. 5.6 can be further extended by considering a 2-dimensional lattice with $(N+1)^2$ sites, with an appropriate placement of BSs, perfect mirrors and phase shifters as mentioned earlier (Fig. 5.3), and one can redistribute entanglement over a 1-dimensional lattice with N lattice points $(1,1)$, $(2,2)$, ..., (N,N).

Chapter 6

Thesis in a Nutshell: Conclusion and Future Prospects

In this thesis we have analyzed various information theoretic aspects of a class of two-mode non-Gaussian entangled states light, generated by a BS from input single mode nonclassical non-Gaussian states. These input states generated under two distinct NC inducing operations, namely photon addition/subtraction and quadrature squeezing, applied on the vacuum state in different orders, could be seen as the states generated under multiple nonclassicality inducing operations (MNIO). The particular single mode states that we have considered are photon added squeezed vacuum state (PAS), photon subtracted squeezed vacuum state (PSS) and squeezed number state (SNS).

We have brought out some interesting nonclassical features of these states in terms of the presence and/or absence of sub-Poissonian and squeezing character, in different parameter regimes. The BS output entanglement in the case of SNS as input is found to be a monotonic function of the input NC as measured by the input state parameters, viz., number of photon addition (m) and the squeeze parameter (r); however, in the case of input PAS, the BS output entanglement has exhibited a non-monotonic dependence. We have attempted to understand this counterintuitive result in terms of an effective NC measure of the states SNS and PAS in terms of the existing measures. However, we have found that the results obtained with the existing measures do not corroborate the BS entanglement curves. We have qualitatively explained this non-monotonic behavior in terms of the mutual competition between the NC-inducing operations, i.e., photon addition and quadrature squeezing, as manifest in the contours of the associated Husimi-Kano Q distributions.

To explain the non-monotonicity in the BS generated entanglement with input PAS we

have further proposed a new Wehrl entropy based measure of NC for the single mode pure states. We have demonstrated that the newly proposed measure reproduces the curves of NC for the input states PAS and SNS, consistent with the corresponding entanglement. We have also shown that our measure is a monotonically increasing function of a well-known measure known as the nonclassical depth, in the case of Gaussian pure states.

We have further studied quantitative and qualitative aspects of QT, using the BK protocol with the BS generated entangled non-Gaussian resources with input MNIO class of states. The primary objective of our study has been to identify what are, besides entanglement, the necessary and/or sufficient conditions on the two-mode entangled states to achieve QT. We have observes that while squeezed vacuum affinity (SVA) is not a genuine attribute of the two-mode entangled resource states, as it is identically zero for a large subclass of the BS generated states, EPR correlation is found not to be sufficient for QT. In conjunction with the earlier results where the EPR correlation has been found not to be always necessary for QT, our work leads us to the conclusion that EPR correlation is neither necessary nor sufficient for QT, in general. We then have investigated the question of whether $U(2)$-invariant two-mode squeezing could be relevant for QT. Our numerical results on the BS entangled resource states as well as the de-Gaussified TMSV indicate that $U(2)$-invariant squeezing appears to be necessary for QT, but not sufficient. In view of the numerical results we propose that $U(2)$-invariant squeezing could be a necessary criterion for QT.

Finally, we have revisited the question of the extent to which input NC is converted into BS output entanglement that was studied earlier by Ge *et. al.* [104]. Our results obtained with a different measure of entanglement, corroborate the conservation law relating input NC, output NC and BS output entanglement. We have further looked into the question of conversion of input NC into BS output entanglement in the non-Gaussian case by focussing on two particular aspects of NC, viz., sub-Poissonian and quadrature squeezing character. We have shown analytically that, compared to the squeezing character, sub-Poissonian character is used up by the BS to greater extent for generating entanglement. We have also addressed the question of regenerating and redistributing the BS entanglement at some different locations. In this regard we have proposed a scheme, using BSs and other linear optical elements such as phase shifter and perfect mirrors, that accomplishes the task of redistributing the BS generated entanglement at different sites on a 1-dimensional lattice.

Lastly, there exists a well known analogy between two-mode quantum states of light and classical paraxial beams [106]. The paraxial beams propagate in the z direction while x and y are the coordinates in the transverse plane. Analogous to the electric field of the beam

projected along the transverse plane $\mathscr{E}(x,y)$ is the wave function associated with the two-mode quantum state of light $\psi(X,Y)$ [107]. Note that X and Y here refer to the quadrature variables, $X = \frac{1}{\sqrt{2}}(a + a^\dagger)$ and $Y = \frac{1}{\sqrt{2}}(b + b^\dagger)$. A lot of work has been around in the literature exploiting the above-mentioned analogy and several interesting results have been reported in respect of vortices [108, 109], non-quantum entanglement [110], violation of Bell inequalities [111] *etc.*

From our perspective it is desirable to look into the connection between NG and vorticity (clearly Gaussian beams do not support vortex), both quantitatively as well as qualitatively using an adaptation of the NG measure for quantum states given by Ivan *et. al.* [67] to paraxial beams.

Appendices

A $R(z,\eta)$ for PAS and SNS

Introducing the expression of $P(\gamma)$ in terms of density operator ρ, the η convoluted function $R(z,\eta)$ can be written in terms of ρ as,

$$R(z,\eta) = \frac{e^{\frac{|z|^2}{1-\eta}}}{1-\eta}\int \frac{d^2\beta}{\pi}\langle -\beta|\rho|\beta\rangle e^{-\frac{(2\eta-1)|\beta|^2+(z^*\beta-z\beta^*)}{1-\eta}}. \tag{A.1}$$

For PAS, we have $\langle\beta|\psi_{\rm PAS}\rangle = \frac{\beta^{*m}}{\sqrt{\mu N_m}}e^{-\frac{|\beta|^2}{2}+\frac{\tau}{2}\beta^2}$. Thus, the $R(z,\eta)$ for PAS becomes,

$$\begin{aligned} R(z,\eta)_{\rm PAS} &= \frac{e^{\frac{|z|^2}{1-\eta}}}{1-\eta}\int \frac{d^2\beta}{\pi}\langle -\beta|\psi_{\rm PAS}\rangle\langle\psi_{\rm PAS}|\beta\rangle\ \exp\Big(-\frac{(2\eta-1)|\beta|^2+(z^*\beta-z\beta^*)}{1-\eta}\Big) \\ &= \frac{e^{\frac{|z|^2}{1-\eta}}}{\mu N_m(1-\eta)}\int \frac{d^2\beta}{\pi}(-|\beta|^{2m})\ \exp\Big(-\frac{\eta|\beta|^2}{1-\eta}+\frac{\tau(\beta^2+\beta^{*2})}{2}+\frac{z\beta^*-z^*\beta}{1-\eta}\Big) \end{aligned} \tag{A.2}$$

One can derive the above non-Gaussian integral using parametric differentiation as,

$$\begin{aligned} R(z,\eta)_{\rm PASVS} &= \frac{(-1)^m}{\mu N_m(1-\eta)}e^{\frac{|z|^2}{1-\eta}}\partial_a^m\partial_b^m\Big[\exp\Big(-\frac{\eta}{1-\eta}|\beta|^2+\frac{\tau}{2}(\beta^2+\beta^{*2})-\frac{z^*}{1-\eta}\beta+\frac{z}{1-\eta}\beta^*\Big) \\ &\qquad \exp\Big(a\beta+b\beta^*\Big)\Big]_{a=0,b=0} \\ &= \frac{(-1)^m}{\mu N_m(1-\eta)}e^{\frac{|z|^2}{1-\eta}}\partial_a^m\partial_b^m\Big[\int\frac{d^2\beta}{\pi}\exp\Big(-\frac{\eta}{1-\eta}|\beta|^2+\frac{\tau}{2}(\beta^2+\beta^{*2})\Big) \\ &\qquad \exp\Big((a-\frac{z^*}{1-\eta})\beta+(b+\frac{z}{1-\eta})\beta^*\Big)\Big]_{a=0,b=0} \end{aligned} \tag{A.3}$$

For any Gaussian integral, we know that

$$\int\frac{d^2z}{\pi}e^{\zeta|z|^2+\xi z+\eta z^*+fz^2+gz^{*2}} = \frac{e^{\frac{-\zeta\xi\eta+f\eta^2+g\xi^2}{\zeta^2-4fg}}}{\sqrt{\zeta^2-4fg}}. \tag{A.4}$$

provided $\zeta^2-4fg>0$. Using formula (A.4), for $R(z,\eta)_{\rm PAS}$, we get,

$$\begin{aligned} R(z,\eta)_{\rm PAS} &= \frac{A_1^m e^{\frac{|z|^2}{1-\eta}}}{\mu N_m\sqrt{\eta^2-\tau^2(1-\eta)^2}}W_0(z,z^*,\eta)\partial_a^m\partial_b^m\Big[e^{A_1a^2+B_1a-B_1^*+D_1ab+A_1b^2}\Big]_{a=0,b=0} \\ &= \frac{A_1^m e^{\frac{|z|^2}{1-\eta}}}{\mu N_m\sqrt{\eta^2-\tau^2(1-\eta)^2}}W_0(z,z^*,\eta)\sum_{k=0}^{m}(-1)^m\frac{m!}{k!(m-k)!}\Big(\frac{D_1}{A_1}\Big)^k L_{m-k}\Big(\frac{|B_1|^2}{4A_1}\Big). \end{aligned} \tag{A.5}$$

where,

$$\begin{aligned} W_0(z,z^*,\eta) &= \exp\Big(-\frac{\frac{\eta}{1-\eta}|z|^2-\frac{\tau}{2}(z^2+z^{*2})}{\eta^2-\tau^2(1-\eta)^2}\Big),\ \ A_1 = \frac{\tau(1-\eta)^2}{2[\eta^2-\tau^2(1-\eta)^2]} \\ B_1 &= \frac{\eta z-\tau(1-\eta)z^*}{\eta^2-\tau^2(1-\eta)^2},\ \ D_1 = \frac{\eta(1-\eta)}{\eta^2-\tau^2(1-\eta)^2}. \end{aligned} \tag{A.6}$$

Similarly, using the technique of parametric differentiation, one can easily derive $R(z,\eta)$ for an SNS. Since $\langle\beta|\psi_{\rm SNS}\rangle = \frac{e^{-\frac{|\beta|^2}{2}+\frac{\tau}{2}\beta^{*2}}}{\sqrt{\mu m!}}\partial_a^m\Big[e^{-\frac{\tau}{2}a^2+\frac{\beta^*}{\mu}a}\Big]_{a=0}$, we have

$$
\begin{aligned}
R(z,\eta)_{\rm SNS} &= \frac{1}{1-\eta}e^{\frac{|z|^2}{1-\eta}}\int\frac{d^2\beta}{\pi}\langle-\beta|\psi_{\rm SNS}\rangle\langle\psi_{\rm SNS}|\beta\rangle\,\exp\Big(-\frac{(2\eta-1)|\beta|^2+(z^*\beta-z\beta^*)}{1-\eta}\Big)\\
&= \frac{e^{\frac{|z|^2}{1-\eta}}}{\mu m!(1-\eta)}\partial_a^m\partial_b^m\Big\{\exp\Big(-\frac{\tau}{2}(a^2+b^2)\Big)\\
&\qquad\int\frac{d^2\beta}{\pi}\exp\Big[-\frac{\eta}{1-\eta}|\beta|^2+(\frac{b}{\mu}-\frac{z^*}{1-\eta})\beta-(\frac{a}{\mu}-\frac{z}{1-\eta})\beta^*+\frac{\tau}{2}(\beta^2+\beta^{*2})\Big]\Big\}_{a=0,b=0}\\
&= \frac{A_2^m e^{\frac{|z|^2}{1-\eta}}}{\mu\sqrt{\eta^2-\tau^2(1-\eta)^2}}W_0(z,z^*,\eta)\partial_a^m\partial_b^m\Big[e^{A_2a^2+B_2a+B_2^*-D_2ab+A_2b^2}\Big]_{a=0,b=0}\\
&= \frac{A_2^m e^{\frac{|z|^2}{1-\eta}}}{\mu\sqrt{\eta^2-\tau^2(1-\eta)^2}}W_0(z,z^*,\eta)\sum_{k=0}^{m}(-1)^{m-k}\frac{m!}{k!(m-k)!}\Big(\frac{D_2}{A_2}\Big)^k L_{m-k}\Big(\frac{|B_2|^2}{4A_2}\Big).
\end{aligned}
\tag{A.7}
$$

where,

$$
W_0(z,z^*,\eta) = exp\Big(-\frac{\frac{\eta}{1-\eta}|z|^2-\frac{\tau}{2}(z^2+z^{*2})}{\eta^2-\tau^2(1-\eta)^2}\Big),\ A_2=\frac{A_1}{\mu^2}-\frac{\tau}{2},\ B_2=\frac{B_1}{\mu},\ D_2=\frac{D_1}{\mu^2}
\tag{A.8}
$$

B $W(z,z^*)$ for PAS and SNS

Here, using the technique discussed in appendix A, we calculate the Wigner function for PAS and SNS. The Wigner distribution for any density operator is given as,

$$
W(z,z^*) = 2e^{2|z|^2}\int\frac{d^2\beta}{\pi}\langle-\beta|\rho|\beta\rangle e^{2(z\beta^*-z^*\beta)}.
\tag{B.1}
$$

Thus, the Wigner distributions for PAS and SNS are given as

$$
\begin{aligned}
W_{\rm PAS}(\alpha,\alpha^*) &= 2e^{2|\alpha|^2}\int\frac{d^2\beta}{\pi}\langle-\beta|\psi_{\rm PAS}\rangle\,\langle\psi_{\rm PAS}|\beta\rangle\exp\Big(2(\alpha\beta^*-\alpha^*\beta)\Big)\\
&= \frac{2e^{2|\alpha|^2}}{N_m\mu}\int\frac{d^2\beta}{\pi}e^{-|\beta|^2+2(\alpha\beta^*-\alpha^*\beta)}\partial_p^m\Big[\int\frac{d^2\gamma}{\pi}e^{-|\gamma|^2-\beta^*\gamma+p\gamma^*+\frac{\tau}{2}\gamma^{*2}}\Big]_{p=0}\\
&\qquad\qquad\partial_q^m\Big[\int\frac{d^2\eta}{\pi}e^{-|\eta|^2+q\eta+\beta\eta^*+\frac{\tau}{2}\eta}\Big]_{q=0}\\
&= \frac{2e^{2|\alpha|^2}}{N_m\mu}\partial_p^m\partial_q^m\Big[\frac{1}{\sqrt{1-\tau^2}}e^{\frac{1}{1-\tau^2}\Big(-(p-2\alpha)(q-2\alpha^*)+\frac{\tau}{2}\overline{(p-2\alpha)^2+(q-2\alpha^*)^2}\Big)}\Big]_{p=0,q=0}\\
&= \frac{2e^{2[(\mu^2+\nu^2)|\alpha|^2-\mu\nu(\alpha^2+\alpha^{*2})]}}{N_m}\partial_p^m\partial_q^m\Big[e^{\frac{\mu\nu}{2}(p^2+q^2)-\mu^2pq+2\mu\overline{q(\mu\alpha-\nu\alpha^*)+p(\mu\alpha^*-\nu\alpha)}}\Big]_{p=0,q=0}\\
&= \frac{2(-1)^m m!e^{-2|\bar\alpha|^2}\mu^m\nu^m}{2^mN_m}\Sigma_{k=0}^{m}\frac{m!(\frac{\tau}{2})^{-k}}{k!(m-k)!}L_{m-k}\Big(\frac{2|\bar\alpha|^2}{\tau}\Big).
\end{aligned}
\tag{B.2}
$$

and

$$\begin{aligned}
W_{\rm SNS}(\alpha,\alpha^*) &= 2e^{2|\alpha|^2}\int\frac{d^2\beta}{\pi}\langle-\beta|\psi_{\rm SNS}\rangle\langle\psi_{\rm SNS}|\beta\rangle e^{2(\alpha\beta^*-\alpha^*\beta)}\\
&= \frac{2e^{2|\alpha|^2}}{m!\mu}\partial_p^m\partial_q^m\left[e^{-\frac{\tau}{2}(p^2+q^2)}\int\frac{d^2\beta}{\pi}e^{-|\beta|^2+(\frac{q}{\mu}-2\alpha^*)\beta-(\frac{p}{\mu}-2\alpha)\beta^*+\frac{\tau}{2}(\beta^2+\beta^{*2})}\right]_{p=0,q=0}\\
&= \frac{2e^{2[(\mu^2+\nu^2)|\alpha|^2-\mu\nu(\alpha^2+\alpha^{*2})]}}{m!}\partial_p^m\partial_q^m\left[e^{-pq+2q(\mu\alpha-\nu\alpha^*)+2p(\mu\alpha^*-\nu\alpha)}\right]_{p=0,q=0}\\
&= 2(-1)^m e^{-2|\bar\alpha|^2}L_m(4|\bar\alpha|^2),
\end{aligned}\tag{B.3}$$

where $\mu=\cosh r,\nu=\sinh r,\bar\alpha=\mu\alpha-\nu\alpha^*$. Evidently, for $\eta=\frac{1}{2}$, Eqs. (A.5) and (A.7) coincide with Eqs. (B.2) and (B.3) respectively, since for $\eta=\frac{1}{2}$, $R(z,\eta)$ coincides with the Wigner function, $W(z,z^*)$.

C $U(2)$ Squeezing for BS Output State for Single Mode Gaussian Input State

Let's consider the column vectors $R_{\rm in}$ and $R_{\rm out}$ for the input and output quadrature operators as

$$R_{\rm in}=\begin{bmatrix}x^a_{\rm in}\\ p^a_{\rm in}\\ x^b_{\rm in}\\ p^b_{\rm in}\end{bmatrix},\quad R_{\rm out}=\begin{bmatrix}x^a_{\rm out}\\ p^a_{\rm out}\\ x^b_{\rm out}\\ p^b_{\rm out}\end{bmatrix}.\tag{C.1}$$

The quadrature operators $\{x^a_{\rm in},p^a_{\rm in}\}$ corresponding to annihilation and creation operators $a_{\rm in},a^\dagger_{\rm in}$ are defined as $x^a_{\rm in}=\frac{1}{\sqrt{2}}(a_{\rm in}+a^\dagger_{\rm in})$ and and $p^a_{\rm in}=\frac{1}{i\sqrt{2}}(a_{\rm in}-a^\dagger_{\rm in})$. Other related operators are defined in the same way.

Using the transformation matrix between input and output mode operators Eq. (**??**) for a 50 : 50 BS, it is easy to show that $R_{\rm out}$ is related to $R_{\rm in}$ by the transformation, $R_{\rm out}=SR_{\rm in}$, i.e.,

$$\begin{bmatrix}x^a_{\rm out}\\ p^a_{\rm out}\\ x^b_{\rm out}\\ p^b_{\rm out}\end{bmatrix}=\begin{bmatrix}\frac{1}{\sqrt{2}} & 0 & \frac{1}{\sqrt{2}} & 0\\ 0 & \frac{1}{\sqrt{2}} & 0 & \frac{1}{\sqrt{2}}\\ -\frac{1}{\sqrt{2}} & 0 & \frac{1}{\sqrt{2}} & 0\\ 0 & -\frac{1}{\sqrt{2}} & 0 & \frac{1}{\sqrt{2}}\end{bmatrix}\begin{bmatrix}x^a_{\rm in}\\ p^a_{\rm in}\\ x^b_{\rm in}\\ p^b_{\rm in}\end{bmatrix}.\tag{C.2}$$

It is well known that, under the linear transformation $S:R_{\rm in}\to SR_{\rm in}$, the input variance matrix $V_{\rm in}$ transforms as $S:V_{\rm in}\to SV_{\rm in}S^T$. Let's consider that, a single mode Gaussian state with variance matrix σ is fed to one of the input ports of a 50 : 50 BS while the other input port is left with vacuum. Since the total input state is a product state, variance matrix of the

total input state will be in a block diagonal form as $V_{\rm in} = \begin{pmatrix} \sigma & 0 \\ 0 & \frac{I}{2} \end{pmatrix}$. Using the transformation S given in Eq. (C.2) we get the output variance matrix as,

$$V_{\rm out} = S\,V_{\rm in}S^T = \frac{1}{2}\begin{pmatrix} \sigma + \frac{I}{2} & -\sigma + \frac{I}{2} \\ -\sigma + \frac{I}{2} & \sigma + \frac{I}{2} \end{pmatrix}, \tag{C.3}$$

where I is the 2×2 identity matrix. For the sake of simplicity let's consider a diagonal form of the single mode variance matrix σ as $\sigma = {\rm diag}\{\eta_{\rm a}, \zeta_{\rm a}\}$. The $U(2)$ squeezing of the matrix $V_{\rm out}$ is defined in terms of its minimum eigenvalue. The eigenvalues of $V_{\rm out}$ could be obtained solving the characteristic equation

$$\begin{aligned} &\det\,(V_{\rm out} - \lambda\, I) = 0 \\ &\Rightarrow \Big\{(\eta_a + \frac{1}{2} - 2\lambda)^2 - (\eta_a - \frac{1}{2})^2\Big\}\Big\{(\zeta_a + \frac{1}{2} - 2\lambda)^2 - (\zeta_a - \frac{1}{2})^2\Big\} = 0 \\ &\Rightarrow 4(\eta_a - \lambda)(\zeta_a - \lambda)(1 - 2\lambda)^2 = 0 \\ &\Rightarrow \lambda = \frac{1}{2},\ \eta_a,\ \zeta_a. \end{aligned} \tag{C.4}$$

As quite explicit from the Eq. (C.4), the least eigenvalue of $V_{\rm out}$ is given by $\lambda_{\rm min} = \min[1/2, \eta_a, \zeta_a]$. As quite explicit from the expression of $\lambda_{\rm min}$, BS output variance matrix represents squeezing ($\lambda_{\rm min} < \frac{1}{2}$) only if either of η_a and ζ_a becomes smaller than $\frac{1}{2}$. To be specific, let's assume that $\eta_a \geq \zeta_a$. In this case the minimum eigenvalue will be given by $\lambda_{\rm min} = \min[1/2, \zeta_a]$. This indicates that the BS output state will be quadrature squeezed only if the input single mode state is quadrature squeezed.

It is noteworthy that in the derivation of the squeezing condition in Eq. (C.4) we have used the input variance matrix σ to be of diagonal form, for the sake of simplicity. However, this condition is not specific to the diagonal form of σ only. By using a suitable symplectic operation $Sp(2, R)$ one can recast any single mode variance matrix in the diagonal form as we have considered for σ. Since, the eigen spectrum doesn't change under symplectic transformations, the squeezing criterion remains invariant under such symplectic transformations [56].

D Mandel Q parameter for BS Output Reduced State

Mandel Q parameter for any state is defined as

$$Q \;=\; \frac{\langle N^2\rangle \,-\, \langle N\rangle^2}{\langle N\rangle} \;-\; 1, \tag{D.1}$$

where, $N = a^\dagger a$ is the number operator. Let's consider a single mode quantum optical state $\rho = \sum_{k,l=0}^{\infty} C_{k,l} \, |k\rangle\langle l|$, where, $\sum_{k=0}^{\infty} |C_{k,k}|^2 = 1$. The quantities $\langle N^2\rangle$ and $\langle N\rangle$ are defined as

$$\langle N^2\rangle = \sum_{k=0}^{\infty} |C_{k,k}|^2 \, k^2 \;\; \& \;\; \langle N\rangle = \sum_{k=0}^{\infty} |C_{k,k}|^2 \, k. \tag{D.2}$$

It is well known that the BS output state, with ρ as input to one of the input ports while other port is left with vacuum, is given by [17]

$$\rho_{\text{out}} = \sum_{k,l=0}^{\infty} \sum_{p=0}^{k} \sum_{q=0}^{l} C_{k,l} \, C_k^p \, (C_l^q)^* \, |k-p\rangle\langle l-q| \otimes |p\rangle\langle q|, \tag{D.3}$$

where, $\sum_{p=0}^{k} |C_k^p|^2 = \sum_{q=0}^{l} |C_l^q|^2 = 1$. The reduced state, obtained by taking partial trace of ρ_{out} over any of the modes, is given by

$$\rho_{\text{out}}^{\text{red}} = \sum_{k,l=0}^{\infty} \sum_{p=0}^{\min(k,l)} C_{k,l} \, C_k^p \, (C_l^p)^* \, |k-p\rangle\langle l-p|. \tag{D.4}$$

The quantities $\langle N^2\rangle$ and $\langle N\rangle$ for $\rho_{\text{out}}^{\text{red}}$ are given as

$$\begin{aligned}
\langle N\rangle_{\text{out}}^{\text{red}} &= \sum_{k,l=0}^{\infty} \sum_{p=0}^{\min(k,l)} C_{k,l} \, C_k^p \, (C_l^p)^* \, \langle l-p|N|k-p\rangle \\
&= \sum_{k,l=0}^{\infty} \sum_{p=0}^{\min(k,l)} C_{k,l} \, C_k^p \, (C_l^p)^* \, (k-p) \, \delta_{k,l} \\
&= \sum_{k=0}^{\infty} C_{k,k} \left\{ k \sum_{p=0}^{k} |C_k^p|^2 + \sum_{p=0}^{k} |C_k^p|^2 \, p \right\} \\
&= \sum_{k=0}^{\infty} C_{k,k} \, \frac{k}{2} = \frac{\langle N\rangle}{2} \;\; \& \qquad \text{(D.5a)} \\
\langle N^2\rangle_{\text{out}}^{\text{red}} &= \sum_{k,l=0}^{\infty} \sum_{p=0}^{\min(k,l)} C_{k,l} \, C_k^p \, (C_l^p)^* \, \langle l-p|N^2|k-p\rangle \\
&= \sum_{k,l=0}^{\infty} \sum_{p=0}^{\min(k,l)} C_{k,l} \, C_k^p \, (C_l^p)^* \, (k-p)^2 \, \delta_{k,l} \\
&= \sum_{k=0}^{\infty} C_{k,k} \left\{ k^2 \sum_{p=0}^{k} |C_k^p|^2 - 2k \sum_{p=0}^{k} |C_k^p|^2 \, p + \sum_{p=0}^{k} |C_k^p|^2 \, p^2 \right\} \\
&= \sum_{k=0}^{\infty} C_{k,k} \, \frac{k^2+k}{2} = \frac{\langle N^2\rangle + \langle N\rangle}{4}. \qquad \text{(D.5b)}
\end{aligned}$$

Putting the expressions of $\langle N\rangle_{\text{out}}^{\text{red}}$ and $\langle N^2\rangle_{\text{out}}^{\text{red}}$ in the definition of Q parameter (Eq. D.1)

we get

$$\begin{aligned} Q_{\text{out}}^{\text{red}} &= \frac{\langle N^2\rangle_{\text{out}}^{\text{red}} - \langle N\rangle_{\text{out}}^{\text{red}}}{\langle N\rangle_{\text{out}}^{\text{red}}} - 1 \\ &= \frac{\frac{\langle N^2\rangle + \langle N\rangle}{4} - \frac{\langle N\rangle^2}{4}}{\frac{\langle N\rangle}{2}} - 1 \\ &= \frac{1}{2}\left\{\frac{\langle N^2\rangle - \langle N\rangle^2}{\langle N\rangle} + 1\right\} - 1 = \frac{1}{2}\left(Q + 1 + 1\right) - 1 = \frac{Q}{2}. \end{aligned} \tag{D.6}$$

E On the Condition of Inseparability for the BS Output Gaussian State with Identical Gaussian Input State at both Input Ports

Let's consider a single mode nonclassical Gaussian state $\rho_{\text{nc}}^{\text{G}}$ as a squeezed thermal state $\rho_{\text{STS}} = S(\zeta)\,\rho_{\text{th}}(\bar{n})\,S^{\dagger}(\zeta)$, where, $S(\zeta) = e^{\frac{\zeta\, a^{\dagger 2} - \zeta^{*}\, a^2}{2}}$ and $\zeta = r\, e^{i\phi}$. The NC of ρ_{STS} is ensured by the fact $r > \frac{1}{2}\ln[2\bar{n}+1]$. For the sake of simplicity, one can neglect the rigid phase space displacement in the expression of a general single mode Gaussian state given by Chaturvedi and Srinivasan [54]. Let's consider a passive 50 : 50 BS with both of input ports are fed with the squeezed thermal states ρ_{STS} with same r and $\bar{n}$ but different phase/direction of squeezing, say, ϕ_a and ϕ_b, where, a and b denote two-input spatial modes. Then the total input state is given by

$$\rho_{\text{in}} = S_a(\zeta)\,\rho_{\text{th}}(\bar{n})\,S_a^{\dagger}(\zeta) \otimes S_b(\zeta)\,\rho_{\text{th}}(\bar{n})\,S_b^{\dagger}(\zeta), \tag{E.1}$$

where, S_a corresponds to ϕ_a and S_b corresponds to ϕ_b. With the input state given in Eq. (E.1), the BS output state is given by

$$\begin{aligned} \rho_{\text{out}} &= U_{\text{BS}}^{\dagger}\,\rho_{\text{in}}\,U_{\text{BS}} \\ &= \{U_{\text{BS}}^{\dagger}\,S_a(\zeta)\,S_b(\zeta)\,U_{\text{BS}}\}\,\{U_{\text{BS}}^{\dagger}\,\rho_{\text{th}}(\bar{n}) \otimes \rho_{\text{th}}(\bar{n})\,U_{\text{BS}}\}\,\{U_{\text{BS}}^{\dagger}\,S_a^{\dagger}(\zeta)\,S_b^{\dagger}(\zeta)\,U_{\text{BS}}\}, \end{aligned} \tag{E.2}$$

where, U_{BS} is the BS transformation on the mode annihilation operators a and b.

Since, to yield inseparability/entanglement at the output of a passive BS, atleast one of the input states must be nonclassical [13, 16], it is quite straightforward to infer that under the BS transformation input thermal state product still remains as the product of two thermal states, i.e., $U_{\text{BS}}^{\dagger}\,\rho_{\text{th}}(\bar{n}) \otimes \rho_{\text{th}}(\bar{n})\,U_{\text{BS}} = \rho_{\text{th}}(\bar{n}) \otimes \rho_{\text{th}}(\bar{n})$. Hence, the only part that might give rise to entanglement in Eq. (E.2) is the BS evolved operator, i.e., $U_{\text{BS}}^{\dagger}\,S_a(\zeta)\,S_b(\zeta)\,U_{\text{BS}}$.

A 50 : 50 BS can be modeled by the transformation $U_{\text{BS}} = e^{\frac{i}{\sqrt{2}}(a^{\dagger}a - b^{\dagger}b)}$ that makes the transformation on the mode annihilation operators given in Eq. 2.1. Using the BS transfor-

mation on the mode operators, a and b, it is quite straightforward to check that

$$U_{\rm BS}^{\dagger}\, S_a(\zeta)\, S_b(\zeta)\, U_{\rm BS} \;=\; \exp\,\frac{r}{2}\Big[a^{\dagger 2}\Big(\frac{e^{i\phi_a}\,+\,e^{i\phi_b}}{2}\Big)\,-\,a^2\Big(\frac{e^{-i\phi_a}\,+\,e^{-i\phi_b}}{2}\Big) + b^{\dagger 2}\Big(\frac{e^{i\phi_a}\,+\,e^{i\phi_b}}{2}\Big)\,-\,b^2\Big(\frac{e^{-i\phi_a}\,+\,e^{-i\phi_b}}{2}\Big) + 2r(a^{\dagger}b^{\dagger}\Big(\frac{e^{i\phi_a}\,-\,e^{i\phi_b}}{2}\Big)\,-\,ab\Big(\frac{e^{-i\phi_a}\,-\,e^{-i\phi_b}}{2}\Big))\Big]. \tag{E.3}$$

As is evident from Eq. (E.3), with the setting $\phi_a \,=\, \phi_b \,=\, \phi$, while the first two terms within the bracket survives, the last term vanishes. This leads to the result

$$U_{\rm BS}^{\dagger}\, S_a(\zeta)\, S_b(\zeta)\, U_{\rm BS} \;=\; e^{\frac{r}{2}\Big[(a^{\dagger 2}e^{i\phi}\,-\,a^2e^{-i\phi})\,+\,(b^{\dagger 2}e^{i\phi}\,-\,b^2e^{-i\phi})\Big]} \;=\; S_a(\zeta)\, S_b(\zeta), \tag{E.4}$$

that in turn reduces Eq. (E.2) to

$$\rho_{\rm out}\Big|_{\phi_a\,=\,\phi_b} \;=\; S_a(\zeta)\,\rho_{\rm th}(\bar{n})\,S_a^{\dagger}(\zeta)\,\otimes\,S_b(\zeta)\,\rho_{\rm th}(\bar{n})\,S_b^{\dagger}(\zeta), \tag{E.5}$$

i.e., a separable state. On the other hand, with $\phi_a \,=\, \phi_b \,+\, \pi \,=\, \phi$, the first two terms within bracket in Eq. (E.3) vanishes while the last term reduces to $r\,(e^{i\phi}\;a^{\dagger}b^{\dagger}\;-\;e^{-i\phi}\;ab)$. As a consequence, with $\phi_a \,=\, \phi_b \,+\, \pi$, Eq. (E.2) reduces to

$$\rho_{\rm out}\Big|_{\phi_a\,=\,\phi_b\,+\,\pi} \;=\; S_{ab}(\zeta)\,\rho_{\rm th}(\bar{n})\,\otimes\,\rho_{\rm th}(\bar{n})\,S_{ab}^{\dagger}(\zeta), \tag{E.6}$$

i.e., an inseparable or entangled state. It is also noteworthy that with $\phi_a \,=\, \phi_b \,+\, \pi$, one obtains a maximally entangled state in Eq. (E.6) depending upon the thermal parameter $\bar{n}$.

References

[1] A. Einstein, B. Podolsky, and N. Rosen, Phys. Rev. **47**, 777 (1935).

[2] E. Schrodinger, Naturwiss **23**, 807 (1935).

[3] M. Nielsen and I. Chuang, *Quantum Computation and Quantum Information*, 10^{th} Anniversary Ed., Cambridge University Press, Cambridge (2010).

[4] R. Horodecki, P. Horodecki, M. Horodecki and K. Horodecki, Rev. Mod. Phys. **81**, 865 (2009).

[5] P. Kok and B. W. Lovett, *Introduction to Optical Quantum Information Processing*, Cambridge University Press, New York (2010).

[6] S. L. Braunstein and A. Pati, *Quantum Information with Continuous Variables*, Kluwer Academy, Dordrecht (2003).

[7] S. L. Braunstein and P. V. Loock, Rev. Mod. Phys. **77**, 513 (2005).

[8] J. Marcinkiewicz, Math. Z. **44**, 612 (1939)

[9] A. K. Rajagopal, E. C. G. Sudarshan, Phys. Rev. A **10**, 1852 (1974).

[10] D. F. Walls and J. G. Milburn, *Quantum Optics*, 2^{nd} Edition, Springer-Verlag Berlin, Heidelberg (2008).

[11] C. Weedbrook, S. Pirandola, R. Garcia-Patron, N. J. Cerf, T. C. Ralph, J. H. Shapiro and L. Llyod, Rev. Mod. Phys. **84**, 621 (2012).

[12] G. Adesso and F. Illuminati, J. Phys. A: Math. Theor. **40**, 7821 (2007).

[13] M. S. Kim, W. Son, V. Buzek and P. L. Knight, Phys. Rev. A **65**, 032323 (2002).

[14] X.-b Wang, Phys. Rev. A **66**, 024303 (2002).

[15] M. M. Wolf, J. Eisert and M. B. Plenio, Phys. Rev. Lett. **90**, 047904 (2003).

[16] J. S. Ivan, S. Chaturvedi, E. Ercolessi, G. Marmo, G. Morandi, N. Mukunda, and R. Simon, Phys. Rev. A **83**, 032118 (2011).

[17] G. S. Agarwal and J. Banerji, J. Phys. A **39**, 11503 (2005).

[18] W. P. Schleich, *Quantum Optics in Phase Space*, 1st Edition, WILEY-VCH, Berlin (2001).

[19] W. Vogel and D. G. Welsch, *Quantum Optics*, 3rd Edition, WILEY-VCH, Weinheim (2006).

[20] C. C. Gerry and P. L. Knight, *Introductory quantum Optics*, Cambridge University Press, New York (2005).

[21] M. S. Kim, F. A. M. de Oliveira, and P. L. Knight, Phys. Rev. A **40**, 2494 (1989).

[22] Z. Zhang and H. Fan, Phys. Lett. A **165**, 14 (1992).

[23] P. Král, J. Mod. Opt. **37**, 889 (1990).

[24] Z.-Z. Xin *et al.*, J. Phys. B **29**, 4493 (1996).

[25] V. I. Man'ko and A. Wünsche, Quantum Semiclassical Opt. **9**, 381 (1997).

[26] E. P. Wigner, Phys. Rev. **40**, 749 (1932).

[27] G. S. Agarwal and E. Wolf, Phys. Rev. D **2**, 2187 (1970);

[28] R. J. Glauber, Phys. Rev. Lett. **10**, 84 (1963); E. C. G. Sudarshan, Phys. Rev. Lett. **10**, 277 (1963).

[29] K. Husimi, Proc. Phys. Math. Soc. Jpn. **22**, 264 (1940); Y. Kano, J. Math. Phys. **6**, 1913 (1965).

[30] K. E. Cahill and R. J. Glauber, Phys. Rev. A **177**, 1882 (1969).

[31] G. S. Agarwal and E. Wolf, Phys. Rev. Lett. **21**, 180 (1968); *ibid.* Phys. Lett. A **26**, 485 (1968); M. Hillery, R. F. O'Connell, M. O. Scully and E. P. Wigner, Phys. Rep. **106**, 121 (1984).

[32] L. Mandel, Phys. Scr. **T12**, 34 (1986).

[33] H. P. Yuen, J. H. Shapiro, Opt. Lett. **4**, 334 (1979); R. S. Bondurant, P. Kumar, J. H. Shapiro and M. Maeda, Phys. Rev. A **30**, 343 (1984); G. H. Milburn and D. F. Walls, J. Opt. Soc. Am. B **1**, 390 (1984).

[34] G. Milburn and D. F. Walls, Opt. Commun. **39**, 401 (1981); L. A. Lugiato and G. Strini, Opt. Commun. **41**, 67 (1982); K. Wodkiewicz and M. S. Zubairy, Phys. Rev. A **27**, 2003 (1983).

[35] L. Mandel, Opt. Commun. **42**, 437 (1982); M. Kozierowski and S. Kielich, Phys. Lett. A **94**, 213 (1983); S. Friberg and L. Mandel, Opt. Commun. **48**, 439 (1984).

[36] M. Hillery, Phys. Lett. A **111A**, 409 (1985).

[37] G. S. Agarwal and K. Tara, Phys. Rev. A **43**, 492 (1991); G. S. Agarwal and K. Tara, *ibid*. **46**, 485 (1992); A. R. Usha Devi, R. Prabhu and M. S. Uma, Eur. Phys. J. D **40**, 133 (2006).

[38] H. P. Yuen, Phys. Rev. A **13**, 2226 (1976); C. M. Caves Phys. Rev. D. **23**, 1693 (1981).

[39] M. Kitagawa and Y. Yamamoto, Phys. Rev. A **34**, 3974 (1986); Y. Yamamoto, N. Imoto, and S. Machida, Phys. Rev. A **33**, 3243 (1986).

[40] R. Short and L. Mandel, Phys. Rev. Lett. **51**, 384 (1983).

[41] S. Schiller, G. Breitenbach, S. F. Pereira, T. Muller and J. Mlynek, Phys. Rev. Lett. **77**, 2933 (1996).

[42] R. Simon, M. Selvadoray, Arvind and N. Mukunda, arXiv: **970903** (1997).

[43] R. Loudon, Rep. Prog. Phys. **43**, 913 (1980)

[44] V. V. Dodonov, J. Opt. B: Quantum Semiclass. Opt. **4**, R1 (2002).

[45] V. Dodonov and V. Man'ko, *Theory of Nonclassical States of Light*, (Taylor & Francis, New York, 2003).

[46] M. Hillery, Phys. Rev. A **35**, 725 (1987).

[47] V. V. Dodonov, O. V. Man'ko, V. I. Man'ko, and A. Wünsche, J. Mod. Opt. **47**, 633 (2000); V. V. Dodonov and M. B. Reno, Phys. Lett. A **308**, 249 (2003).

[48] C. T. Lee, Phys. Rev. A **44**, R2775 (1991).

[49] A. Kenfack and K. Zyczkowski, J. Opt. B **6**, 396 (2004).

[50] K. Zyczkowski and W. Slomczynski, J. Phys. A: Math. Gen. **31**, 9095 (1998).

[51] C. Gehrke, J. Sperling and W. Vogel, Phys. Rev. A **86**, 052118 (2012); A. Miranowicz, M. Bartkowiak, X. Wang, Y. X. Liu, and F. Nori, Phys. Rev. A **82**, 013824 (2010).

[52] W. Vogel and J. Sperling, Phys. Rev. A **89**, 052302 (2014).

[53] N. Lutkenhaus and S. M. Barnett, Phys. Rev. A **51**, 3340 (1995).

[54] S. Chaturvedi and V. Srinivasan, Phys. Rev. A **40**, 6095 (1989).

[55] H. Cramer, *Mathematical Methods of Statistics*, 1st Indian Edition, Asia Publishing House, Bombay (1962).

[56] R. Simon, N. Mukunda and B. Dutta, Phys. Rev. A **49**, 1567 (1994); Arvind, B. Dutta, N. Mukunda and R. Simon, Pramana-J. Phys. **45**, 471 (1995).

[57] Arvind, B. Dutta, N. Mukunda and R. Simon, Phys. Rev. A **52**, 1609 (1995).

[58] M. G. Genoni, M. L. Palma, T. Tufarelli, S. Olivares, M. S. Kim, and M. G. A. Paris, Phys. Rev. A **87**, 062104 (2013).

[59] C. Hughes, M. G. Genoni, T. Tufarelli, M. G. A. Paris, and M. S. Kim, Phys. Rev. A **90**, 013810 (2014).

[60] I. Straka *et. al.*, Phys. Rev. Lett. **113**, 223603 (2014).

[61] J. Park, J. Zhang, J. Lee, Se-Wan Ji, M. Um, D. Lv, K. Kim, and H. Nha, Phys. Rev. Lett. **114**, 190402 (2015).

[62] J. Park, J. Lee, Se-Wan Ji, and H. Nha, Phys. Rev. A **96**, 052324 (2017).

[63] L. Happ, M. A. Efremov, H. Nha and W. P. Schleich1, New J. Phys. **20**, 039601 (2018).

[64] M. G. Genoni, M. G. A. Paris and K. Banaszek, Phys. Rev. A **76**, 042327 (2007).

[65] M. Genoni, M. G. A. Paris and K. Banaszek, Phys. Rev. A **78**, 060303 (R) (2008); M. G. Genoni and M. G. A. Paris, Phys. Rev. A **82**, 052341 (2010); P. Marian and T. A. Marian, Phys. Rev. A **88**, 012322 (2013).

[66] A. Wehrl, Rev. Mod. Phys. **50**, 221 (1978); A. Wehrl, Rep. Math. Phys. **16**, 353 (1979).

[67] J. Solomon Ivan, M. Sanjay Kumar and R. Simon, Quantum Inf. Process **11**, 853 (2012).

[68] R. F. Werner, Lett. Math. Phys. **17**, 359 (1989); R. F. Werner, Phys. Rev. A **40**, 4277 (1989).

[69] A. Peres, Phys. Rev. A **54**, 2685 (1996).

[70] M. Horodecki, P. Horodecki and R. Horodecki, Phys. Lett. A **223**, 1 (1996).

[71] L. M. Duan, G. Giedke, J. I. Cirac and P. Zoller, Phys. Rev. Lett. **84**, 2722 (2000).

[72] R. Simon, Phys. Rev. Lett. **84**, 2726 (2000).

[73] E. V. Shchukin and W. Vogel, Phys. Rev. A **72**, 043808 (2005).

[74] A. Miranowicz and M. Piani, Phys. Rev. Lett. **97**, 058901 (2006).

[75] J. Eisert, Ch. Simon and M.B. Plenio, J. Phys. A **35**, 3911 (2002).

[76] C. H. Bennett, D. P. DiVincenzo, J. A. Smolin and W. K. Wootters, Phys. Rev. A **54**, 3824 (1996); S. Hill and W. K. Wootters, Phys. Rev. Lett. **78**, 5022 (1997); W. K. Wootters, Phys. Rev. Lett. **80**, 2245 (1998).

[77] G. Giedke, M. M. Wolf, O. Kruger, R. F. Werner, and J. I. Cirac, Phys. Rev. Lett. **91**, 107901 (2003); M. M. Wolf, G. Giedke, O. Kruger, R. F. Werner, and J. I. Cirac, Phys. Rev. A **69**, 052320 (2004).

[78] G. Vidal and R. F. Werner, Phys. Rev. A **65**, 032314 (2002); M. B. Plenio, Phys. Rev. Lett. **95**, 090503 (2005).

[79] M. Hillery and M. S. Zubairy, Phys. Rev. Lett. **96**, 050503 (2006).

[80] V. Vedral, M. B. Plenio, M. A. Rippin and P. L. Knight, Phys. Rev. Lett. **78**, 2275 (1997); V. Vedral and M. B. Plenio, Phys. Rev. A **57**, 1619 (1998).

[81] G. Vidal, J. Mod. Opt. **47**, 355 (2000).

[82] M. B. Plenio and S. Virmani, arXiv:**0504163v3** (2006).

[83] C. H. Bennett, G. Brassard, C. Crepeau, R. Jozsa, A. Peres, and W. K. Wootters, Phys. Rev. Lett. **70**, 1895 (1993).

[84] S. L. Braunstein and H. J. Kimble, Phys. Rev. Lett. **80**, 869 (1998).

[85] D. Bouwmeester, Jian-Wei Pan, K. Mattle, M. Eib, H. Weinfurter and A. Zeilinger, Nature **390**, 575 (1997).

[86] A. Furusawa, J. L. Sorensen, S. L. Braunstein, C. A. Fuchs, H. J. Kimble and E. S. Polzik, Science **282**, 706 (1998).

[87] T. C. Zhang, K. W. Goh, C. W. Chou, P. Lodahl, and H. J. Kimble, Phys. Rev. A **67**, 033802 (2003).

[88] W. P. Bowen et al, Phys. Rev. A **67**, 032302 (2003).

[89] M. Yukawa, H. Benichi, and A. Furusawa, Phys. Rev. A **77**, 022314 (2008).

[90] S. Pirandola and S. Mancini, Laser Physics **16**, 1418 (2006); A. Furusawa and N. Takei, Phys. Rep. 443, 97 (2007); S. Pirandola, J. Eisert, C. Weedbrook, A. Furusawa and S. L. Braunstein, Nature Photonics **9**, 641 (2015).

[91] G. S. Agarwal and K. Tara, Phys. Rev. A **46**, 485 (1992).

[92] M. S. Kim, F. A. M. de Oliveira, and P. L. Knight, Opt. Commun. **72**, 99 (1989).

[93] E. H. Lieb, Commun. Math. Phys. **62**, 35 (1978)

[94] A. Ourjoumtsev, A. Dantan, R. Tualle-Brouri and P. Grangier, Phys. Rev. Lett. **98**, 030502 (2007).

[95] F. Dell'Anno, S. De Siena, L. Albano and F. Illuminati, Phys. Rev. A **76**, 022301 (2007).

[96] Y. Yang and Fu-Li Li, Phys. Rev. A **80**, 022315 (2009).

[97] S. Y. Lee, S. W. Ji, H. J. Kim and H. Nha, Phys. Rev. A **84**, 012302 (2011).

[98] C. Navarrete-Benlloch, R. Garcia-Patron, J. H. Shapiro and N. J. Cerf, Phys. Rev. A **86**, 012328 (2012).

[99] S. Wang, L. L. Hou, X. F. Chen and X. F. Xu, Phys. Rev. A **91**, 063832 (2015).

[100] K. P. Seshadreesan, J. P. Dowling and G. S. Agarwal, Physica Scripta **90**, 074029 (2015).

[101] L. Hu, Z. Liao and M. S. Zubairy, Phys. Rev. A **95**, 012310 (2017).

[102] A. V. Chizhov, L. Knoll, and D. G. Welsch, Phys. Rev. A **65**, 022310 (2002); P. Marian and T. A. Marian, *ibid.* **74**, 042306 (2006).

[103] H. Y. Fan and J. R. Klauder, Phys. Rev. A **49**, 704 (1994); H. Y. Fan, H. L. Lu, and Y. Fan, Ann. Phys. **321**, 480 (2006).

[104] W. Ge, M. E. Tasgin and M. S. Zubairy, Phys. Rev. A **92**, 052328 (2015).

[105] M. M. Wolf, J. Eisert and M. B. Plenio, Phys. Rev. Lett. **90**, 047904 (2003).

[106] N. R. Heckenberg, M. E. J. Friese, T.A. Nieminen and H. Rubinsztein-Dunlop, *Optical Vortices*, Nova Science Publishers (1999).

[107] S. Danakas and P. K. Aravind, Phys. Rev. A **45**, 1973 (1992).

[108] L. Allen, M. W. Beijersbergen, R. J. C. Spreeuw, and J. P. Woerdman, Phys. Rev. A **45**, 8185 (1992); G. Indebetouw, J. Mod. Opt. **40**, 73 (1993); M. W. Beigersbergen, L. Allen, H.E.L.O. Van der Veen, and J. P. Woerdman, Opt. Commun. **96**, 123 (1993); H. He, M. E. J. Friese, N. R. Heckenberg, and Rubinsztein-Dunlop, Phys. Rev. Lett. **75**, 826 (1995).

[109] G. S. Agarwal, R. R. Puri, and R. P. Singh, Phys. Rev. A **56**, 4207 (1997); J. Courtial, K. Dholakia, D. A. Robertson, L. Allen, and M. J. Padgett, Phys. Rev. Lett. **80**, 3217 (1998); L. Allen, M. J. Padgett, and M. Babiker, Prog. Opt. **39**, 291 (1999).

[110] B. N. Simon, S. Simon, F. Gori, M. Santarsiero, R. Borghi, N. Mukunda, and R. Simon, Phys. Rev. Lett. **104**, 023901 (2010).

[111] P. Chowdhury, A. S. Majumdar, and G. S. Agarwal, Phys. Rev. A **88**, 013830 (2013).